SYNTHESIS, PROPERTIES AND MODIFICATIONS OF ENGINEERING POLYMERS

by

James L. Hedrick

Dissertation submitted to the Faculty of the
Virginia Polytechnic Institute and State University
in partial fulfillment of the requirements for the degree of

DOCTOR OF PHILOSOPHY

in

Materials Engineering Science

APPROVED:

J. E. McGrath, Chairman

G. L. Wilkes

T. C. Ward

J. P. Wightman

K. L. Reifsnider

August, 1985

Blacksburg, Virginia

SYNTHESIS, PROPERTIES AND MODIFICATIONS OF
ENGINEERING POLYMERS

by

James L. Hedrick

Committee Chairman: James E. McGrath
Chemistry

(ABSTRACT)

Amorphous and semi-crystalline poly(arylene ether sulfone) homo- and copolymers and related structures were systematically synthesized via nucleophilic, aromatic substitution reactions using the potassium carbonate/N-methylpyrrolidone synthesis route. In particular, deuterated poly(arylene ether sulfones) were synthesized in order to investigate molecular motion via deuterium NMR. The mechanical, dynamic mechanical and fracture properties of these materials were also examined. Polysulfones were characterized to be tough, ductile materials and it was found that polysulfone-poly(dimethylsiloxane) block copolymers blends with homopolysulfone serves to further increase their ductility as indicated by fracture toughness $K_{I,C}$ measurements. In addition, it was demonstrated that functionalized polysulfone was an excellent thermoplastic modifier for brittle epoxy networks. The morphology and properties of these copolymers and copolymer-homopolymer blends were studied as a function of molecular weight and chemical structure. A number of techniques were utilized to elucidate the possible toughening mechanisms that are operative.

ACKNOWLEDGMENTS

The author would like to gratefully acknowledge the support, guidance and patience of Prof. J. E. McGrath during the preparation of this thesis. In addition, the research, travel and writing experiences provided by Prof. McGrath during the thesis work were very valuable. The author would also like to acknowledge the contributions of Prof. G. L. Wilkes, Prof. T. C. Ward and the other members of my committee. My colleagues, Dr. Dillip Mohanty and Dr. Iskendar Yilgor, are thanked for their significant contributions to my understanding of the synthesis, characterization and properties of polymers.

The author would also like to acknowledge the financial support of NASA through the late Dr. George Sykes, which included partial support of my summer research study in Australia with Prof. O'Donnell.

Finally, I would like to thank my parents for their support during the course of this thesis.

Table of Contents

1.0 INTRODUCTION

Poly(arylene ether sulfones) and related structures comprise a class of materials known as engineering thermoplastics. These materials may be fabricated by conventional techniques including extrusion and compression molding, or they may be used as solvent castable amorphous matrix resins for high performance graphite reinforced composites. Their desirable properties include dimensional stability, low coefficient of thermal expansion, retention of modulus at high temperatures (150°C), radiation resistance and tough, ductile mechanical properties. Unfortunately, the "Achilles heel" of these amorphous thermoplastics is their sensitivity to organic environments which leads to their catastrophic premature failure at low stresses and strains. These latter phenomena are known as environmental stress cracking (ESC).

This thesis will first discuss the desirable properties associated with these engineering polymers. For instance, the tough, ductile mechanical properties which have often been associated with the major secondary transition (β-relaxation) in the dynamic mechanical spectra. Both the origin of the secondary relaxation as well as its relationship to mechanical behavior is still somewhat of a controversial issue. Several selectively deuterated poly(arylene ether sulfones) were synthesized in high molecular weight for deuterium NMR investigations in a collaborative effort with Dr. L. W. Jelinski at AT&T Bell Laboratories. Deuterium NMR provides highly specific information about molecular motion which compliments the molecular motion obtained using dynamic mechanical analysis. Fracture mechanics techniques were also used to quantify the mechanical behavior of homo- and block polymers.

Poly(arylene ether sulfone) materials, like many other thermoplastics of sufficient molecular weight, have the ability to craze and deform in a plastic or ductile fashion. The initiation of these energy absorption mechanisms leads to a material of sufficiently improved impact strength. Perfectly alternating block copolymers of polysulfone with poly(dimethylsiloxane) were synthesized and blended with homopolysulfone to form a finely dispersed "mechanically compatible" blend. The block copolymer was shown to exist as discrete composite particles within the homopolysulfone matrix and served as a stress concentrator capable of initiating craze formation. The morphology and mechanical properties of the copolymers and the block copolymer-homopolymer blends were investigated using a wide variety of techniques.

The most obvious way to improve a materials resistance to environmental stress cracking, is by crosslinking, which will render it insoluble. However, with crosslinking, the desirable ductile mechanical properties associated with these materials are often lost. Therefore, a compromise must be achieved between toughness and solvent resistance if this approach is chosen.

One of the most solvent resistant organic materials which have achieved significant commercial status are the epoxy networks. Many applications such as coatings, structural adhesives and matrix resins for composite structures have been developed. Unfortunately, because of their highly crosslinked structure, these networks are inherently brittle and have limited utility in those applications which require high impact strength. In recent years, functionally terminated

elastomeric oligomers have been used to improve the toughness of these materials. However, the incorporation of a low modulus elastomer often effects the bulk properties, especially the modulus. In an effort to obtain a better balance of properties (toughness and stiffness) engineering thermoplastics were used to modify the epoxy networks. Functionally, terminated Bisphenol-A based polysulfone oligomers of controlled molecular weight were chemically reacted into the epoxy resin prior to curing. The morphology of these materials were examined and demonstrated to display interesting two phase structures which led to significantly enhanced fracture toughness, without loss of flexural modulus.

2.0 HISTORICAL: Ductile Engineering Thermoplastics and Thermosets

2.1 Synthesis

2.1.1 Synthesis of Poly(arylene ether sulfones)

Synthetic routes for the preparation of poly(arylene ether sulfones) and related structures were discovered independently and nearly simultaneously by Union Carbide Corporation (1-4), 3M Corporation (5) and ICI (6-9). Each of these firms commercialized their "polysulfone's", but the 3M product is no longer produced. Table 1 contains the structures and some important thermal properties for these materials.

The two main synthetic routes developed for the preparation of these high molecular weight novel macromolecules are polyetherification and polysulfonylation. In polyetherification, the sulfone containing activated halide and bisphenol monomers are suitably reacted to form an ether linkage via nucleophilic aromatic substitution. In contrast, polysulfonylation involves a Friedel-Crafts reaction (electrophilic aromatic substitution) with aromatic ethers such as diphenyl ether. It is interesting to note that similar structures may be obtained by each synthetic route, and also that subtle isomeric structural variations can play a major role in mechanical behavior.

2.1.1.1 Polyetherification

Johnson and coworkers (1,4) at Union Carbide were perhaps the first to describe the synthesis of poly(arylene ether sulfones and ketones) via nucleophilic aromatic substitution. A large number of novel high

Table 1

Structures of Important Aromatic Poly(arylene ether sulfones)

Structure	Tg, °C
Udel 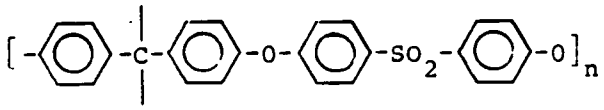	190
Astrel 300 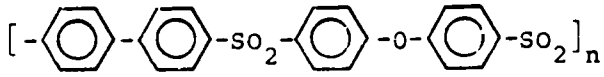	285
Polyethersulfone 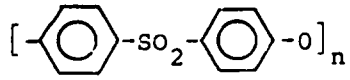	230

molecular weight structures were investigated. The basic synthetic scheme is shown in Scheme 1. Several solvents were examined (1) and dimethyl sulfoxide (DMSO) was found to give the highest molecular weight. DMSO is an aprotic, dipolar solvent and was found to be the most efficient of the solvents examined at solubilizing the polar reaction intermediates as well as the subsequent amorphous polymer. In Scheme 1, X was normally an isopropylidene and Y was a sulfone group.

SCHEME 1

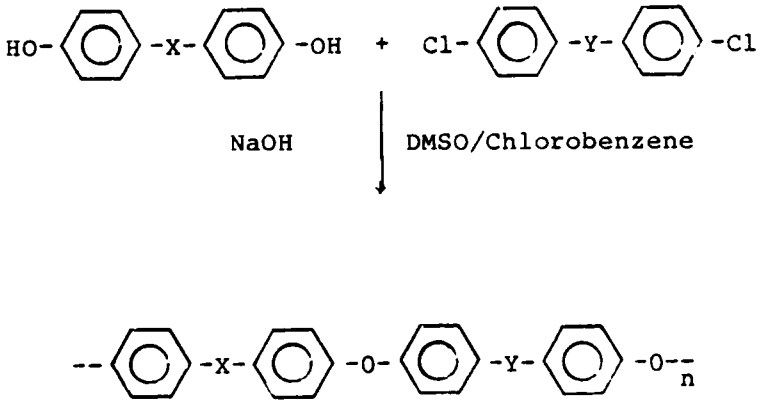

Sulfolane was also found to give good results, but side reactions with the base at elevated temperatures caused several problems which could limit molecular weight. Chlorobenzene was chosen as a dehydrating agent to remove the water which is produced during the bisphenate formation. It was demonstrated that water removal was crucial, principally to prevent hydrolysis of the activated aromatic halide which would in turn upset the required 1:1 stoichiometry. In addition, chlorobenzene was a suitable solvent for the polymer.

Sodium hydroxide was found to be a good choice for producing bisphenates with the high reactivity with dichlorodiphenylsulfone (approximately one hour at 160°C). Unfortunately, hydrolytic side reactions have been associated with this strong base. Specifically, even a slight excess of the sodium hydroxide can hydrolyze the dihalide monomer, which thus creates a stoichiometric imbalance. In this case only one chlorine is usually replaced, since the second is considerably less reactive (3). Thus, a two step process is required in which the bisphenate is first formed using sodium hydroxide and the water removed by azetropic distillation with chlorobenzene. In the second step, the activated dihalide is added slowly as a solution in chlorobenzene and reacted at 1:1 stoichiometry to obtain high molecular weight.

It is well known that in general, aromatic halides are unreactive. However, the electron withdrawing ability of the sulfone group activates these para-linked halides, thus promoting the nucleophilic aromatic displacement (1). A ketone group will also activate an aromatic halide but to a lesser extent. Importantly, in this case, fluorine groups may be required as the more active leaving group.

The mechanism of the aromatic substitution reaction is fairly well understood, at least in small molecules (10-12). It is accepted that these reactions usually proceed through an intermediate complex such as that outlined below:

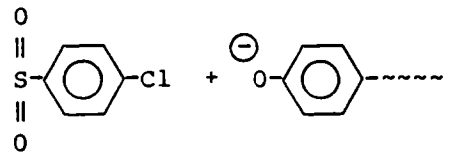

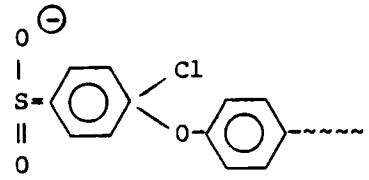

Activated Complex

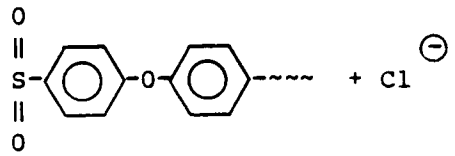

The ability of the sulfone group to accept a negative charge from the ring serves to stabilize the complex.

The electron withdrawing ability of the sulfone group is more effective for the ortho or para positions, however, the ortho position may be subjected to steric hindrance. The order of reactivities of the halides has been observed (4) to be p > o >> m and F > Cl >> Br>I.

Johnson and coworkers (1) synthesized a number of high molecular weight poly(arylene ethers) where both X and Y (Scheme 1) were varied. Table 2 contains many of these structures (1,4).

Rose (6-9,12) and coworkers synthesized a wide variety of novel intermediates for the preparation of poly(arylene ether sulfones) and related structures. Halogenophenylsulphonylphenols were synthesized by partial hydrolysis of the corresponding dihalides. In addition, other novel monomers were synthesized via Freidel-Crafts electrophilic addition reactions. Subsequent polymerizations were then carried in solution (DMSO or sulfolane), or bulk, in the presence of KF. Polymerizations employing KF required high temperatures (220-280°C) and extended times (20-30 hours) using dimethyl sulfone or sulfolane as the solvent.

More recently, Viswanathan and coworkers (13) reported a detailed description of a somewhat different synthetic route for the preparation of poly(arylene ether sulfones). The dimethyl acetamide/potassium carbonate route was developed for the synthesis of novel materials as shown in Scheme 2. Potassium carbonate is a weak base and only reacts with phenols at elevated temperatures (140°C and above). Thus, hydrolytic side reactions associated with strong bases are minimized. They (13) investigated the effect of excess K_2CO_3 on several appropriate model compounds and polymers and found no evidence of hydrolysis of the halide or reaction with the polymer. Furthermore, an excess of this weak base may be used, which minimizes stoichiometric errors.

DMAC is a typical aprotic, dipolar solvent for these nucleophilic displacement reactions which allows moderately high reaction

Table 2

Poly(arylene ethers) Structures

Polymer no.	Polymer repeat unit	$\eta_{sp/c}$ 100ml/g	Tg°C	Water Absorption wt. %
1	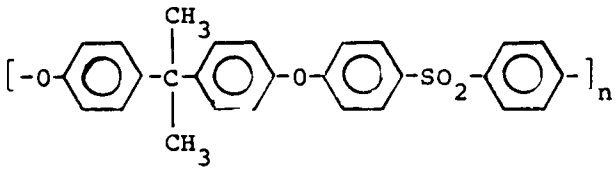	0.48	184	0.72
2	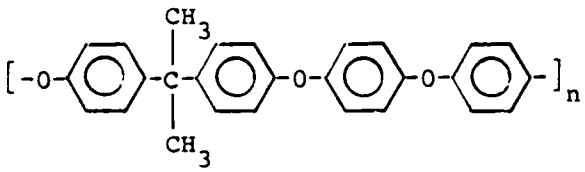	0.50	122	0.13
3	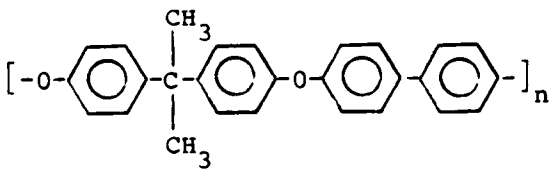	0.70	154	0.17
4	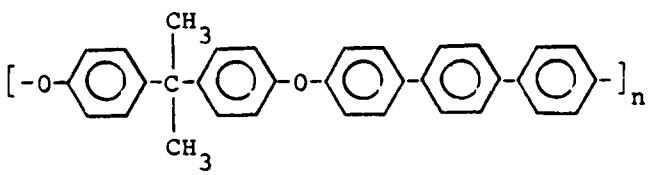	1.1	182	0.18
5	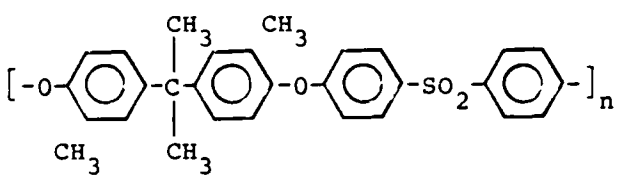	0.61	178	0.66

Table 2 (Continued)

Poly(arylene ethers)

Polymer no.	Polymer repeat unit	η_{sp}/c 100ml/g	Tg°C	Water Absorption wt. %
6	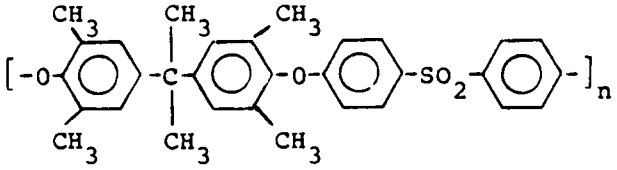	0.41	230	1.30
7	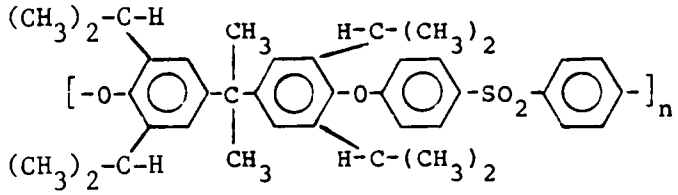	0.55	175	0.32
8	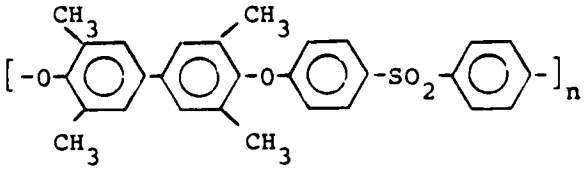	0.87	262	1.36
9	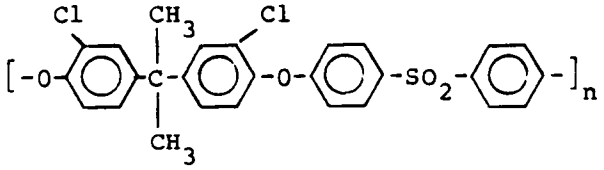	0.50	190	0.67
10	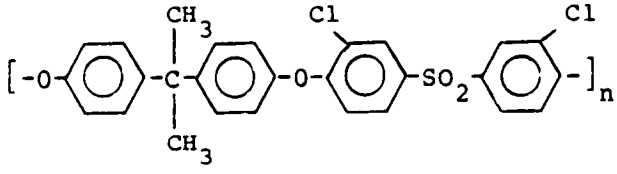	0.51	172	0.52

Scheme 2

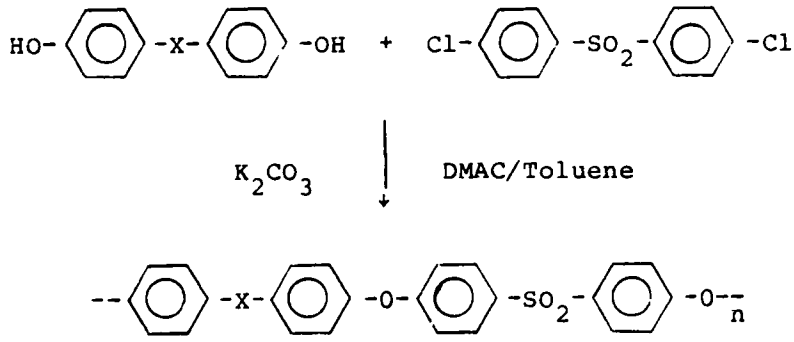

temperatures (~160°C). Furthermore, it was observed that certain polar bisphenate intermediates in the polymerizations have limited solubility in the DMSO, thus limiting the molecular weight. Apparently, DMAC, and especially the weak base K_2CO_3, circumvents many of these problems, possibly because the bisphenol hydroxyls are converted to phenates one at a time, and hence tend to quickly react to form more soluble nonionic species. Toluene was used as a dehydrating agent in these studies.

Another advantage in such a synthetic route is the order of addition of the reactants. That is, in the DMSO/sodium hydroxide route a two step procedure is required. However, by the utilization of a weak base such as K_2CO_3 the monomers may be added all at once or sequentially, as desired. Unfortunately, this synthetic route may require longer reaction times because of the slow dehydration step and the heterogeneous nature of the base.

Viswanathan et al. (13) have synthesized a series of statistical hydroquinone/bisphenol-A (Hq/BisA) copolymers as shown in Scheme 3. It was believed that the incorporation of the hydroquinone would possibly lead to a semi-crystalline polymer especially from solution. This is thought to have important ramifications in improving environmental

Scheme 3

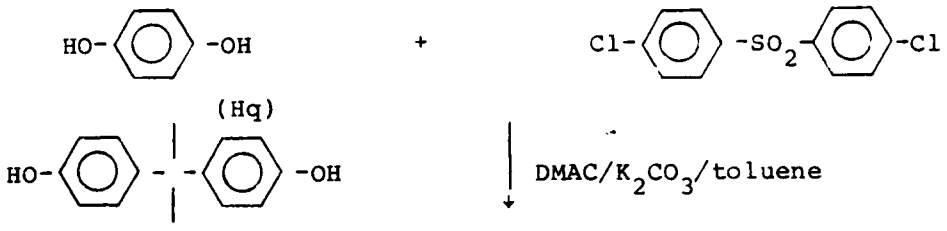

(Bis-A)

(variable compositions)

Statistical Copolymer

stress cracking resistance. However, at higher levels of hydroquinone content the reaction mixture became extremely viscous and the polymer often prematurely precipitated prior to reaching high molecular weight.

In an effort to circumvent many of the problems associated with the relatively low boiling solvent DMAC, another higher boiling amide solvent was chosen for the synthesis of these more rigid poly(arylene ethers). Mohanty and McGrath (14) have found that N-methyl-2-pyrrolidone (NMP) is a suitable solvent which allows reaction temperatures at 190°C, or even briefly up to its boiling point (202°C). In addition, NMP is a relatively non-toxic aprotic dipolar solvent which

SCHEME 4

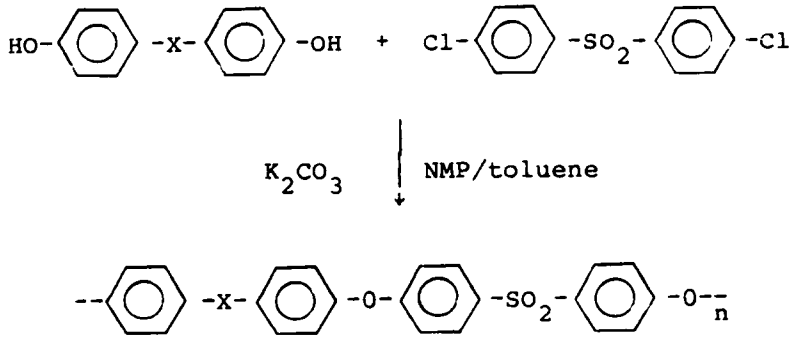

solubilizes the polar intermediates as well as the subsequent polymers. K_2CO_3 was once again chosen as the base. These workers synthesized a large number of poly(arylene ether sulfone, ketone and nitrile) homo and copolymers as shown in Table 3.

Water is miscible with both DMAC and NMP, therefore it is necessary to use a dehydrating agent such as toluene. Unfortunately, toluene is a nonsolvent for the growing polymer and may interfere to some extent with the reaction. Recently, Johnson and McGrath (15) have used N-cyclohexyl-2-pyrrolidone (CHP) which is immiscible with water at elevated temperatures. Thus, a hydrocarbon-like dehydrating agent is not required. Furthermore, a mixture of NMP and CHP can be used to solubilize the polar intermediates, because CHP is not as polar as NMP.

In each of the synthesis procedures described thus far, well defined block copoly(arylene ethers) have not been synthesized. Ether linkages between aromatic rings are typically stable to phenoxides, but when these linkages are activated by sulfone groups they are labile under the basic step-growth or polycondensation conditions. It has been reported by Rose and others (1,4,12) that a significant amount of ether interchange occurs at temperatures above 120°C. In fact, kinetic data obtained (12) indicate that these activated ether linkages are nearly as reactive as the corresponding halides.

This reaction involves the attack of a phenoxide on these activated ethers as shown in Scheme 5 below. It is this scrambling of the polymeric chains that leads to a statistical copolymer.

Kircheldorf et al. (16,17) have recently reported that they can prepared block copoly(arylene ethers) from silylated bisphenols and

Table 3

POLY(ARYLENE ETHER SULFONES)

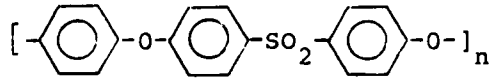

POLY(ARYLENE ETHER NITRILES)

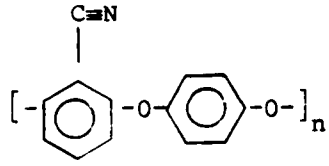

POLY(ARYLENE ETHER KETONES)

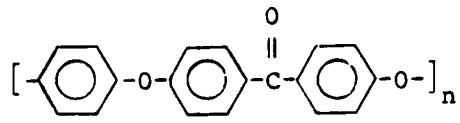

SCHEME 5

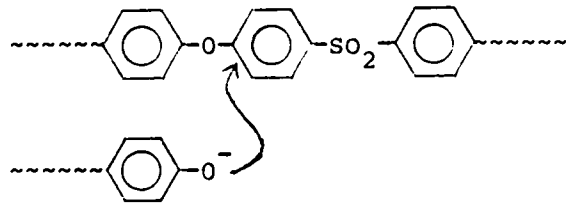

activated dihalides in a bulk reaction as shown in Scheme 6. The silylated bisphenols were synthesized by reacting the appropriate bisphenol with either chlorotrimethylsilane or hexamethyl disilazane in refluxing toluene or dioxane (16,17).

SCHEME 6

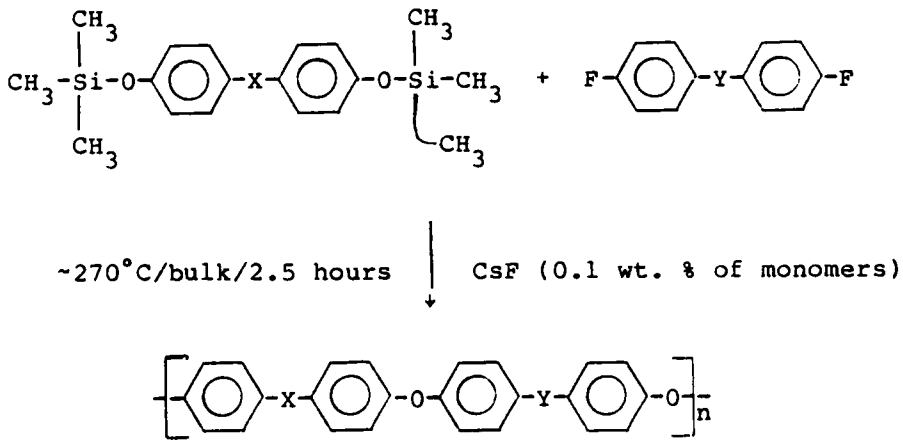

Cesium fluoride was found to be the most effective catalyst (16) and the following reaction mechanism was proposed:

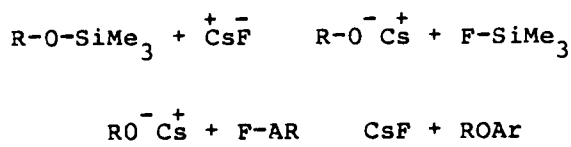

The effectiveness of the catalyst depends on the formation of the dissolved fluoride ions, which are believed to cleave the Si-O bond of the silylated bisphenols. The fluoride ion is most useful because it is a strong nucleophile and the subsequent Si-F bond in the leaving group is more stable than any other silicon bond.

The reaction temperature used depends on the nucleophilicity of the bisphenol and its anion. Silylated bisphenol-A and related structures required reaction temperatures between 220 and 230°C. However, weaker nucleophiles such as dihydroxydiphenylsulfone required reaction temperatures around 300°C. At these reaction temperatures the by-product fluorotrimethylsilane is evolved apparently leaving a clean homo- or copolymer. By this novel synthetic technique both random and block copolymers were synthesized. The statistical or random copolymers were synthesized by a one step process in which all the monomers were added simultaneously. The block copoly(arylene ether sulfone ketone) materials were synthesized in a two step process in which the ketone block was prepared first, followed by the sulfone block. Two glass transition temperatures were obtained at segment molecular weights of (5000 Mn) which is indicative of a block copolymer and a two phase morphology. It is believed (16,17) that the use of the relatively weak fluoride ion catalyst precludes the transetherification reactions during the polymerization. However, a more likely explanation is the reactivity of the ≡Si-O bond relative to the ether linkage. In addition, fluorotrimethylsilane is a good leaving group. Very recently, Wu (18) has improved these procedures and has obtained crystallizable copolymers.

2.1.1.2 Polysulfonylation

A second important route to poly(arylene ether sulfones) is a polysulfonylation process or Friedel-Crafts reaction, in which sulfone linkages are formed by the reaction of arylsulfonyl chlorides with an aromatic nuclei as shown in Scheme 7 (5,19,20). This could also utilize an A-B type polymerization which could lead to high molecular weight and may be done in solution or melt.

Typical solvents used in this synthesis are nitrobenzene, dimethylsulfone or chlorinated biphenyl. The solvent helps to controls

SCHEME 7

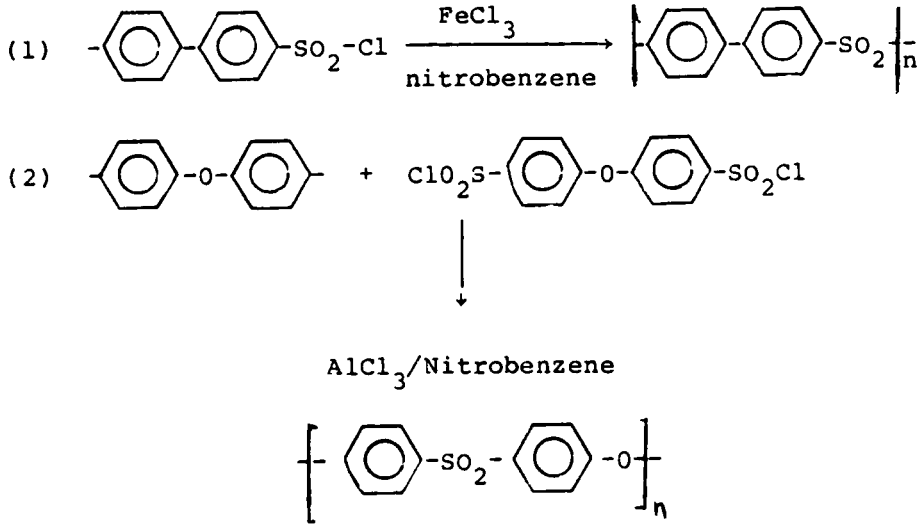

the viscosity and allows the by-product (HCl) to be more easily removed, as compared to bulk processes. The preferred catalysts are $FeCl_3$, $SbCl_5$, $InCl_3$, $AlCl_3$ as well as other typical Friedel-Crafts catalysts.

Sulfonylation is generally thought (12) to proceed through a intermediate complex of the type shown below.

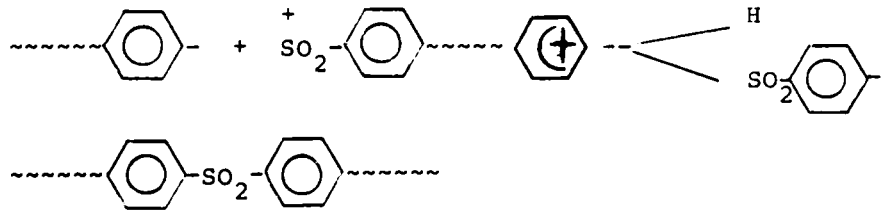

The electron deficient reagent attacks the aromatic ring which provides an electron pair to form the sulfone linkage. Thus, it is important that the aromatic ring being attacked not contain electron withdrawing groups such as SO_2 or CO.

It is generally understood that electrophilic substitution may involve attack at both the ortho and para positions. However, Friedel-Crafts polymerization of aryl sulfonyl chlorides, particularly with monochlorosulfonated compounds, show a high tendency towards para substitution. More ortho attack was observed with the A-B type monomers.

In addition, significant amounts of branching in the polysulfonation reactions have been observed by Cadby (21) in an NMR investigation. Although, the exact mechanism of this branching is not clearly understood it appears that a small amount of ortho position reaction competes with the more desired para coupling. It does appear that even modest branching seriously detracts from the usual ductile behavior of the all para systems.

2.1.2 Synthesis of Aromatic Poly(Arylene Ether Ketones)

Aromatic poly(arylene ether ketones) belong to the class of semi-crystalline polymers known as engineering thermoplastics which have recently achieved significant commercial status. Their desirable

properties include excellent electrical and mechanical properties even at elevated temperatures and resistance to both fire (ignition) and chemicals. The two major poly(arylene ether ketones) which were introduced commercially are tradenamed PEEK^{R} (ICI) and STILAN 1000^{R} (Raychem Corporation) and are shown in Table 4. However, Raychem has since withdrawn their product. Another product named KADEL was developed at Union Carbide and is now in commercial development by Amoco.

In a similar fashion to the aromatic polysulfones, the poly(arylene ether ketones) may be polymerized by either polyacylation or by polyetherification depending on the monomers used.

2.1.2.1 Polyacylation

The first synthesis of a fully aromatic poly(arylene ether ketone) was described by Bonner (22) who obtained a polymer of low molecular weight (IV = 0.18 dl/gm) by the Friedel-Crafts polycondensation using nitrobenzene as a solvent and aluminium chloride as the catalyst.

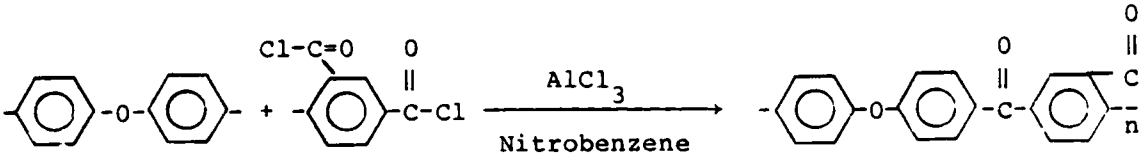

Goodman et al. (23) reported a similar structure using a Friedel-Crafts reaction with methylene chloride as solvent and obtained relatively high molecular weight (IV = 0.5 dl/gm). These workers condensed the A-B monomer p-phenoxybenzoyl chloride/phenoxybenzoyl chloride.

Iwakura et al. (24) used polyphosphoric acid (PPA), to polymerize p-phenoxybenzoic acid as shown below. They noted that the polymer was

Table 4

Structures of Important Aromatic Poly(arylene ether ketones)

PEEK

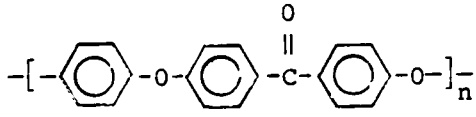

STILAN 1000

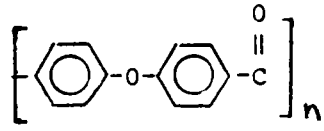

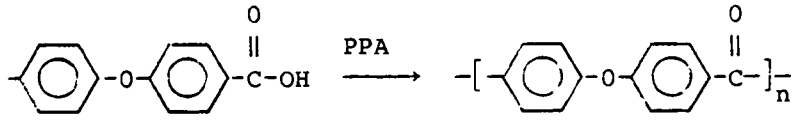

insoluble in most normal organic solvents, which in turn allowed only limited molecular weight prior to premature precipitation. Apparently PPA dissolves the polymer by protonation of the ketone group. However, a more effective BF_3HF acid "solvent" system was devised by Marks (25), which complex was also an excellent catalyst for polyacylations. High molecular weight aromatic polyketones were obtained by the latter synthetic technique (IV = 1.0-2.7 dl/gm). Dahl (26) further refined Mark's procedure and concluded that the semi-crystalline poly(arylene ether ketones) required an intrinsic viscosity of 0.8 dl/gm in H_2SO_4 to obtain ductile mechanical properties.

Recently, Rose (27) and others (28) have synthesized aromatic polyketones by an electrophilic arylation processes which involves a reaction between a mixture of aromatic diacyl halide and an aromatic compound containing at least two aromatically bound hydrogen atoms, or a self reacting monoacyl halide containing at least one aromatically bound hydrogen atom. The solvents used in this case were fluoroalkane sulfonic acids such as trifluoromethane sulfonic acid , difluoromethane sulfonic acid, tetrafluoromethane sulfonic acid and others. It is believed that the acid serves as both a solvent and Lewis acid in the polymerization. The fluoroalkane sulfonic acids are preferred over the liquid hydrogen fluoride solvents. In addition, this synthesis technique did not require metal catalysts which are often difficult to remove.

2.1.2.2 Polyetherification

Farnham et al. (1) synthesized a number of amorphous and semicrystalline aromatic poly(arylene ether ketone) via the polyetherification route. The amorphous high molecular weight materials were synthesized in typical aprotic, dipolar solvents such as DMSO or sulfolane via nucleophilic aromatic substitution. Table 5 contains the various bisphenols reacted with difluorobenzophenone and the subsequent polymers. However, these workers were unsuccessful at synthesizing high molecular weight semicrystalline, aromatic polyketones, due to premature crystallization from their preferred solvent, sulfolane. In addition, it was noted that these materials tended to be brittle unless obtained in the amorphous form. A clear indication that aromatic polyketones synthesized by this route were indeed low molecular weight.

Mohanty et al. (14) synthesized amorphous, aromatic poly(arylene ether ketones) based on tetramethyl bisphenol A or bisphenol-S using the NMP/K_2CO_3 route. However, semicrystalline polymers of high molecular weight derived from hydroquinone or bisphenol were not obtained.

Rose pioneered the use of diphenylsulfone as a heat transfer agent to allow the synthesis of high molecular weight poly(arylene ether ketones) at elevated temperatures. However, this is an inconvenient solid "solvent" (melting point 123°C). Thus, it is very difficult to remove this high boiling solvent upon completion of the polymerization, although acetone extraction techniques are reasonable effective. Residual solid solvent may, of course, effect the mechanical behavior, crystallization kinetics as well as other properties.

Table 5

Various Poly(arylene ether ketones)

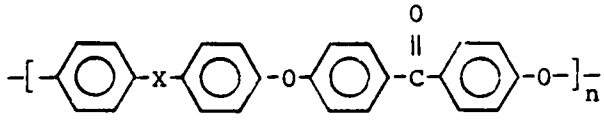

X	Tg°C
-O-	150
$-C(CH_3)_2-$	155
$-C(CF_3)_2-$	175
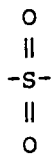	200

Recently, lower boiling solvents have been used (14,29) such as CHP, benzophenone and dimethylsulfone, to synthesize aromatic polyketones. However, Kirchoff et al. (16,17) have recently provided one solution to this problem by silylating the bisphenols and conducting the reactions in bulk.

2.2 Characterization and Physical Behavior

2.2.1 Ductile Properties and the β-Transition

Poly(arylene ether sulfones) and related structures exhibit tough, ductile mechanical properties. These desirable properties have been associated with the major secondary relaxation (β relaxation) in

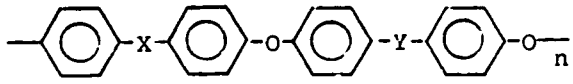

the dynamic mechanical spectra (30) which is shown in Figure 1. This transition has a maximum at -100°C at 1 Hz with a magnitude of 0.02 on the tan δ scale. In addition, it is interesting to note the large breadth of the transition, indicating the possibility of a wide range of molecular motions. This transition has been observed in many other ductile thermoplastics such as polycarbonate, poly(aryl esters) and poly(arylene ether ketones). It has been suggested by many polymer scientists that this molecular motion is at least related to an energy absorption mechanism. That is, the transition observed in the dynamic mechanical spectra at -100°C occurs at very low frequencies. During an actual impact situation (high deformation rates or high frequencies) the transition shifts on the temperature scale towards room temperature and the molecular motion can be involved in the dissipation of the energy

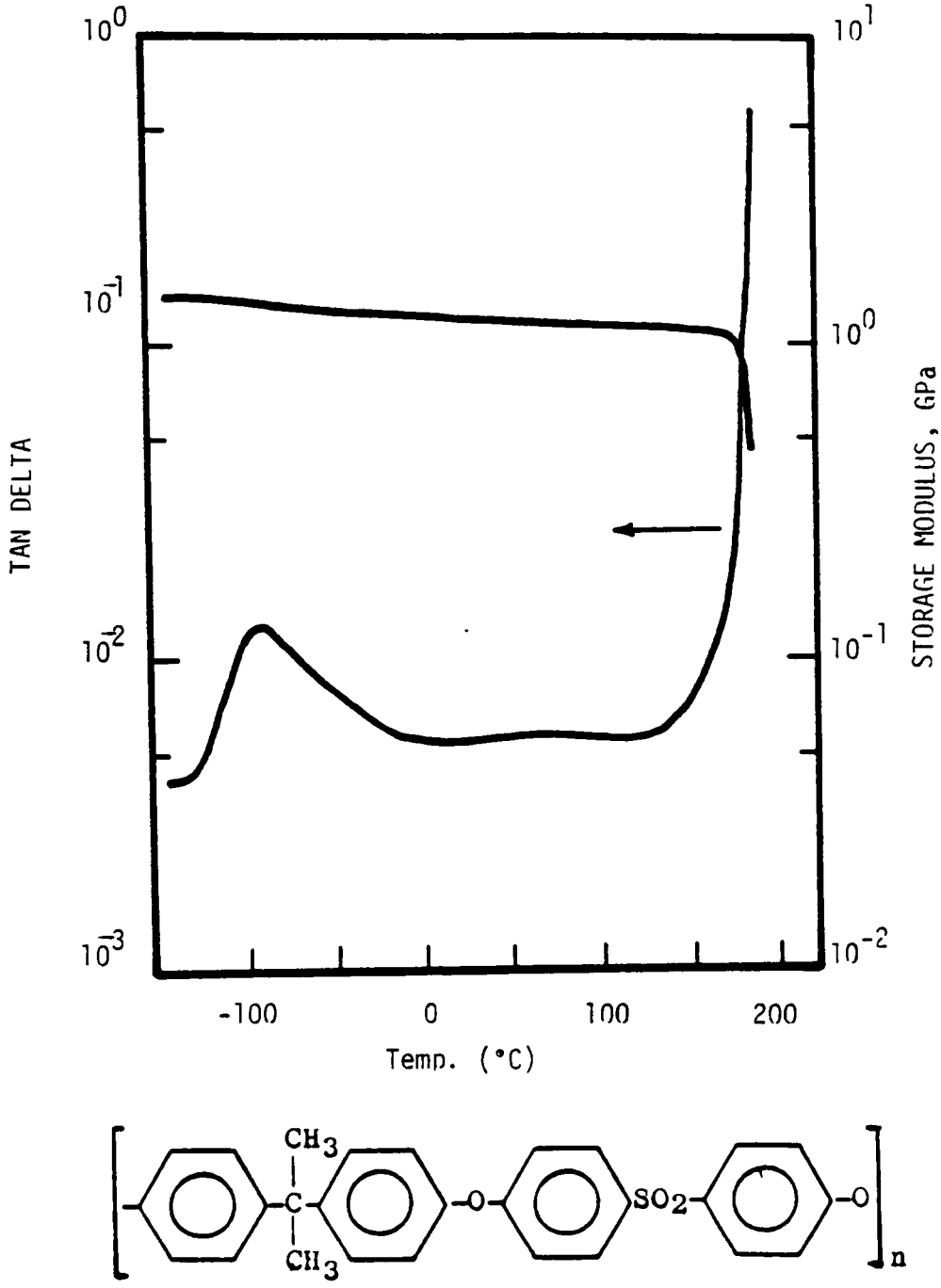

Figure 1. Plot of tand and storage modulus as a function of temperature for bisphenol-A polysulfone. (Reference 29).

associated with impact. However, both the possible origins of the secondary relaxation as well as its effect on the mechanical properties are still somewhat of a controversial issue and the phenomenon has been investigated by a variety of dynamic mechanical and dielectric techniques.

Heiboer (31) was one of the first investigators to report the major secondary relaxation associated with bisphenol-A polysulfone. He found that both the magnitude and position of the mechanical loss to be affected by annealing. Struik (32) and Petrie (33) have studied the effect of annealing of amorphous glasses and it is generally found that annealing shifts the secondary relaxation spectrum to longer times and the magnitude of the transition of a quenched sample is higher than that of an annealed sample. It is believed that aging (annealing) at a temperature close to the Tg decreases the free volume, hence limiting the mobility of the glass. Accordingly, Kinloch (34) reported that fracture toughness values decreased with annealing.

Robeson and coworkers (35) found that the addition of low molecular weight dilutants reduced the magnitude of the β relaxation in polysulfone. This effect has been termed antiplasticization and resulted in a decrease in impact strength and toughness. They suggested that the polymer's free volume decreased with increasing antiplasticizer content. Furthermore, Robeson also showed that CO_2 permeability also decreased with the addition of antiplasticizer.

Several others (35-41) observed that water sorption increased the magnitude of the relaxation. For instance, in a dynamic mechanical analysis, Baccaredda (36) observed a transition at -45°C (6100 Hz) for

the bisphenol-A based polysulfone, whose magnitude showed a strong dependence on water sorption. The activation energy for the relaxation was estimated to be about 12 kcal/mol. These workers attributed the β peak to rotational movements of absorbed water molecules bound to the polar groups along the polymer chain.

Kurz and coworkers (37) extended Baccaredda's work to several other aromatic polysulfones and observed a transition at -100°C (1 Hz) that was sensitive to water uptake. These workers attributed the molecular moiety responsible for this transition to the sulfone group as it was the most polar and hence the logical group in the backbone.

Suzuki et al. (38) studied the dielectric behavior of a variety of amorphous polymers and observed that these secondary relaxations disappeared as the water was removed from the polymer. In a similar dielectric investigation, Allen (39) concluded that water associated with the polar groups in the polysulfone backbone strongly influenced the β relaxation. However, it should be noted that dielectric measurements are more sensitive to polarizable groups than mechanical measurements.

Chung and Sauer (40) investigated the major secondary relaxation in a number of polymers including the polysulfone (UDEL^{R}) which contained aromatic groups in the backbone. Using a torsion pendulum apparatus they observed a broad β relaxation at 162K (0.67 Hz) in polysulfone similar to those previously reported by Kurz and Heiboer. In addition, they calculated an activation energy of 10.5 kcal/mol which is in close agreement to previous reports. However, they observed that this transition was common to many structures which contained phenylene

rings, and attributed the relaxation to reorientational motion of the phenylene rings. Chung et al. also observed that the ring motion was sensitive to atoms adjacent to the rings, i.e., phenyl rings connected by ether linkages which have a low potential energy barrier show a secondary relaxation at a lower temperature. Furthermore, water sorption increased the magnitude of the transition. However, the transition was still present in dry samples. Hence, several important conclusions resulted from this investigation; (1) the transition was believed to result from phenyl ring rotations, and reorientation and not from motion of the sulfone linkage as reported by Kurz, and (2) water enhanced the transition by hydrogen bonding to the polar groups along the backbone.

Robeson et al. (35,41,42) investigated the dynamic mechanical analysis of a large number of novel poly(arylene ether) structures in an attempt to assess the molecular moieties responsible for the large secondary relaxation. The structures investigated are contained in Table 2. The poly(arylene ethers) synthesized by the Ullman reaction (2 and 3 from Table 2), which do not contain the sulfone moiety, do indeed show a major relaxation at -100°C (1 Hz). Furthermore, the effect of water sorption is minimal in these structures as shown in Figure 2. However, the sulfone containing poly(arylene ether) showed a strong dependence on water uptake as shown in Figure 3. The dimethyl bisphenol-A polysulfone showed no transition at -100°C as shown in Figure 4. Apparently, the transition has shifted to 45°C with the structural variation. However, water sorption still produces a transition at -100°C (1 Hz) with no effects on the other transitions.

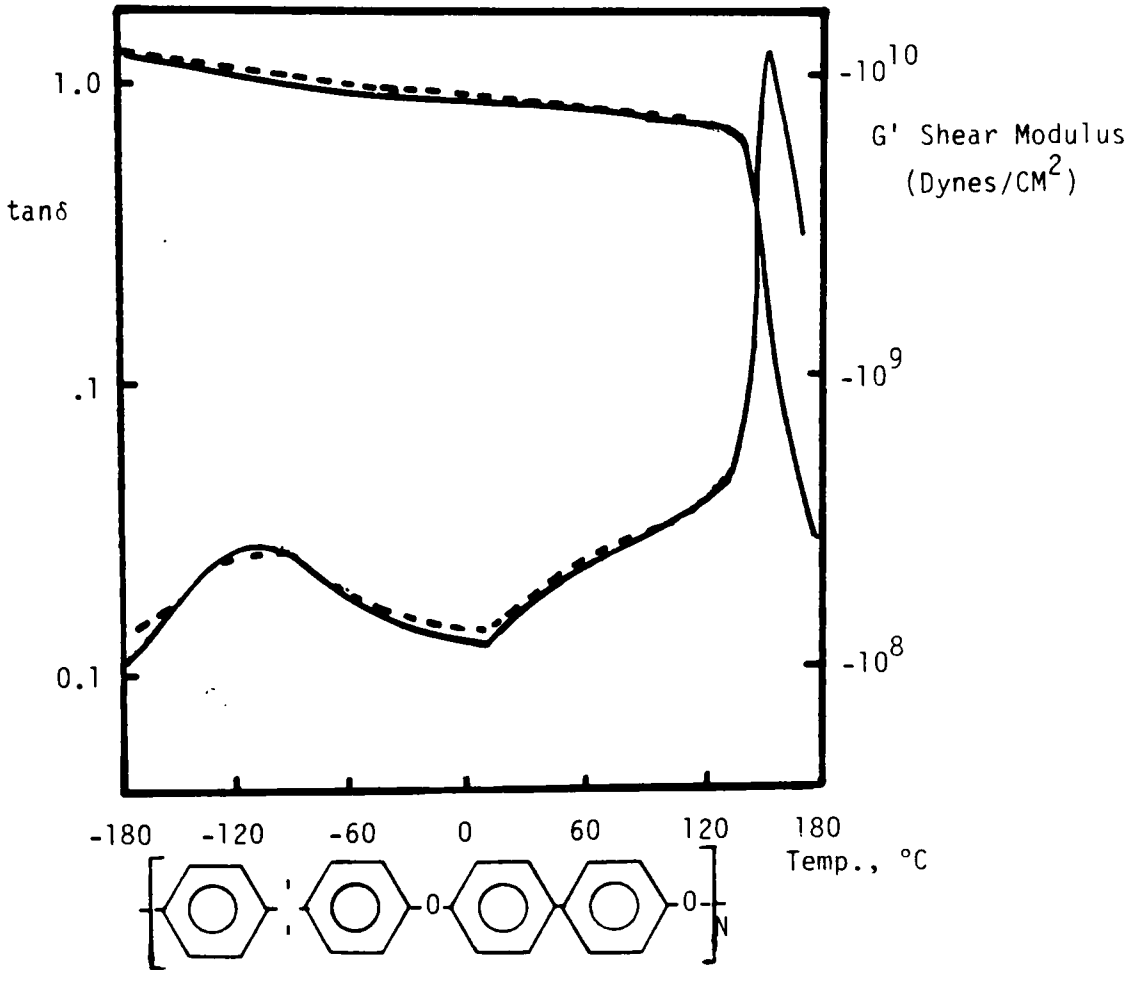

Figure 2. Shear modulus and mechanical loss versus temperature data for bisphenol A, biphenyl poly(aryl ether). (-----) dry, (———) wet. (Reference 35).

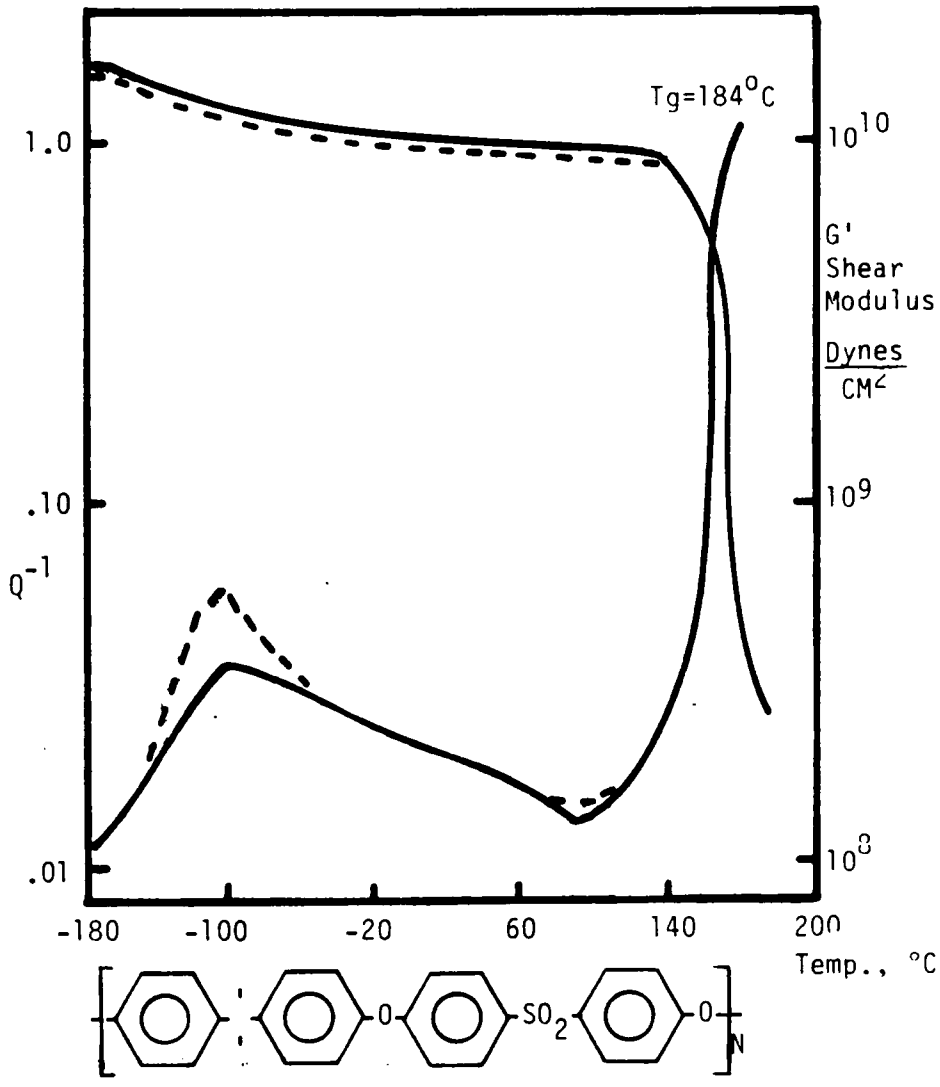

Figure 3. Shear modulus and mechanical loss versus temperature for bisphenol A based polysulfone. (———) 0% and (-----) 100% rel. humidity. (Reference 35).

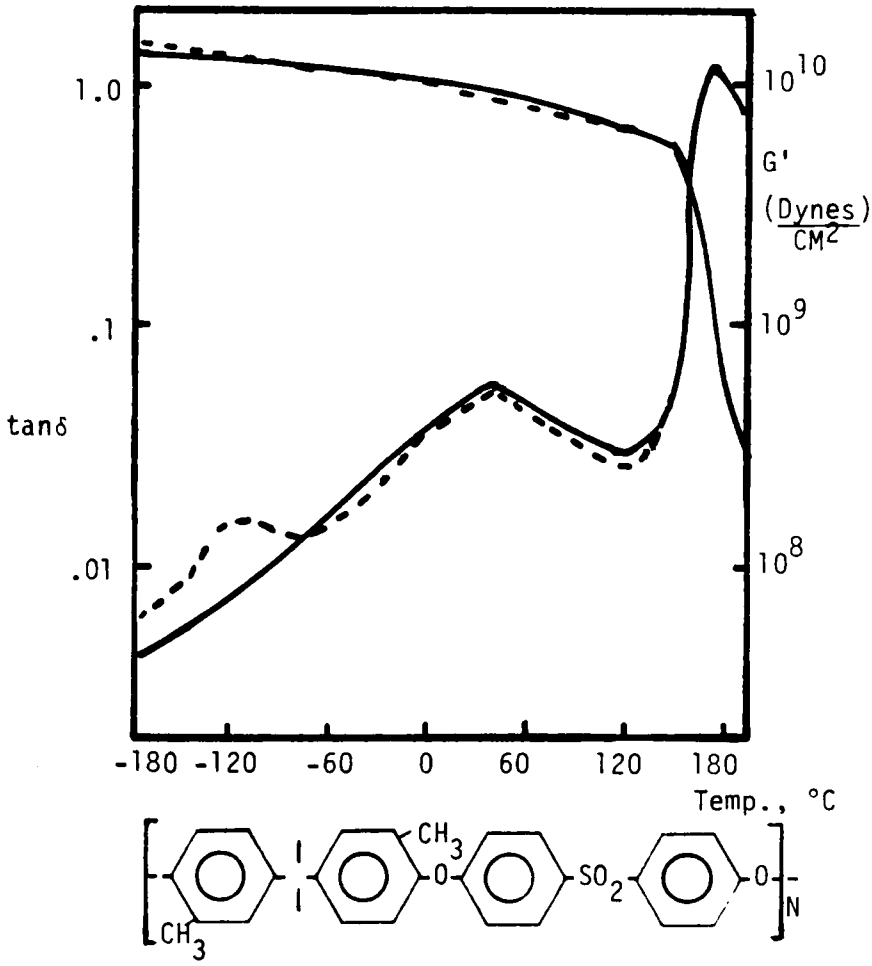

Figure 4. Shear modulus and mechanical loss versus temperature data for dimethyl bisphenol A based polysulfone. (———) dry, (-----) wet. (Reference 35).

It was concluded that the transition for the dry polysulfone is a relaxation basically due to the aryl ether group. Water sorption produces another transition due to the polar sulfone linkage being complexed with water. This transition apparently overlaps with the aryl ether relaxation.

Although the dynamic mechanical analysis provides the frequency and temperature dependence of molecular motions, the identification of the species involved is often difficult. Recently, the use of NMR has provided insight not only to the frequency of molecular motion, but also to the molecular moieties responsible for the motion. Schaefer and coworkers (43) reported a direct correlation in certain carbon 13 NMR relaxation times, which is a function of the molecular dynamics, to one measure of particular impact strength of amorphous glasses under certain selected conditions. The ratio of the cross polarization relaxation time $\langle T_{CH} \rangle$ to the spin lattice relaxation time in the rotating frame, $\langle T_{\rho e} \rangle$, gives information on the dynamic molecular components capable of dissipating energy relative to the rigid or static segments which are unable to respond to an impact. It has been suggested (43) that the ability of a polymer to handle an impact in the kilohertz range is considered crucial for toughness. Thus, a material with small value of $\langle T_{\rho e} \rangle$ could have sufficient molecular motion to dissipate an impact in the crucial range. A small value of $\langle T_{\rho e} \rangle$ produces a large value of $\langle T_{CH} \rangle / \langle T_{\rho e} \rangle$. Therefore a direct correlation may exist between the relaxation ratios and the impact strength. Figure 5 contains a plot of the ratio of the relaxation times as a function of impact strength according to Schaefer et al. (43). Polymers having high impact strength

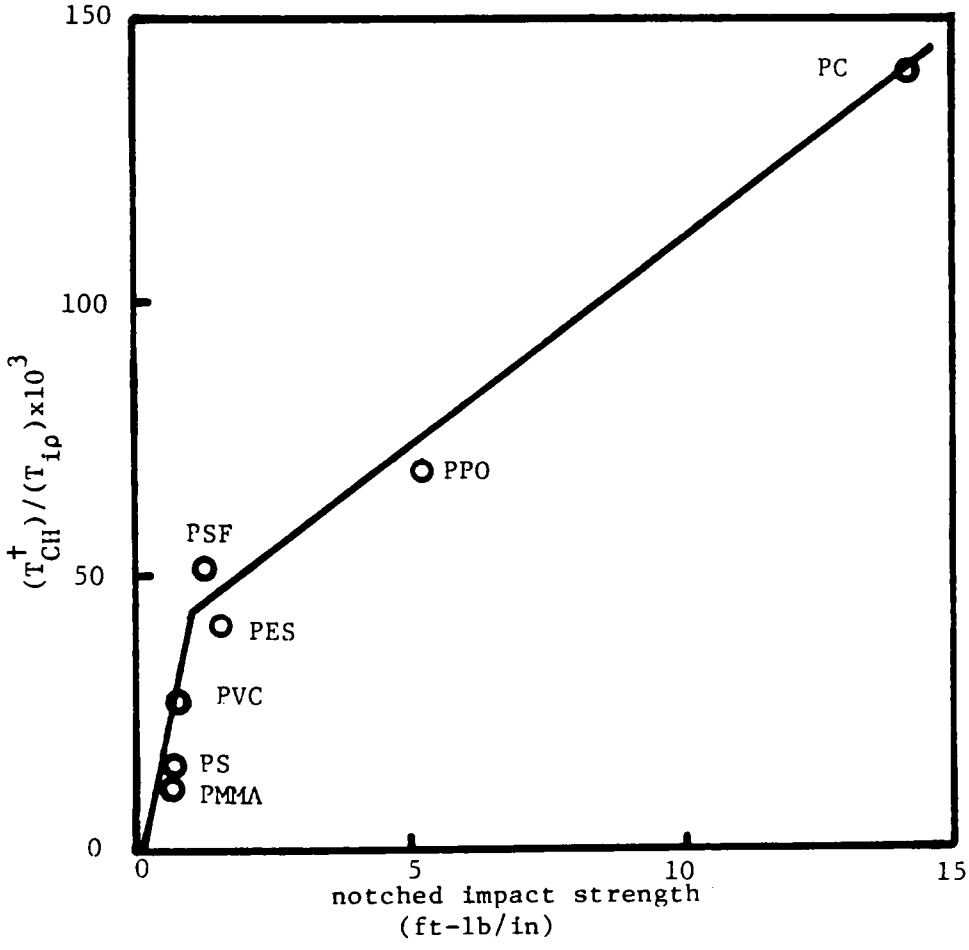

Figure 5. The correlation between notched impact strength in ft lb/(in. of notch radius), and a ratio of C NMR relaxation parameters. The abbreviations are polycarbonate, PC; poly(phenylene oxide), PPO; polysulfone, PSF; poly(ether sulfone), PES; poly(vinyl chloride), PVC, polystyrene, PS; poly(methyl methacrylate), PMMA. (Reference 43).

such as polycarbonate and polysulfone have large ratio values, while those materials having low impact properties have low ratio values.

Others have used spin lattice relaxation times to investigate solid state molecular motion in thermoplastics (44-48), thermosets (49) and crystalline polymers (50-53) in an effort to relate this molecular motion to the dynamic mechanical and bulk properties. In addition, the effects of thermal history (annealing) (44) and the addition of antiplasticizer (45) have been investigated.

Carbon-13 NMR no doubt provides insight in molecular motion in polymeric materials and the molecular moieties responsible for this motion. In addition, the spin lattice relaxation times have been correlated to the impact properties of various engineering polymers. However, recently the technique of solid state deuterium NMR has been shown to provide highly specific information about molecular motion (dynamics) and structure in polymers. Recently, H. W. Spiess (54) has published an extensive review of deuterium NMR and the various techniques developed in obtaining molecular motion information over a wide frequency range.

Deuterium NMR spectra are dominated by the electronic quadrupole interactions of the I=1 spin, which is almost exclusively from intramolecular contributions. The deuterium NMR lineshapes are extremely broad and are sensitive to motions that have characteristic frequency ranges proportional to the inverse of the quadrupolar splitting, i.e., 10^4-$10^6 sec^{-1}$ or 250 kHz (55). The range can be extended to higher frequencies by the use of deuterium NMR relaxation times (56). In addition, for those materials with extremely slow

motions, spin alignment experiments can be used to detect molecular motion in the low frequency range (57,58). Figure 6 illustrates the various correlation times available by the various deuterium NMR techniques (55).

The application of Fourier transform techniques to deuterium NMR lineshape investigations was not successful until 1976 (54). In order to circumvent the dead time of the receiver, i.e., effects due to pulse length, recovery times, magnetoacoustic ringing etc., Powles and coworkers (59) have developed a solid echo technique. This technique utilizes two 90° pulses which are separated by a time t and a 90° phase shift. Thus, in principle, the Fourier transform of the free induction decay gives the true absorption spectrum.

Jelinski and coworkers (55) have used deuterium NMR investigations to assess the molecular motions in semicrystalline poly(butylene terephthalate). By varying the quadrupole echo pulse sequence, the molecular motions associated with both the crystalline and amorphous regions have been distinguished. Furthermore, it was determined that a heterogeneous distribution of phenyl ring flips occur with an activation energy of 5.9 Kcal/mol.

Deuterium NMR has also served as a useful probe in determining the nature of the interaction of water (deuterium oxide) with epoxy networks (60). In addition, deuterium NMR has been used to investigate the effects of tacticity on molecular motion in deuterated poly(methyl methacrylates). Such information should thus be powerful in assessing molecular motion in appropriately designed polymeric materials. It has indeed been utilized in this thesis, as will be discussed later.

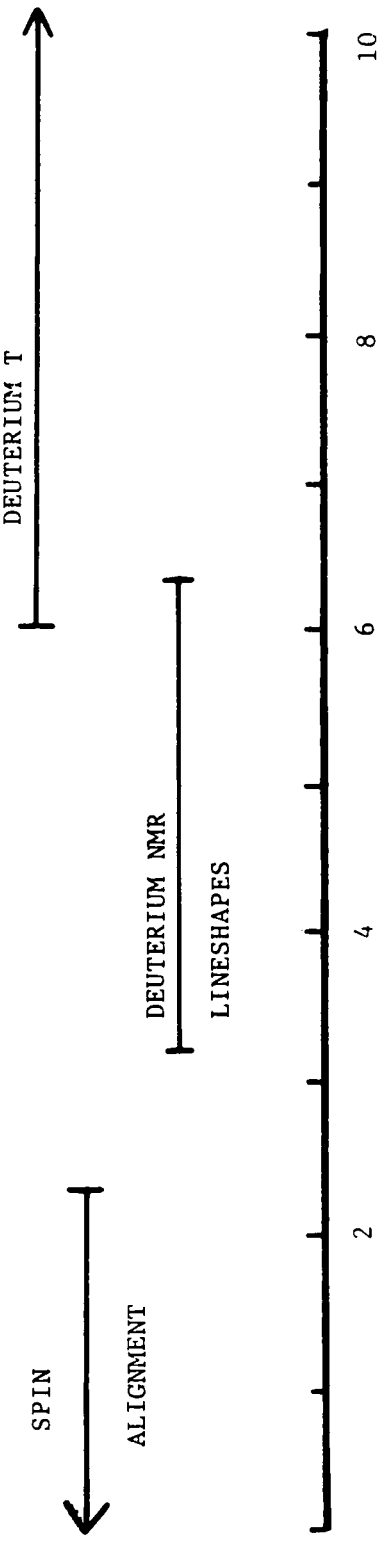

Figure 6. Schematic representation of the correlation times that are probed by using various techniques (Reference 55).

2.2.2 Impact Modification

2.2.2.1 Thermoplastic Systems

Thermoplastics such as polyesters, polycarbonate, polysulfone and others have relatively high Tg values and are considered ductile. However, they are typically susceptible to brittle failure, especially in sharply "notched" specimen. The stress concentration developed at the crack front of the precrack serves to initiate crazing or shear yielding in the local region about the crack tip. Thus, in notched specimen, the energy absorption mechanism initiated is localized and often low.

Therefore, if one wishes to further improve the fracture toughness of such high performance materials it is necessary to increase the number of energy absorption mechanisms available to the material. This is often done by the incorporation of a second dispersed phase. In principle, rubber particles, voids or even hard inclusions can serve as the second phase and initiate crazing or shear deformations. A classic example is high impact modified polystyrene (HIPS), where styrene is polymerized (and partially grafted) in the presence of polybutadiene. Polybutadiene has a lower solubility parameter than the polystyrene phase and thus separates as discrete pure rubber or "composite" particles. During the polymerization some of the polystyrene is grafted on to the unsaturated sites in the polybutadiene. This is beneficial because it serves to compatibilize (stabilize the interface) the particle with the polystyrene matrix. Thus, the particle achieves good interfacial adhesion which is considered crucial in impact modification. The type (61-65), size (66) and distribution (67) of particles are several of the important variables in impact modification. The early

theories on the role of the rubber particle stems back to the late fifties where Merz et al. (68) and others (69,70) proposed that the rubber bridged the crack as it propagated and which resulted in an increase in fracture toughness. However, later it was realized that deformation mechanisms within the matrix, which were enhanced by the dispersed phase led to the increase in impact strength.

Goodier (71) derived equations for the stress field of a rubber particle within a isotropic matrix. The rubber particle having a different modulus than the matrix serves as a stress concentrator. This stress was shown to be that of triaxial tension. Furthermore, this concentration was found to be greatest at the equator of the particle. If the volume fraction of rubber is sufficiently high, the stress fields of the particles can interact, leading to larger stresses.

The triaxial tension promoted by the rubber particles is now believed to initiate the energy absorption processes available to a material. However, whether crazing or shear deformations occur depend on structural features of the polymer. For instance, it is well known that polystyrene and poly(methyl methacrylate) craze, whereas materials such as polycarbonate and poly(phenylene oxide) yield by shear deformations. In general, the mechanism which is dominate in a toughened system is usually the same mechanism operative in the unmodified matrix. However, the size of the modifying particle dictates to a large extent which energy absorption mechanism will be initiated. Thus, prior to impact modification it is best to understand the energy absorption mechanisms available to a material then design a second dispersed phase of the appropriate size. Donald and Kramer (66) have

found that smaller rubber particles (approximately 0.1 μm) were capable of initiating shear deformations promoted by rubber particle cavitation. However, in the same material modified with larger particles (about 1.5 μm in diameter), the elastomer successfully initiated crazes. For instance, the optimum particle size in HIPS is 2-5 μm (61,70,72) and current wisdom suggests that these relatively large rubber particles are required not only to initiate crazes but terminate them as well. Buchnall (73-75) suggests that crazes are initiated at the equator of the particles perpendicular to the applied load. In addition, the rubber particle also terminates the craze, preventing premature crack initiation and growth. Kramer and coworkers (66), among others, have reported that the optimum morphology for the rubber particles in HIPS consists of: a large number of polystyrene occlusions within the polybutadiene dispressed phase. It was found that this morphology served to stabilize the craze and prevent craze breakdown. Kambour (76) also suggested that the rubber particle spanned and stabilized the craze, thus preventing craze breakdown and failure.

Another interesting example of an impact modified system is a blend of HIPS and PPO as mentioned earlier. It is well-known that PS and PPO (Noryl) are completely miscible in all combinations. Thus, a 50/50 blend of HIPS and PPO serves to impact and modify the "Noryl" blend. In this case, the polystyrene-polybutadiene rubber-like graft phase separates out of the miscible matrix blends . PS and PPO each have different energy absorption mechanisms (i.e., crazing and shear yielding, respectively). Thus, the fracture mechanisms in this situation are fairly complex and controversial. Bucknall (74,77)

observed shear bands intersecting crazes at 45° angles which suggested that the shear bands act as craze terminators. Kambour (78) supports this argument, however, Kramer and coworkers (66,79) did not.

The exact nature of how the second discrete phase functions and the optimum morphology of the particle is still a fairly controversial area. However, it is commonly believed that the second discrete phase serves to initiate the energy absorption mechanism available to these amorphous thermoplastics and the size of the particle can influence the efficiency of this initiation.

2.2.2.2 Thermoset Networks

Epoxy resins are one of the most important classes of thermosetting polymers. These networks have many desirable properties including high tensile strength and modulus, excellent chemical and corrosion resistance and good dimensional stability (80-83). Consequently, these materials are widely used for many important applications such as coatings, structural adhesives, reinforced plastics and matrix resins for advanced composite materials (83-85). Unfortunately, these highly crosslinked systems have limited molecular motion and are inherently rather brittle. Consequently have limited utility in applications requiring high impact fracture strength, and even thermal cycle resistance.

In recent years, the incorporation of elastomeric modifiers has served as a successful means of enhancing the fracture strength of brittle materials, as discussed earlier. The rubber particles act as stress concentrating sites, thus initiating energy absorbing processes

such as crazing and shear band formation in these thermosets allowing a tougher material to be obtained (34,86-89).

Recently, this technology has been applied to epoxy resins where low molecular weight liquid butadiene acrylonitrile copolymers having either carboxyl (CTBN) and amine (ATBN) end groups have been utilized (80-83). Other elastomeric modifiers that have been studied include acrylate elastomers (85), poly(oxypropylene amines) (86) and polysiloxane copolymers containing not only dimethyl groups but also trifluoropropyl and diphenyl groups (82,84). By copolymerizing the more polar trifluoropropylmethylsiloxane or diphenylsiloxane unit with the polydimethylsiloxane, the solubility parameter of the oligomers could be increased so that they were closer to that of the uncured epoxy resin. This is desirable, so that one has a homogeneous resin/modifier mixture for the system to be used. During the curing process, the elastomeric component separates within the reaction medium to form a second dispersed phase.

As expected, the $K_{I,C}$, fracture toughness values of the rubber modified epoxy networks are considerably higher in some cases than those for the unmodified materials. These $K_{I,C}$ values are also strongly dependent on the testing rate, (34), temperature (84), crosslink density (90), volume fraction of rubber (91) and the type and structure of the curing agent (93). The mechanism of energy dissipation for the epoxy networks is probably different than that for polystyrene or the engineering thermoplastics. Kramer (93) has studied the fracture mechanisms of polystyrene of various molecular weights. At molecular weights above 30,000 (the critical molecular weight for entanglements),

crazing was observed in the fractured samples. This feature significantly improved the fracture toughness and a plot of fracture toughness versus molecular weight was similar to the well known zero shear rate viscosities versus molecular weight plots discussed by polymer rheologists. However, crazing was not important in fractured specimens made from lower molecular weight polymers where only local shear deformation was observed. The ramifications of this investigation may be very important in understanding polymer fracture. That is, highly crosslinked epoxy networks do not craze (93) and the only energy absorbing mechanism observed is what is termed microshear banding.

Various theories have been proposed to explain the toughening effect of the rubbery particles on these highly crosslinked structures. Douglass (70) proposed that the rubber particle bridges the crack before stretching and tearing the rubber until failure. Others have observed microcracking (94), crazing (95) and local shear yielding (69) which is thought to be induced by the stress concentrating particles. Today, the mostly accepted theory involves the basic deformation processes and their interaction (34,88,89). The first process involves a dilatation or void formation at the particle or its interface produced by triaxial stress ahead of the crack tip along with the stresses at the particles. The second process involves initiation of local shear deformations at the equator of the particles where the stresses are the greatest. The latter process is primarily responsible for the toughening of the resin networks.

The improvement in fracture toughness by the addition of the rubber modifier is at the expense of some bulk properties. This is not

surprising because the modulus of the modifier is much lower than the matrix.

In principle, the use of hard or rigid particles may initiate the energy absorption mechanisms available to an amorphous thermoplastics or thermosets. Modification with rigid materials could thus produce a better balance of properties (i.e., toughness and stiffness). However, there are many problems associated in modifying materials with rigid particles.

Bucknall (73) has investigated whether glass particles could impact modify polystyrene. Unfortunately, the fracture strength of these modified materials decreased. It was suggested that the poor interfacial adhesion between the particle and the matrix as well as the brittle material of the inorganic glass contributed to the decrease in impact strength. Similar effects have also been observed in both epoxy (96-101) and polyester (102) resins. The observation that rigid particles are not as effective as rubber "fillers" in increasing toughness may also be associated with the inability of a rigid particle to span and stabilize a craze. Furthermore, inadequate bonding or interfacial adhesion may limit the efficiency of a rigid particle to serve as a craze terminator.

Several investigations (99,103) have shown that rigid particle filled epoxy resin can produce an improvement in fracture toughness. However, this improvement is highly dependent on the particle size of the modifier. For instance, Lange and Radford (99,103) used aluminum trihydrate to modify epoxy networks and found an enhancement in toughness, which depended on volume fraction and particle size. They

proposed that the main energy absorption mechanism involved "crack pinning" as schematically shown in Figure 7 (90). As the crack approaches a layer of rigid particles, the crack front is pinned providing sufficient adhesion between the particle and the matrix. The crack is then bowed, creating new surface area before breaking away. Typically, one sees striations on the fracture surface where the pinning had occurred.

Recently, another approach has been taken to modify epoxides using rigid particles which produces a better balance of properties than rubbers. Blending with tough, ductile engineering thermoplastics has been studied. Buchnall (104) and others (105) have used ICI's polyethersulfone; Diament and coworkers (106) have used General Electric's polyetherimide (Ultem). These workers report improvement in fracture toughness provided that a phase separation with good interfacial adhesion is achieved. Bucknall reported that the addition of the polyethersulfone into the epoxy did not significantly improve the fracture toughness. Polyethersulfone is a fairly polar material and has a higher solubility parameter than the epoxy network, therefore the solubility parameter difference may promote the phase separation but it also limits the interfacial adhesion and consequently the fracture toughness.

2.2.3 Fraction Mechanics

2.2.3.1 Development of Fracture Mechanics

The first quantitative developments in fracture mechanics concepts were introduced by Griffith (107,108) in 1920. The hypothesis behind the Griffith concept is that crack propagation will occur when stored

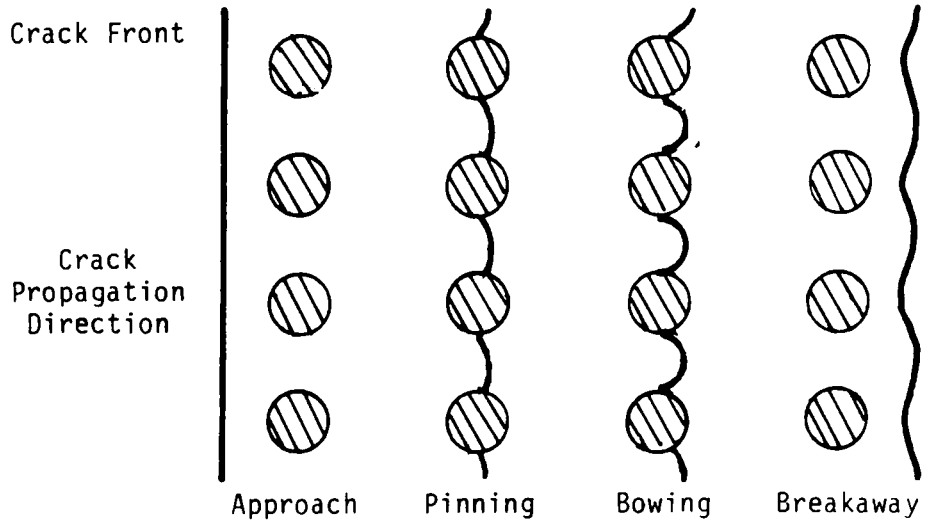

Figure 7. General schematic of crack front approaching and interacting with rigid particles (crack pinning). (Reference 90).

elastic energy reaches a critical value that is equal to the energy required to create new surfaces by the fracture process. Griffith used a stress analysis developed by Inglis (109) for an elliptical plate to derive the strain energy contribution for the initiation of fracture given below. The left hand side of Equation 1 represents the driving

$$\frac{\sigma_c 2\pi a}{E} = 2\delta \qquad (1)$$

δ = surface energy; E = modulus; a = length of flaw;
σ = stress applied to material

force for crack propagation and the right hand side represents the material's resistance to fracture. The rearrangement of Equation 1 leads to the critical stress for fracture. These observations and

$$\sigma_c = \frac{2\delta E}{\pi a} \qquad (2)$$

concepts were primarily developed for brittle materials, i.e., glass.

In the 1950's the Griffith theory was modified and generalized by Irwin (110,111) and Orowan (112) to include other sources of resistance to fracture in addition to surface energy effects. Orowan (112) believed that the fracture stress predicted by the Griffith expression was underestimated for materials other than glass. Orowan (112) proposed that the plastic deformation in the region adjacent to the crack tip where the stresses exceeded the yield strength contributed to the fracture toughness of a material. Orowan (112) suggested that the appropriate form for Equation 2 was:

$$\sigma_c = \frac{2E(\nu+P)}{\pi a} \qquad (3)$$

where P is a plastic work term and ν is the poisson ratio.

Irwin (110,111) extended the Griffith concepts by hypothesizing that fracture will occur when the crack driving force or strain energy release rate, G, reaches a critical value, G_c. G expresses the amount of stored energy that would be released if the crack were to extend and create new surface area. To illustrate this concept, imagine a cracked body of uniform thickness, t, subjected to a load, P, as shown in Figure 8. The linear load-deflection curve is also shown in Figure 8, and the stored energy is given by the area under the curve. If the crack, a, extends by an increment Δa, the effect load on the specimen will drop by an amount ΔP. If the body is now loaded to its new crack length, $a + \Delta a$, the elastic energy will have decreased as shown in Figure 9. Thus, the strain energy release rate or more commonly fracture energy is the change in stored elastic energy per unit area as shown in Equation 4, or in terms of the compliance, C, of the sample as shown in Equation 5.

$$G = \frac{dV}{dA} \tag{4}$$

$$G = \frac{P^2}{2t}\frac{dC}{da} \tag{6}$$

2.2.3.2 Stress Intensity Factor

Fracture mechanics attempts to establish a parameter to characterize the failure of a cracked body under a load. In linear elastic fracture mechanics, the stress intensity factor, K_I, is such a parameter and is sufficient to relate the elastic stress-strain intensification in the vicinity of the crack tip to the load and sample

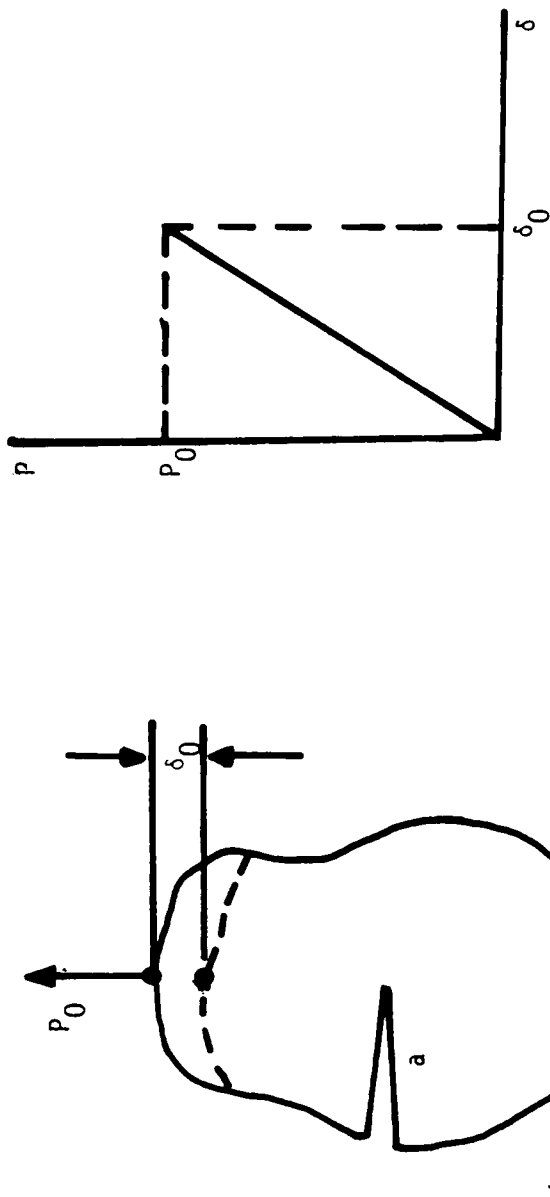

Figure 8. A notched body loaded in a linear elastic fashion. (Reference[13]).

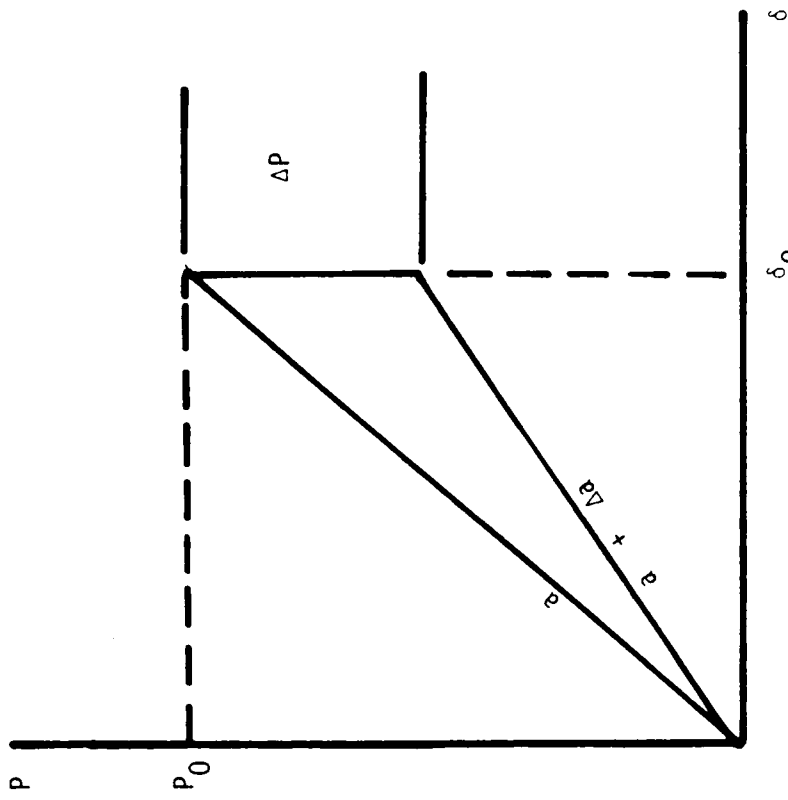

Figure 9. Linear load versus deflection cure for a crack extended a and an increment a + Δa. (Reference 113).

catastrophic crack growth provided sufficient constraint to plastic geometry (114,115). Plane strain fracture toughness, $K_{I,C}$, is a material property which is measured in terms of K_I and is the critical value of K_I which characterizes the susceptibility to unstable or deformation or brittle failure occurs.

The concept of mechanical constraint is crucial in the understanding of fracture mechanics and obtaining valid $K_{I,C}$ values. In order to simplify the models of predicting failure, the state of stress and strain must be expressed, i.e., as plane stress or plane strain. In plane stress the stresses in the thickness direction are assumed to be equal and usually zero and this is typically representative of a thin specimen. Samples which fracture in this manner typically show plastic deformation. However, for samples which are considered to be thick, the assumption of plane strain is appropriate. If the load is applied in the plane of the body, then the strain is assumed to be zero and this defines the condition of plane strain. In such cases, constraint to plastic is achieved and the sample fails by brittle mechanisms. The state of stress and strain in a loaded body is also sensitive to the notch or pre-crack and the thickness.

In order to achieve plane strain fracture, an infinitely sharp crack must be introduced to the sample. Consider a notched sample loaded with a tensile stress σy as shown in Figure 10. This stress causes the element bordering the crack tip to contract in the X direction and to assume the shaded area. A similar element further from the crack front will contract as well as creating a stress, σx, between the elements. In addition, a stress normal to the plane, σz, limits the

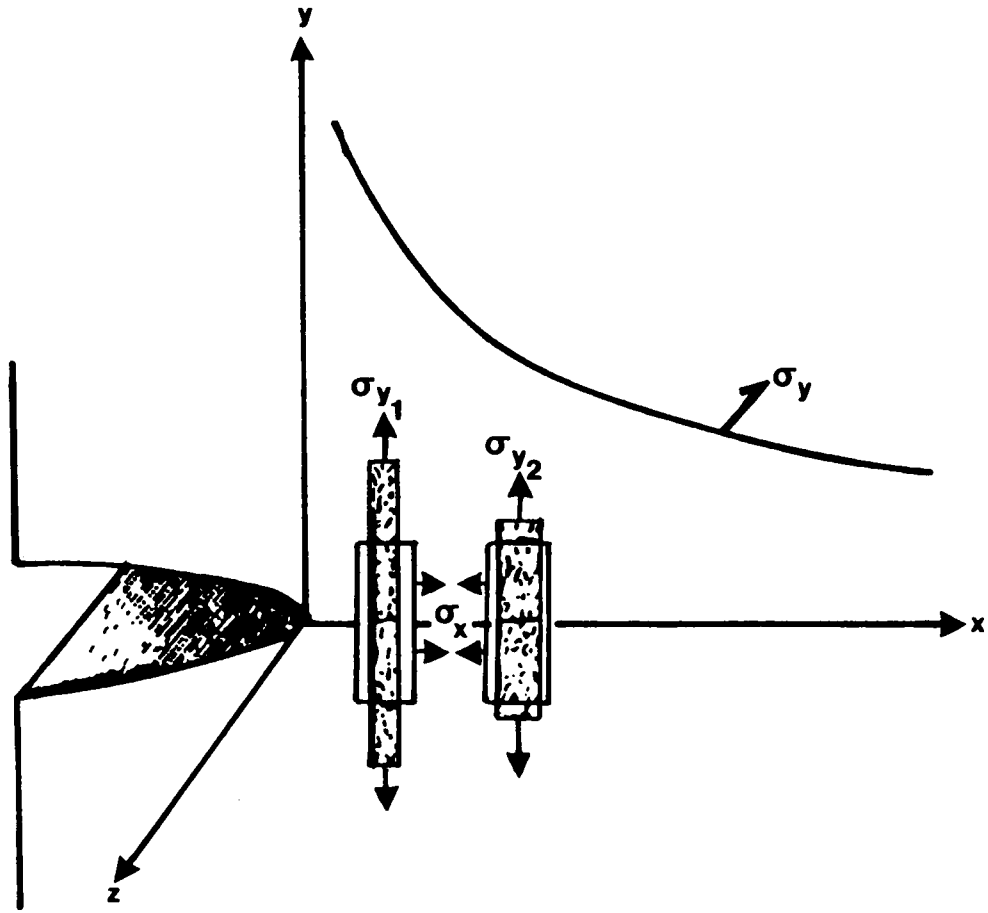

Figure 10 Stress in the x- and z-directions result from nonuniform elongation of the elements in the direction of applies stress (the y-direction). This triaxial stress distribution inhibits plastic flow and produces mechanical constraint. (Reference 119).

contraction in that direction. The triaxial stress distribution which is created limits plastic deformation and subsequently provides mechanical constraint (115). This stress field is dependent on notch depth and section thickness. Typically, as the requirement for mechanical constraint is satisfied and plastic deformations are precluded, the fracture toughness is generally lower.

In addition to producing a triaxial stress field at the crack front, the sample thickness must be sufficient to achieve plane strain fracture conditions. For instance, Ting (116) studied the effects of sample thickness on three commercial polysulfones; Victrex^{R}, Radel^{R} and Udel^{R}. Figure 11 contains the fracture energy, $G_{I,C}$, of these materials as a function of sample thickness. At thin sample thicknesses the sample does not have sufficient constraint and plane stress fracture conditions are prevalent. In this case, plastic deformation mechanism tend to overestimate the fracture toughness of the material (114,116). As the sample thickness increases a mixed mode failure or transition region is observed and the fracture energy decreases. When the fracture energy reaches a value where it is no longer a function of sample thickness, plane strain fracture conditions are satisfied.

There are many test specimen shapes possible which can facilitate these measurements. Essentially, each geometry requires its own stress analysis. There are a number of criteria for choosing the appropriate test specimens, which would certainly include those listed below:

(1) Load capacity of experimental set up;

(2) Accuracy desired in the experiment;

(3) The valid range of K_I;

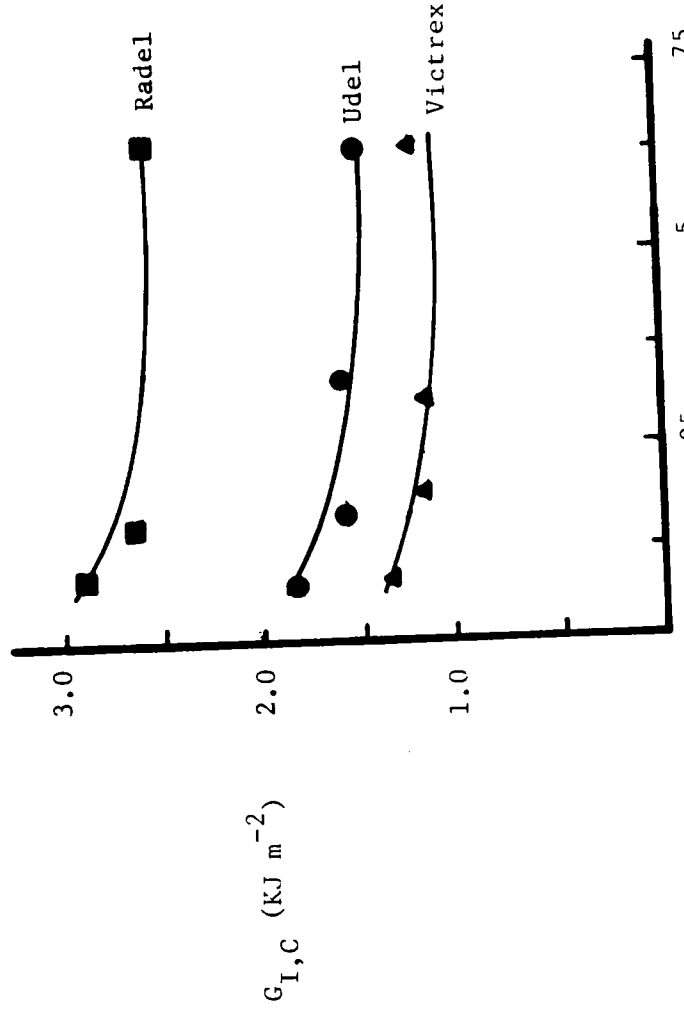

Figure 11. Dependence of specimen thickness on the fracture energies of sulfone polymers. (Reference 116)

(4) Thickness of material;

(5) Toughness of material;

(6) Amount of material;

(7) Ease of precracking;

The most common test specimens are shown in Figure 12. The stress intensity fracture for each of these samples is known (113). Of those shown, the compact tension (CT) and three point bend (3PB) are the most common. In addition, these specimens require the least amount of material and are the easiest to precrack. The center-cracked (CC), single edge cracked (SEC) and double edge cracked (DEC) require the most material and the greatest loads. Furthermore, these specimens are difficult to prenotch. In addition, some of these geometries require two precracks.

The sample geometry chosen for most of our testing was 3PB specimen. In this case, the critical stress intensity factory for catastrophic failure, $K_{I,C}$, is given in the following equation (40):

$$K_{I,C} = \frac{3P_C L}{BW^{3/2}} Y \quad \text{(three point bend sample geometry)} \tag{6}$$

where:

P_C = the critical load for unstable crack growth

L = length

B = thickness

W = width

Y = geometry factor given by

$$Y = [1.93\ (a/w)^{1/2} - 3.07\ (a/w)^{3/2} + 14.53\ (a/w)^{5/2} - 25.11\ (a/w)^{7/2} + 25.80\ (a/w)^{9/2}]$$

a = crack length

a. CENTER CRACKED PLATE (CC)

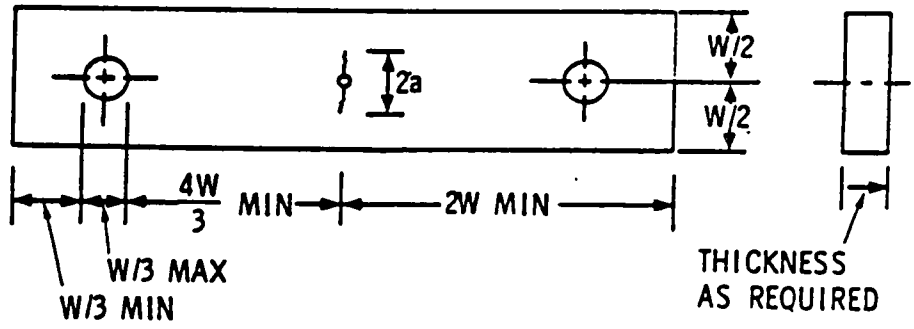

b. DOUBLE EDGE CRACKED PLATE (DEC)

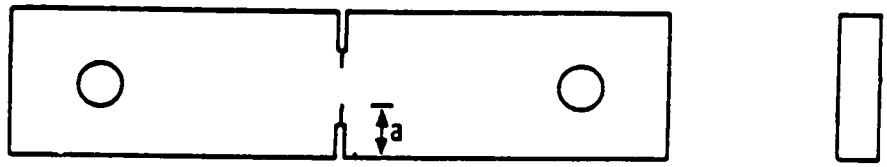

DIMENSIONS AS PER CC SPECIMEN

c. SINGLE EDGE CRACKED PLATE (SEC)

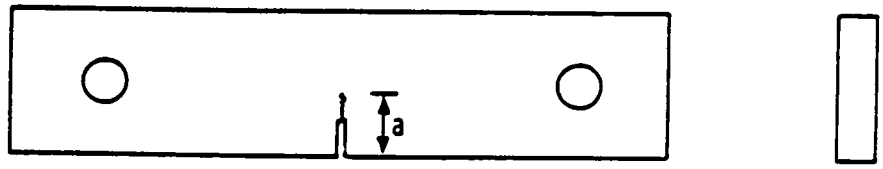

DIMENSIONS AS PER CC SPECIMEN

Figure 12. Common plane strain fracture toughness test specimens. (Reference 113).

d. THREE POINT BEND (3PB)

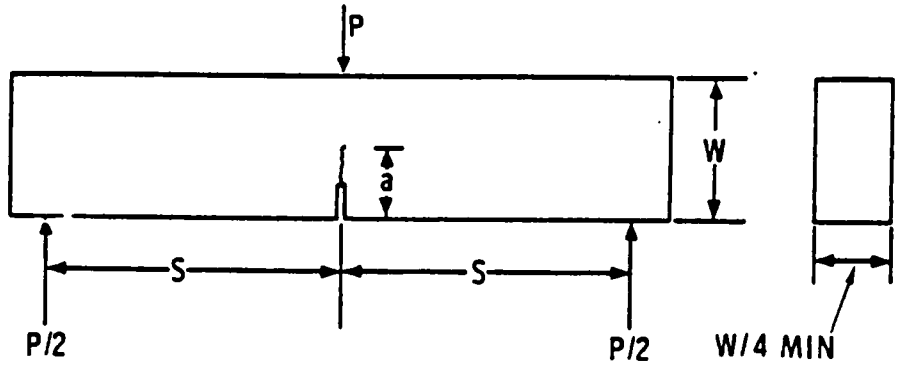

e. COMPACT TENSION (CT)

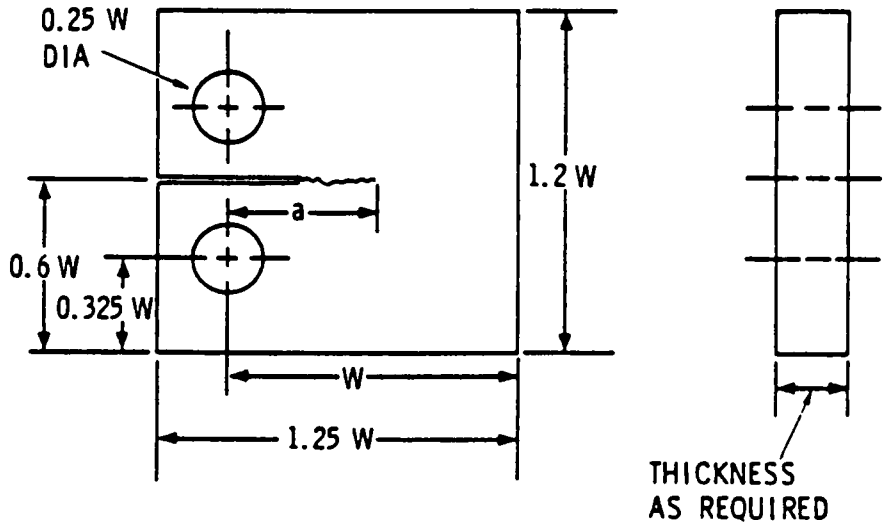

Figure 12. (Continued).

f. WEDGE OPENING LOADED, T TYPE (WOL-T)

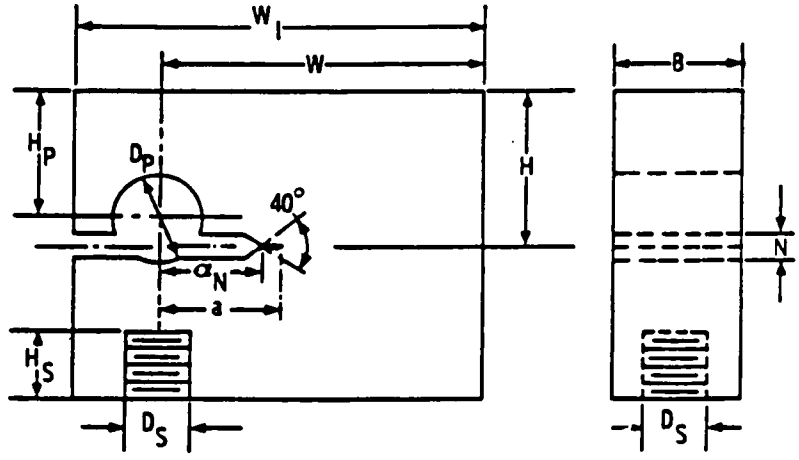

GEOMETRY RATIOS:

B	= 1.00		
W	= 2.55		
W_1	= 3.20		
H_S	= 0.625	$\frac{H}{W}$	= 0.486
D_S	= 0.625 MAX.		
H_P	= 1.00		
D_P	= 0.70 MAX.		
α_N	= 0.77		
N	= 0.094		

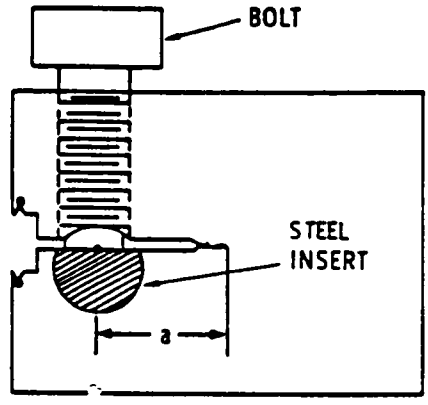

BOLT LOADED
MODIFICATION
OF WOL-T

Figure 12. (Continued).

g. CANTILEVER BEAM (CB)

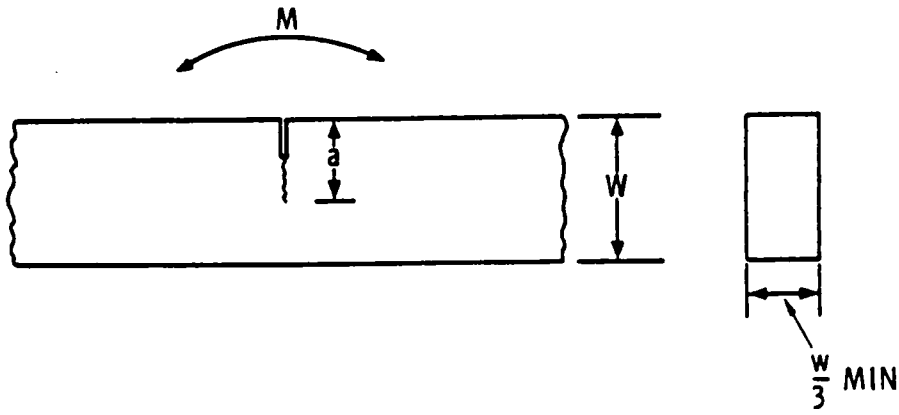

h. DOUBLE CANTILEVER BEAM (DCB)

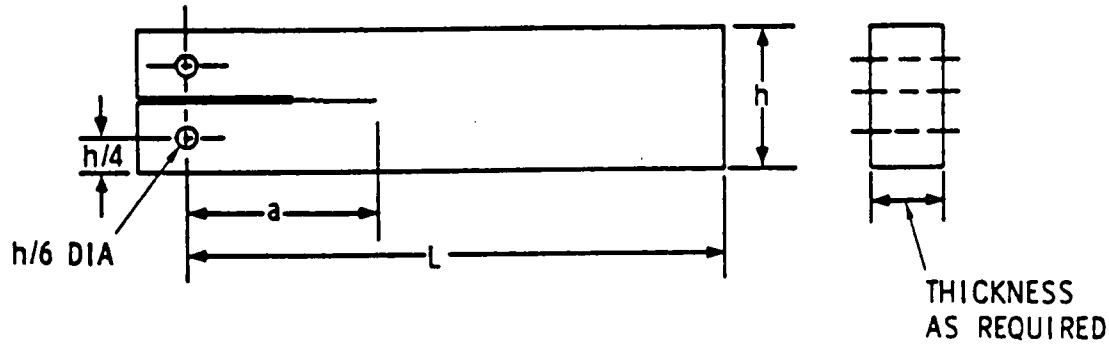

L > 4h

Figure 12. (Continued).

The fracture toughness is proportional to the critical load for unstable crack growth P_C. In addition, the geometry of the specimen is accounted for. Figure 13 contains the Y versus a/w plot for each of the sample geometries. The 3PB specimen has a much higher Y gradient with crack length than the other sample geometries. Therefore, K_I will change as crack extension occurs (i.e., K_I is very sensitive to changes in crack length). However, this is only detrimental when fatigue measurements are made where continuous and accurate measurements of the crack length are required.

However, when one is limited by sample dimensions and working with a tough material, linear elastic fracture mechanics is not always applicable. In such cases where sufficient constraint is not provided and plastic deformation is evident, the J-integral analysis developed by Rice (117-119) is applicable. The J-integral analysis yields a $J_{I,C}$ value which is a critical value for the onset of stable crack growth for a sample which fails in plane stress. In these specimens, the stresses typically exceed the yield stress. This in turn complicates the nature of the crack tip and one must account for this "blunting" or plasticity at the crack front.

Figure 14 gives an illustration of the sequence of events during loading (117-119). A sharp crack is introduced into the sample, a, and upon loading crack extension first takes on the form of plastic flow and blunting, Δa, until conditions for tearing develop, da. The value da proceeds approximately linearly with the value of dJ. Now we must focus our attention on the value of J which is proportional to the area under the load versus displacement curve as illustrated in Figure 15. It is

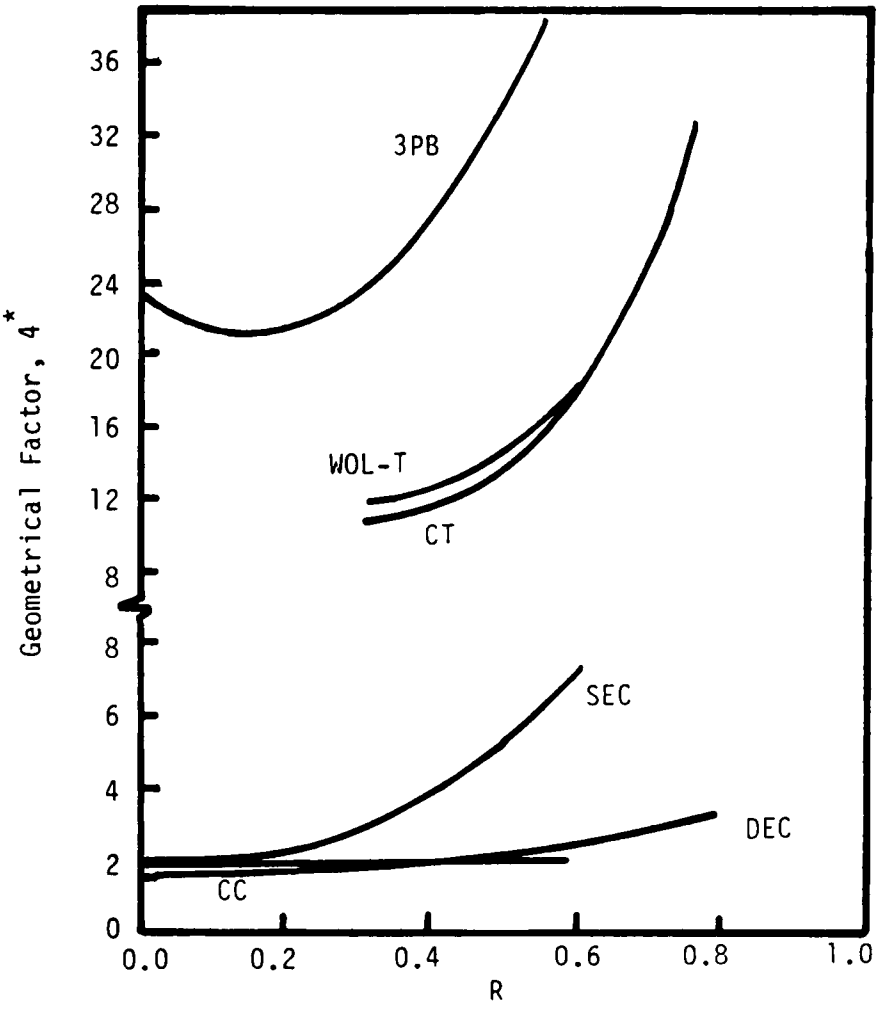

Figure 13. Finite geometry correction factors for selected specimens in Figure . R = 2a/w for CC and DEC, R = a/w for others. Y* = 12Y for 3PB, Y = Y for others. (Reference 113).

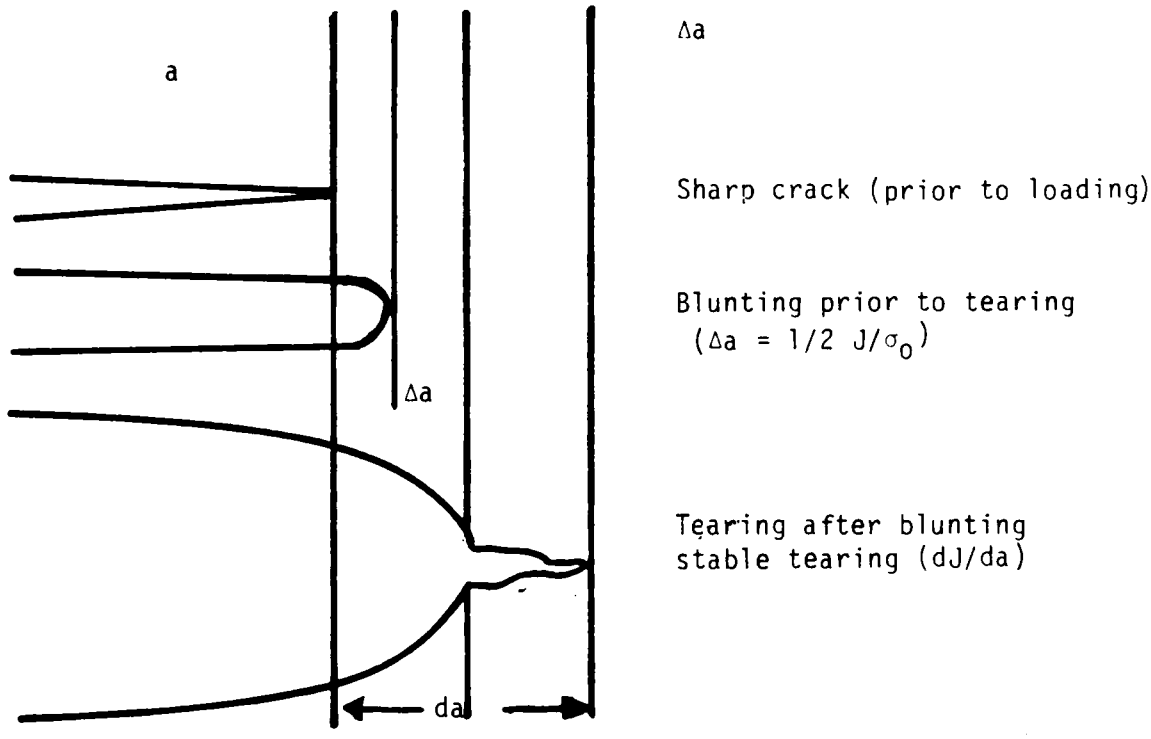

Figure 14. Sequence of events which occur during the loading of a body which fails in plane stress. (Reference 43-45).

important to notice the deviation from linearity in this plot i.e., plastic deformation. The J value is given by the following equation:

$$J = \frac{2(Area)}{Bb} \tag{7}$$

where B and b is the width and thickness, respectively. Knowing that J varies linearly with crack extension, this plot (Figure 16) gives the J-integral curve which represents the energy required for stable crack growth. However, the blunting of the crack front prior to extension tends to overestimate the fracture toughness and must be corrected. This is typically done by the use of a blunting line given by Equation 8. It follows that the blunting is proportional to the yield stress

$$J = 2\sigma_y \Delta a \tag{8}$$

of the material. The blunting line is shown in Figure 16. The intersection of the J-integral and blunting lines yields the fracture toughness $J_{I,C}$: The critical energy required to initiate the onset of stable crack growth.

There are only limited reports in the literature (120) on this technique for assessing the toughness of polymeric materials. Generally, the sample dimensions may be increased to provide constraint to plastic deformation and linear elastic fracture mechanics may be used. The difficulty in obtaining $J_{I,C}$ arises from the measurement of da. Metallic materials may be stained or heat treated and oxidized to distinguish the crack extension. However, in macromolecules this may cause environmental stress cracking or relaxation, respectively. Williams et al. (46) have used crack opening displacement gauges to determine crack extension in polymeric materials.

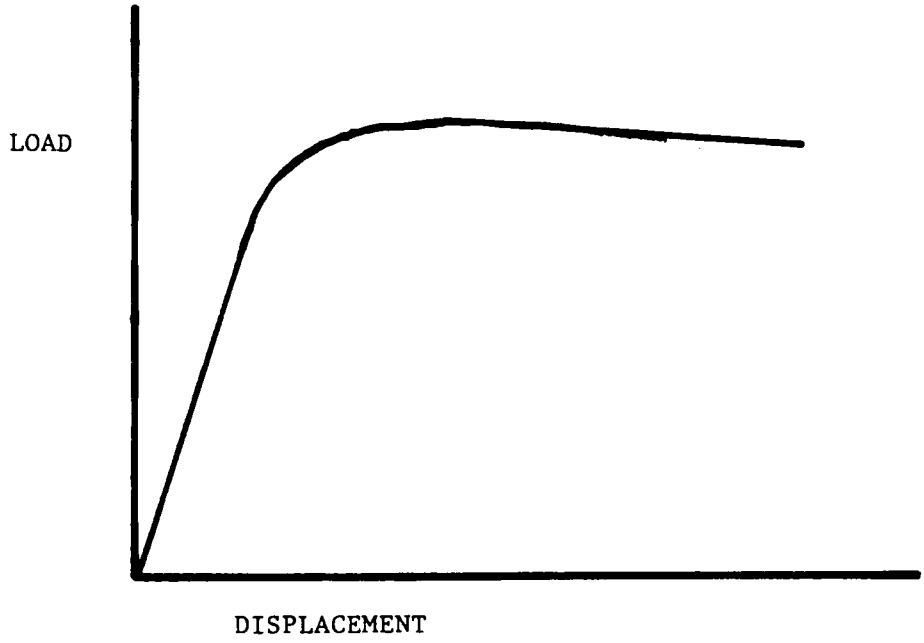

Figure 15. Load versus displacement plot for a material which fails in plane stress.

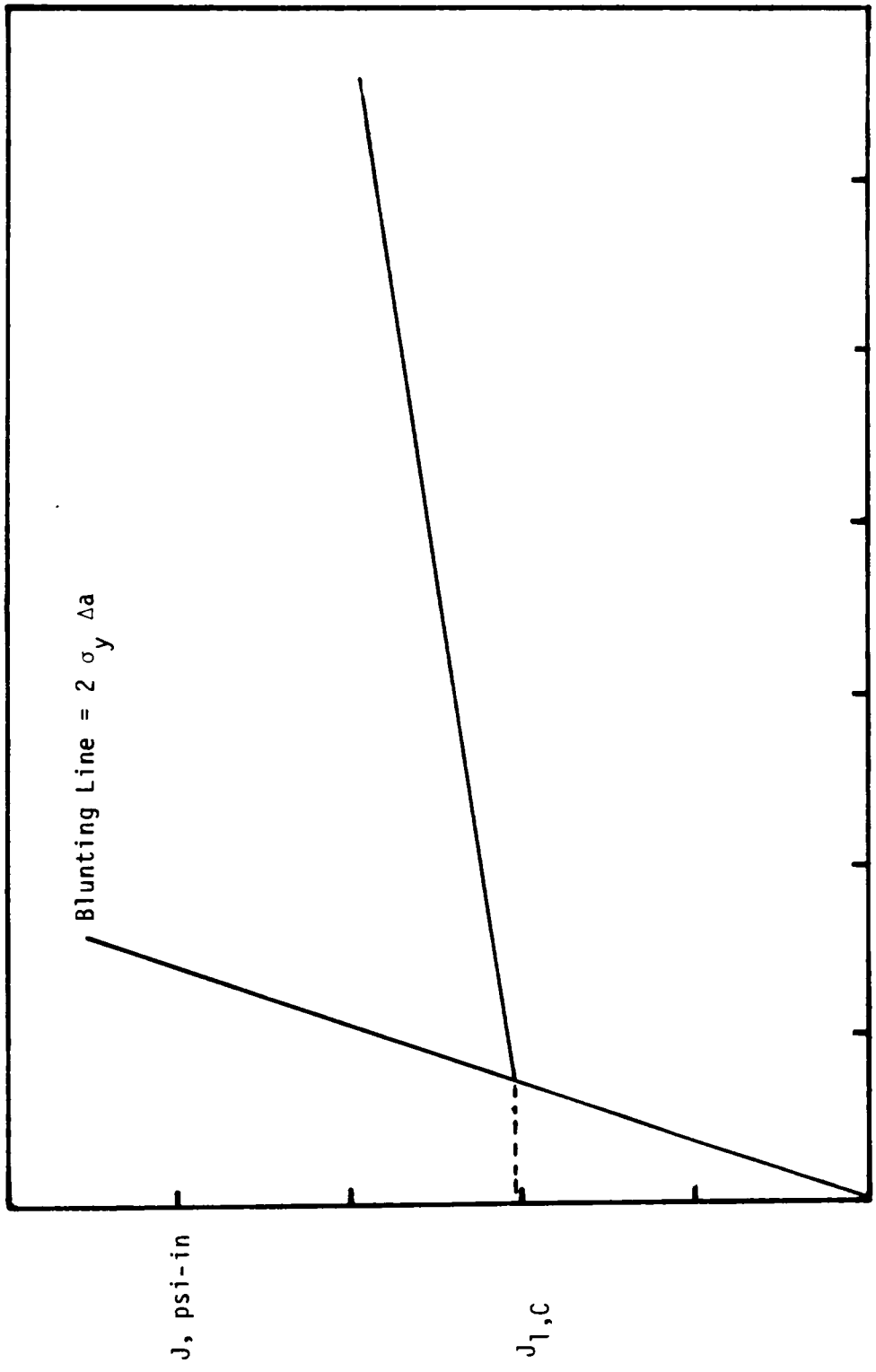

Figure 16. Plot of $J_{I,C}$ versus crack extension for a material which fails in plane stress

2.2.3.3 Crack Tip Deformations

The introduction of a notch into a body produces a stress concentration in the general vicinity of the crack front. In principle, the stresses at this point should be infinite. However, the infinite stress concentration at the crack tip is seldom achieved because the yield stress, σ_y, of most materials is exceeded (114). Consequently, a region at the crack tip is plastically deformed. Figure 17 contains a general schematic of the stresses as a function of distance from the crack front. The yielded region, r_y, around the crack tip is obtained at the intersection of the actual stress at the crack front and the yield stress of the material. It follows that the effective crack tip lies at the center of a small plastic zone, and no doubt this crack tip blunting will effect the fracture toughness of the material.

There are several models accounting for the size and shape of the plasticity effects at crack tips. The two most noted models are those of Irwin (110,111,114) and Dugdale (121). Dugdale predicts a yielding zone, C, extending ahead of the crack tip with a narrow elongated shape as shown in Figure 18.

In contrast, Irwin predicts that the effective crack tip lies in the center of a circular plastic zone with radius r_y also shown in Figure 18. Neither of these models have been reported (113) to be based on totally realistic stress analysis, therefore, they should only be used as estimates. However, it is interesting to note that in each case the size of the plastic zone is considered to be inversely proportional to the yield stress (see Figure 18) of the material. Therefore, it

appears difficult to compare polymers with different material properties such as an epoxy network and an engineering thermoplastic.

Unlike metallic materials which have the ability to nucleate dislocations and other forms of energy absorption, polymers, particularly glassy and semicrystalline materials, craze under an applied load. Crazes are oriented material formed perpendicular to an applied load and is often a precursor to brittle failure. Crazes are usually formed at the crack tip of most of these materials and blunt the crack front, thus overestimating the fracture toughness.

Craze zones have been observed and measured in a variety of engineering thermoplastics including polysulfone (122,123), polycarbonate (123-126) and poly(methyl methacrylate) (127). The measurement of these plastic or crazed zones is typically performed by optical interference techniques. Recently, an experimental set-up has been reported (128,129) where the crack tip region may be investigated during fatigue crack propagation.

The crazed or plastic zone at the crack tip has been reported to be flame shaped (122,127,130) for static loading cases and more unusual features have been observed for discontinuous fatigue crack propagation (123).

The Dugdale model has been successful at describing the craze zone size at the crack tip for most engineering thermoplastics (122,127,131-134), provided the appropriate time and temperature dependent material properties are taken into account (130-134). Using the Dugdale model and knowing the craze size and shape, the Young's modulus and a few other basic parameter estimations on the crack opening displacement in

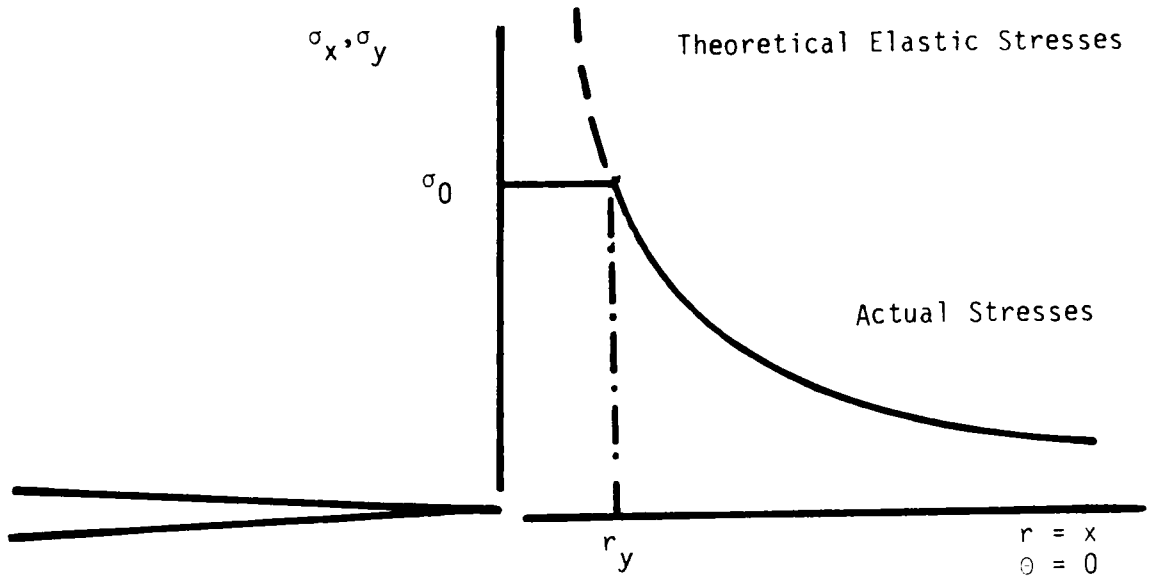

Figure 17. Stress distribution and yield zone at the crack front. (Reference 113).

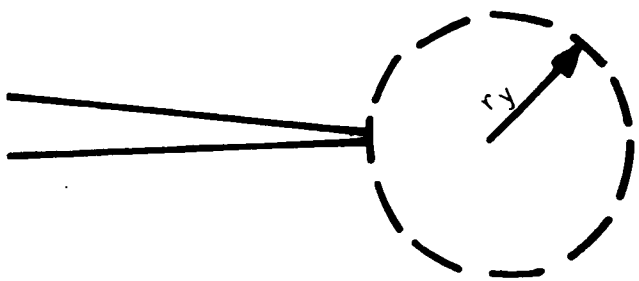

$$2r_y = \frac{1}{\pi}\left(\frac{K}{\sigma_0}\right)^2$$

Irwin Model

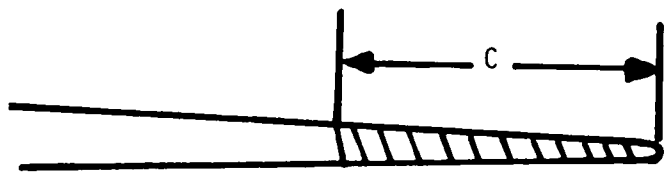

$$C = \frac{\pi}{8}\left(\frac{K}{\sigma_0}\right)^2$$

Dugdale Model

Figure 18. Crack front deformation models of Irwin and Dugdale. (Reference 113).

the craze, craze stress and plane strain fracture toughness may be obtained.

Hine and coworkers (122) found that the Dugdale model was able to describe the craze shape and size in poly(ether sulfone). However, the fracture toughness values predicted from this model were significantly lower than the actual values. On examination of the fracture surfaces, shear lips or regions of plastic deformation (plane stress), similar to those found in polycarbonate (123-126), were found on the edges of the sample. Brittle fracture, or a plane strain region, was observed in the center of the sample where the constraint was the highest. This mixed mode fracture behavior of the poly(ether sulfone) promotes the discrepancy between the fracture toughness experimentally obtained and that predicted by the Dugdale model.

There are numerous factors which effect the nature of the deformation zone at the crack tip. For instance, entanglements have been found by Kramer (135-139) and others to play a significant role in determining whether a crack tip zone will deform plastically or craze. Specifically, it was proposed that the tendency for a polymer to undergo either shear yielding or crazing is controlled by the contour length of the polymer chain between entanglements, l_e. In turn this parameter could then govern the maximum extension ratio, λ_{MAX}, for the network through Equation 9, where $\langle R^2_{rms} \rangle^{1/2}$ is the root mean square end-to-end

$$\lambda_{MAX} = \frac{l_e}{\langle R^2_{rms} \rangle_e^{1/2}} \tag{9}$$

distance of a chain of the entanglement molar mass M_e. In general, polymers with a short l_e and limited extensionability ($\lambda_{MAX}<3$) tend to

deform by shear yielding. Polycarbonate (126,139) is a prime example of a material with high entanglement density which tends to plastically deform in the general vicinity of the crack tip. In contrast, polystyrene has a low entanglement density (high l_e) and tends to craze in crack tip region. Kramer et al., (137,139) have partially crosslinked polystyrene, PS, using electron beam irradiation which he hoped would effectively increase the entanglement density. The deformation zone at the crack tip changed and the polystyrene apparently began to plastically deform at the crack tip. However, the author acknowledges other effects (e.g., branching, chain scission) could be important here.

To further confirm the role of entanglements, miscible Noryl^R blends were examined. Poly(2,6-dimethyl, 1,4-phenylene oxide), PPO, has a high entanglement density and is known to plastically deform in the precrack region. Thus, by varying the relative compositions of PS to PPO one can selectively control the deformation zone at the crack tip (139).

The stress concentration at the crack front can deform (craze or plastic deformation) the local region at the crack tip. In turn, this can blunt the crack tip leading to a fracture toughness which is typically overestimated. These deformation processes are a function of the sample thickness, yield strength and other variables as well. In an effort to minimize the effects of crack tip deformations on the measured fracture toughness valve, ASTM specification E399 (114) develops some basic guidelines for plane strain fracture toughness testing.

The Irwin model predicts a plastic zone with radius r_y shown in Equation 10.

$$r_y = \frac{1}{2\pi} \left(\frac{K_{I,C}}{\sigma o}\right) \tag{10}$$

In principle (ASTM E399), the crack length should be much larger than deformation zone:

$$a \geq 40\ r_y \tag{11}$$

In practice, the above criteria is not always satisfied and the following conditions are acceptable:

$$a \geq 16 r_y \tag{12}$$

Furthermore, the length of the remaining ligament (i.e., w, width, -a) be large relative to the deformation zone:

$$(w-a) \geq 16 r_y \tag{13}$$

It has also been found that the thickness, B, must also follow size guidelines. Experimentally it has been shown that ideally, to minimize the deformation at the crack tip, brittle or low toughness materials should be used which have a high yield strength.

$$B \geq 2.5 \left(\frac{K^2_{I,C}}{\sigma_y}\right) \tag{14}$$

3.0 EXPERIMENTAL

Step growth or condensation polymerization involves the stepwise condensation of functional monomers to form high molecular weight polymers. In order to achieve high molecular weight linear materials, several criteria must be satisfied. These include difunctionality, one-to-one stoichiometry, high monomer and solvent purity and very high conversions are crucial for obtaining high polymer. The following sections describe the careful purification procedures required to obtain polymerizable monomers.

In each of the materials synthesized (oligomers and polymers), the control of the molecular weight and end groups was considered to be very important. The mechanical and thermal properties depend on molecular weight up to a point and then tend to level off with increasing molecular weight. However, with increasing molecular weight above the critical molecular weight for the development of entanglements, the melt viscosity dependency on molecular weight increases to the 3.4 power thus making melt processing difficult. Therefore, there is an optimum in molecular weight needed in order to achieve good mechanical properties while retaining processability.

In an effort to control the molecular weight of each of the polymers synthesized, the Carothers equation was used. A stoichiometric imbalance (excess of the dihalide monomer in the case of "non-functional" polymers) was calculated and used to obtain molecular weights which were, similar to those materials commercially available, (e.g., 29,000-32,000 Mn range). This usually gives intrinsic

viscosities in the range of 0.5-0.8 dl/g in NMP at 25°C, depending on the monomers used and the polymer-solvent interaction parameters.

3.1 Solvents and Purification

N-Methyl-2-Pyrrolidone (NMP). NMP was obtained from Fisher Scientific Company and was dried by stirring over phosphorous pentoxide (P_2O_5) or calcium hydride (CaH_2) for 24 hours. The dried solvent was then vacuum distilled at approximately 70°C to avoid degradation.

Toluene. The toluene was obtained from the Fisher Scientific Company and was used without further purification.

Diphenylsulfone. Diphenylsulfone was obtained from Aldrich and is a solid "solvent" with a melting point of 123°C. This solvent was purified by recrystallization from acetone.

Benzophenone. Benzophenone was obtained from Aldrich and is a solid solvent which melts at 63°C. This solvent was used without further purification.

N-Cyclohexyl-2-Pyrrolidone (CHP). N-Cyclohexyl-2-Pyrrolidone was obtained from GAF and was vacuum distilled from calcium hydride at approximately 120°C.

Chlorobenzene. Chlorobenzene was obtained from Fisher Scientific Company and was distilled from calcium hydride.

3.2 Monomer Synthesis and Purification

3.2.1 Bisphenol-A (Bis-A)

High purity Bisphenol-A was obtained from either Union Carbide Corporation or Dow Chemical Company. The Bisphenol-A was recrystallized from toluene by the following procedure. A 1500 ml Erlenmeyer flask was

heated to reflux temperatures (~110°C). At this time the monomer had gone into solution and 2 gms of activated charcoal was added. The solution was allowed to boil for 5 minutes and was filtered through celite. The clear solution was transferred to another Erlenmeyer flask and boiled with stirring to reduce the volume. The solution was then cooled first to room temperature and then in an ice bath. After 1 hour the crystals formed were filtered and dried under vacuum at 60°C for 24 hours. In an effort to remove any remaining solvent, the crystals were crushed and dried for another 6 hours.

3.2.2 Synthesis and Purification of Deuterated Bisphenol-A

The bisphenol-A monomer has two possible sites for deuteration, the isopropylidene linkage and the phenyl rings. The synthesis involves the electrophilic addition of acetone onto phenol catalyzed by hydrogen chloride. For case 1, in which deuterated acetone was used, the monomer obtained is labeled D-BisA-I, and in case 2 using deuterated phenol the monomer obtained is labeled D-BisA-II as shown in Scheme 15.

To a 250 ml three necked round bottom flask equipped with a mechanical stirrer, hydrogen chloride inlet and condenser, 0.5 moles of phenol (Fisher Scientific Co.) in case 1 or deuterated phenol (Aldrich Chemical Co.) in case 2 was added. Deuterated acetone (0.25 moles) (Aldrich) in case 1 or acetone (0.25 moles) (Fisher) in case 2 was then introduced. The acetone served as both a solvent and reactant. Hydrogen chloride gas (Matheson) was bubbled through the reaction for four hours and the reaction was terminated after six hours. Once the reaction was complete, the bisphenol-A monomer precipitated out of

Scheme 15

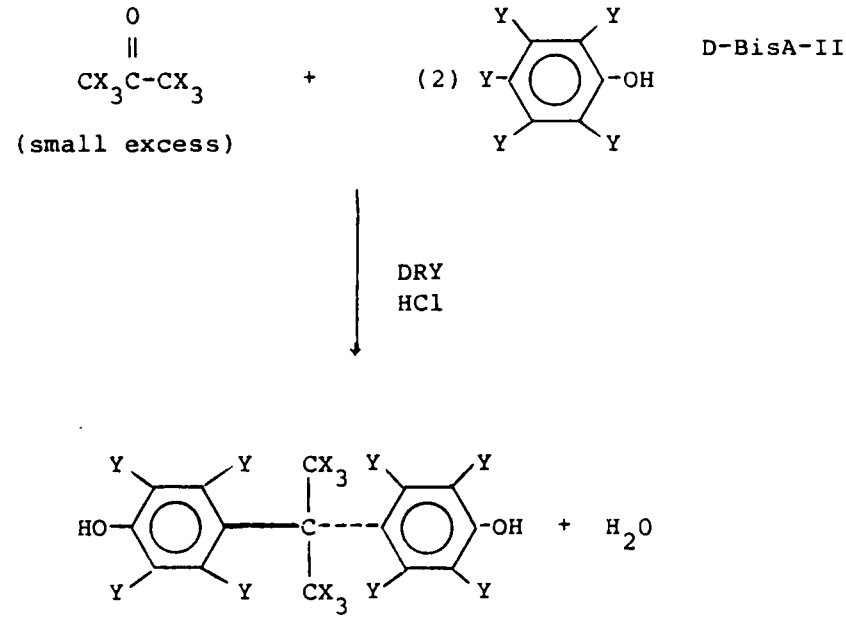

case 1 (D-BisA-I)

$X = {}^{2}H$

$Y = {}^{1}H$

case 2 (D-BisA-II)

$X = {}^{1}H$

$Y = {}^{2}H$

solution. The monomer was added to a large excess of water to remove any unreacted materials or byproducts. The product was crystallized twice from toluene as described previously.

3.2.3 Synthesis and Purification of Deuterated 4,4'-dichlorodiphenyl Sulfone

The partially deuterated 4,4'-dichlorodiphenyl sulfone was synthesized by a Friedel-Crafts reaction in which p-chlorobenzene sulfonyl chloride was reacted with an excess of deuterated chlorobenzene in the presence of aluminum chloride, as shown in Scheme 16.

Scheme 16

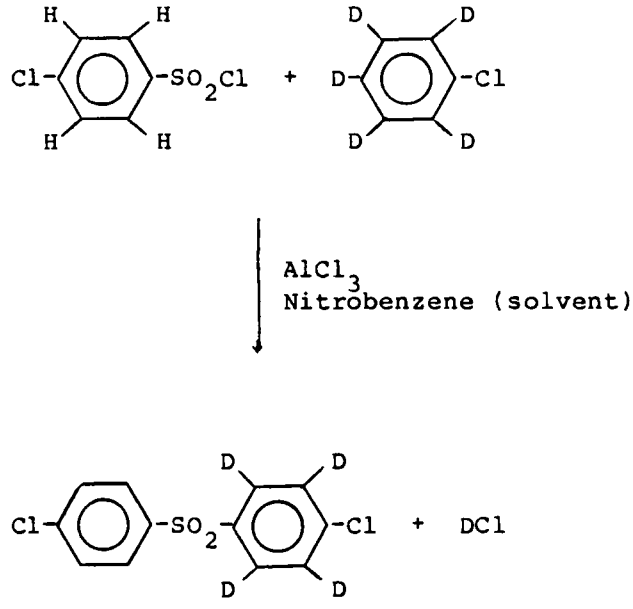

To a four necked 250 ml flask equipped with a mechanical stirrer, nitrogen inlet, condenser and an addition funnel, 20 ml of deuterated chlorobenzene, 5.6 g of aluminum chloride was dissolved in nitrobenzene and transferred into an addition funnel. The reaction mixture was heated to 60°C and the 4-chlorobenzenesulfonyl chloride was added slowly over a two hour period. The reaction was allowed to proceed overnight at 60°C. The product was placed in a large excess of water to remove the aluminum chloride. The nitrobenzene and unreacted chlorobenzene were rotovapped at 180°C, leaving the crude monomer as a residue. The deuterated dichlorodiphenylsulfone (D-DCDPS-I) was recrystallized twice from toluene.

3.2.4 Epon Resin 828

Epoxy oligomers based on bisphenol-A and epichlorohydrin were

obtained from Shell Development Company (EPON resin 828). The molecular weight is 380 g/mol.

3.2.5 4,4'-Diaminodiphenyl Sulfone

The diaminodiphenylsulfone curing agent was obtained from Aldrich Chemical Company and used without further purification.

3.3 Polymer Synthesis

3.3.1 Synthesis of Hydroxyl Terminated Polysulfone Oligomers

A typical synthesis of hydroxyl-terminated polysulfone oligomer was conducted in a four-necked, 500 ml round bottom flask equipped with a mechanical stirrer, gas inlet, thermometer, Dean Stark trap, and condenser. For a synthesis designed to prepare a 14,600 g/mol oligomer the flask was charged with 22.8270 g of Bis-A and 27.9407 g of 4,4'-dichlorodiphenylsulfone. These monomers were carefully washed into the flask with NMP. The final volume of NMP was approximately 250 ml. To this solution, approximately 150 ml of toluene was added as an azeotroping agent. Finally, approximately 19 g of potassium carbonate (Fisher Scientific Company) base was added. Note that K_2CO_3 was used in a 30 to 40 percent excess. This reaction mixture was then heated until the toluene began to reflux. An optimum reflux temperature range appears to be about 140-150°C. Water is released during the phenoxide formation and is azeotroped from the system. Refluxing must proceed until no more water is observed; which may take 3-5 hours. The temperature was increased to 180°C for 3-5 hours; completion or near completion may be qualitatively estimated by the point the viscosity increases dramatically. The polymer was then filtered and coagulated in

a 10X volume of a 50/50 methanol and water mixture. The polymer was then dried for 24 hours in a vacuum oven at 80°C.

3.3.2 Synthesis of Dimethylamino-Terminated Polymethylsiloxane Oligomers

The dimethylamino-terminated poly(dimethylsiloxane) oligomers were prepared by the anionic bulk equilibration of a low molecular weight oligomer with the cyclic tetromer, D_4. The precursor oligomer was obtained either from Union Carbide Corporation or Petrarch Systems, Inc. Its molecular weight was determined by titration. The reaction was carried out in a 3-necked round-bottomed flask equipped with a mechanical stirrer, inert gas inlet, thermometer, condenser, and drying tube. In a typical reaction to produce a 5000 g/mole oligomer, 23.75 g of a 570 g/mole oligomer along with 226.25 g of D_4 were introduced into the reaction flask. Using a silicone oil bath and hot plate, the temperature was raised to 80°C with stirring and 1.5 g of tetramethyl-ammonium siloxanolate catalyst was added. The reaction was maintained at 80°C for 24 hours to ensure complete equilibration. The temperature of the reaction was then raised to 160°C for 3 hours to decompose the catalyst. The titrated molecular weight was 4410 g/mole.

3.3.3 Synthesis of Polysulfone-Poly(dimethylsiloxane) Perfectly Alternating Block Copolymers.

The perfectly alternating block copolymers were synthesized in solution using the silylamine-hydroxyl condensation reaction (143). The reaction was carried out in a 1-liter four necked round bottom flask fitted with a mechanical stirrer, a Dean Stark trap, condenser, thermometer, inert gas inlet, and addition funnel. In a typical

reaction to produce a polysulfone-poly(dimethylsiloxane) block copolymer, 22.3 g of a 4900 g/mole hydroxyl-terminated polysulfone oligomer was placed into the flask with 500 ml of chlorobenzene. With stirring, the temperature was raised to chlorobenzene reflux temperature(132°C) and approximately 80 ml of solvent was removed from the trap to dehydrate the system. The 4400 g/mole siloxane oligomer (20.0 g) was placed into the addition funnel. Half of the oligomer was added to the solution and allowed to react until the evolution of dimethylamine (as detected by pH paper) had significantly decreased. The rest of the siloxane oligomer was added likewise in increments. As the stoichiometric point was approached, a noticeable increase in viscosity was observed. The reaction was allowed to proceed at reflux temperature for another 2 hours. It was then cooled and the product was precipitated in a ten-fold excess of methanol. The fibrous product was dried in a vacuum oven overnight, then redissolved in chloroform, filtered, and reprecipitated in filtered methanol/isopropanol solution. After drying for 24 hours under vacuum at 70°C, the recovered yield was 95 percent and the intrinsic viscosity in chloroform was 0.60 dl/g.

3.3.4 Synthesis of High Molecular Weight Poly(Hydroxy Ether)/Polysulfone Linear Copolymers

The synthesis of the epoxy-polysulfone copolymer was conducted in a 250 ml four-necked round-bottom flask equipped with a mechanical stirrer, Dean Stark trap, condenser, thermometer and nitrogen inlet. In a typical reaction to prepare a high molecular weight epoxy-polysulfone copolymer, 3g hydroxyl functional of 5300 g/mol polysulfone and 0.194 g of Bisphenol-A diglycylether were charged to the flask. These materials

were then washed down the flask with 20 ml of dimethylsulfoxide. In order to dehydrate the system, 20 ml toluene was used as a dehydrating agent. At this time a trace amount of tetramethylamonium hydroxide was added to the system. The reaction mixture was heated to 115-120°C, where the DMSO-toluene mixture began to reflux. After 4 hours the reaction was viscous and considered complete. The polymer was coagulated in a 50/50 mixture of methanol and water. The fibrous product was dried at 80°C under vacuum for 24 hours.

3.3.5 Synthesis of Modified Networks with Phenolic Hydroxyl Terminated Polysulfone Oligomers

A typical reaction of the phenol terminated polysulfone and the EPON 828 resin was conducted in a 125 ml filtering flask equipped with a teflon coated magnetic stirrer and a rubber stopper. To prepare an epoxy resin containing fifteen percent by weight of polysulfone, 10.5g (.002 mole) of 5300 g/mol Bis-A polysulfone oligomer and 45g (0.118 mole) of EPON 828 resin was charged along with 20-30 ml of methylene chloride into the flask. The large molar excess of the epoxy resin to that of the polysulfone oligomer is important. This will mainly result in the capping of the Bis-A-PSF oligomer without any chain extension. Once the oligomers were dissolved in methylene chloride trace amounts of tetramethylammonium hydroxide in a twenty-five percent methanol solution was added as a catalyst. The mixture was then slowly heated under vacuum to 110-120°C for 4.5 hours. At this time the reaction mixture appeared to be clear and homogeneous. Once the reaction was thought to be complete, the temperature was increased to 160°C so as to decompose the "transient" catalyst. The reaction was cooled to 150°C and the

stoichiometric amount, 14.5g (0.058 mole), of the 4,4'-diaminodiphenyl-sulfone was added. The reaction system was heated at this temperature under vacuum until it was homogeneous. The reaction mixture was then cooled to approximately 80°C, poured into a silicone mold and cured at 140°C for 2 hours and then post-cured at 190°C for another 2 hours. The materials were removed form the mold after the curing cycles and cooled to room temperature. The networks prepared in the manner above were utilized for the thermal and mechanical characterizations.

3.3.6 Synthesis of Modified Networks with Amine Terminated Polysulfone Oligomers

The amine terminated polysulfone was added to the EPON Resin 828 at 150°C and allowed to react for ten minutes to allow good mixing. The DDS (diaminodiphenyl sulfone) was then added and the system was kept at 150°C until homogeneous and clear. The reaction mixture was then cooled to approximately 60°C, poured into a silicone mold, cured for 2 hours at 140°C and post cured 2 hours at 190°C. Those networks which were modified with higher molecular weight oligomers required an additional cure, 0.5 hour at 205°C.

3.4 Characterization

3.4.1 Gel Permeation Chromatography

The molecular weight distributions were qualitatively checked using a Waters Liquid Chromatograph Model 244 or 150 C. Microstyrogel columns of 500, 1000, 10,000 and 100,000 angstrom pore size were used in conjunction with a refractive index detector. Approximately 0.25%

solutions of THF or chloroform were used as a solvent with a flow rate of 1 ml/min.

3.4.2 Fourier Transform Infrared Spectroscopy

A Nicolet MX-1 spectrophotometer was used for obtaining the infrared spectrum on all polymers and monomers. Polymers were analyzed in thin films cast from (5%) chloroform solutions. Monomers were run as KBr pellets.

3.4.3 Proton Magnetic Resonance Spectroscopy

NMR spectra were obtained using a Varian EM-390 90 MHz spectrometer. Spectra were obtained in a 10% deuterated chloroform solution for the polymers and from a 10% solution of deuterated DMSO or acetone solution for the monomers. Methylene chloride or TMS was used as a lock reference.

A JEOL FX200 MHz was also used to obtain spectra. Deuterated chloroform was used as the solvent with TMS as the reference. Solution concentration was about 10%.

3.4.4 Differential Scanning Calorimetry (DSC)

Glass transition, melting points and epoxy network curing investigations were determined on a Perkin-Elmer Model-2 DSC. The baseline was checked for flatness at each heating rate, and temperature calibration was accomplished using an indium standard which has a melting point of 60°C and a known heat of fusion of 6.8 cal/g. Subambient transitions were achieved by immersing the cold finger in liquid nitrogen and purging the sample chamber with helium. Except where noted, the heating rate was 10°K/min.

3.4.5 Intrinsic Viscosity Measurements

Intrinsic viscosities of the various polysulfones and related structures were determined using a Cannon-Ubbelhode dilution viscometer. Four concentrations of the polymer solutions in chloroform, NMP or trifluoromethane sulfonic acid at 25°C were used for the measurements.

3.4.6 Dynamic Mechanical Analysis

Dynamic mechanical spectra of 10-15 mil thick films of several of the homo- and copolymers were obtained using a Polymer Laboratories Dynamic Mechanical Thermal Analyzer operating at 1 Hz. Materials were run in a single cantilever mode with a 1 mm free length, and a heating rate of 5°C/min.

3.4.7 Thin Layer Chromatography

The purity of the monomers was checked by thin-layer chromatography on silica gel and using acetone as the developing solvent. All three monomers exhibited one spot which matched the R_F value (within 6%) of the undeuterated recrystallized commercial compound. AUU lamp with a long and short wavelength light source was used to identify the compounds spotted and eluted on the TLC plates.

3.4.8 Thermogravimetric Analysis (TGA)

The relative thermal stabilities of the various homo- and copolymers and the blends were assessed by thermogravimetry in a nitrogen atmosphere. A Perkin-Elmer TGS-2 along with the System 4 Microprocessor was used. The heating rate in each case was 20°C/min.

3.4.9 Mass Spectroscopy

All hydrogeneous and deuterated monomers were analyzed for the molecular ion peak using a Varian 120 Model instrument.

3.4.10 High Pressure Liquid Chromatography

In the HPLC analysis, a Waters M-45 solvent delivery system was used. A precolumn of 5μ ODS packing 3 cm long with an inner diameter of 4.6 mm was used in conjunction with a DuPont Zorbax ODS column, 25 cm long with a inner diameter of 9.5 mm. A Waters Model R401 differential refractometer was the detector used. A 20μl sample loop was used to inject samples. The mobile phase was a (15/85) mixture of methanol and tetrahydrofuran.

3.4.11 Titration of Functional Oligomers

Titration of functional oligomers were carried out using a computer-interfaced Fisher Scientific Titrimeter II automatic titrator operating in the automatic endpoint seeking (AEP) mode. A standard calomel electrode was used with a double junction reference. The electrodes were stored in a pH 4.0 buffer. The electrometer was calibrated according to the manufacturer's instructions. A ten milliliter burette was used for all titrations.

The hydroxyl-terminated poly(arylene ether) sulfone oligomers were titrated with 0.2 N aqueous tetraethylammonium hydroxide in 20 ml of either N,N-dimethylformamide (DMF) or N,N-dimethylacetamide (DMAC) as reported earlier (171).

The dimethylamino terminated poly(dimethylsiloxane) oligomers were titrated with 0.1 N alcoholic HCl in 100 ml of isopropanol.

3.4.12 Scanning Electron Microscopy

Scanning electron microscopy (SEM) was used to study the nature of the domains by observing the fracture surfaces in many of the block copolymer systems. Prior to fracture, the samples were immersed in

liquid nitrogen for approximately fifteen minutes. A notch was usually introduced into the sample to make crack initiation easier. The sample was removed from the liquid nitrogen and quickly fractured. It was then mounted on a sample peg with copper tape.

Two different instruments were used for the SEM studies. An ISI Super III was used with gold-palladium coated samples for most of the routine examinations of fracture surface. When elemental analysis was needed, however, an AMR 900 scanning electron microscope was used with carbon coated samples. This instrument is equipped with an International 707 energy dispersive X-ray analyzer (EDAX) unit. No quantitative EDAX studies were performed.

3.4.13 Transmission Electron Microscopy

Transmission electron microscopy (TEM) was performed on thin cast films of the siloxane containing block copolymers to directly observe the nature of the microphase separation in these block copolymers. Staining of one of the phases was unnecessary due to the great degree of electron density differences between the poly(dimethylsiloxane) and the poly(arylene ether). A chloroform solution of the polymer was cast on water and was then transferred directly to a 150 mesh copper TEM grid. Micrographs were obtained using a JEOL 100 operating at 80 keV.

3.5 Sample Preparation

3.5.1 Compression Molding

Sheets of the homopolymers, copolymers and copolymer-homopolymer blends were compression molded between ferrotype plates in a hot presses. Before use, the plates were thoroughly cleaned with warm soap

and water followed by acetone to remove any impurities or release agents. A stainless steel spacer of the appropriate thickness was used to mold samples with the desired dimensions. Steel plates were also used between the ferrotype plates and platens of the press to provide rigidity. The press was first preheated to the desired temperature, whereupon the mold containing the polymer was inserted and contact pressure applied. After sufficient time was given to melt the polymer (3-4 minutes), full pressure was applied. Pressure and heat were maintained for 2-3 minutes and the press was then cooled by running air and then cold water through the platens.

3.5.2 Detailed Film Casting Procedure for Poly(arylene ether) Sulfones and Related Structures

The first step in the preparation of the films is to dissolve the polymer in an appropriate solvent, so as to yield an approximately ten percent (w/v) solution. Where possible, chloroform is a preferred solvent. In order to prepare four films, 4 gms of polymer were placed in a 250 ml beaker containing a magnetic stirring bar and 40 mls of chloroform. This solution was stirred and was covered with a watch glass to prevent the introduction of large impurities from the atmosphere. After the solution was formed, it was filtered. For this purpose a disposable 10cc syringe was used to transfer the polymer solution. The needle was removed and the solution was filtered through a disposable Gelman's syringe filter into a 250 ml Erlenmeyer flask. The polymer solution was examined to see if refiltering was required. If not, the flask was next gently swirled to displace any bubbles.

The next step was the actual casting of the film. A large

stainless steel base was used as a level base to cast the films. The actual casting was done on a clean 9" x 6" glass plate. A doctor's blade used to spread the polymer solution over the glass plate. Casting was conducted so as to yield a six inch long film. That is, the nine inch length of the plate was perpendicular to the doctor's blade. The actual procedure involves placing 8-10 mls of the dissolved polymer on the edge of the plate, and in one continuous motion, transferring the blade over the solution. The glass plate was then covered with a watch glass to prevent dust from settling on the drying film.

This cast film was allowed to sit overnight (20 hrs) to partially dry. The films were then transferred into a vacuum oven and heated to 60°C at low pressure for at least 8 hours to remove the chloroform. Since the films were ~1 mil or less, this is believed to be sufficient. This film thickness was critical for the radiation degradation studies.

The films were removed from the oven and from the plate by running cold water over the plate. The thin film then can usually be easily stripped off the plate. The films were stored between two Kimwipes which were themselves within 2 pieces of card board. This procedure helps the film to remain straight and prevents creases. The film which is now within the rail board, was transferred into a polyethylene "Ziploc" bag which was left open and placed in the vacuum oven for 24 hours to remove any traces of water. Then the bags were removed from the oven and stored in a desiccator until the radiation degradation or other experiments are initiated.

3.6 Mechanical Property Measurements

3.6.1 Fracture Toughness

The impact strength of both the thermosets and thermoplastics synthesized was characterized by fracture toughness, K_{IC}, measurements. The value of K_{IC} indicates the critical stress intensity for a load which will cause catastrophic failure in mode I testing or tension. For our investigation the three-point bend specimen geometry was used. The relation for K_{IC}, for a three-point bend specimen is

$$K_{IC} = \frac{3PL \quad a^{1/2}Y}{\beta w^2} \tag{15}$$

where P=load, L=2w, β=thickness, w-width, a=crack length and Y=geometric factor given by

$$Y = 29.6 - 186\,(a/w) + 656\,(a/w)^2 - 1017\,(a/w)^3 + 639\,(a/w)^4$$

Equation (15) indicates that the value of K_{IC}, is directly proportional to the load and accounts for the specimen geometry and crack length.

The thickness of the fracture toughness specimens is crucial for obtaining plane strain fracture conditions. I found that the dimensions of 3.2 x 6.4 x 38.1 mm were sufficient in obtaining plane strain fracture conditions for the brittle epoxy samples. However, for the more ductile thermoplastic ductile and larger sample dimensions were required to insure plane strain 6.4 x 12.8 x 76.2 mm.

Figure 19 contains the fracture toughness values for Udel as a function of strain rate. As expected as the strain rate increases the fracture toughness decreases. For these investigations, a strain rate

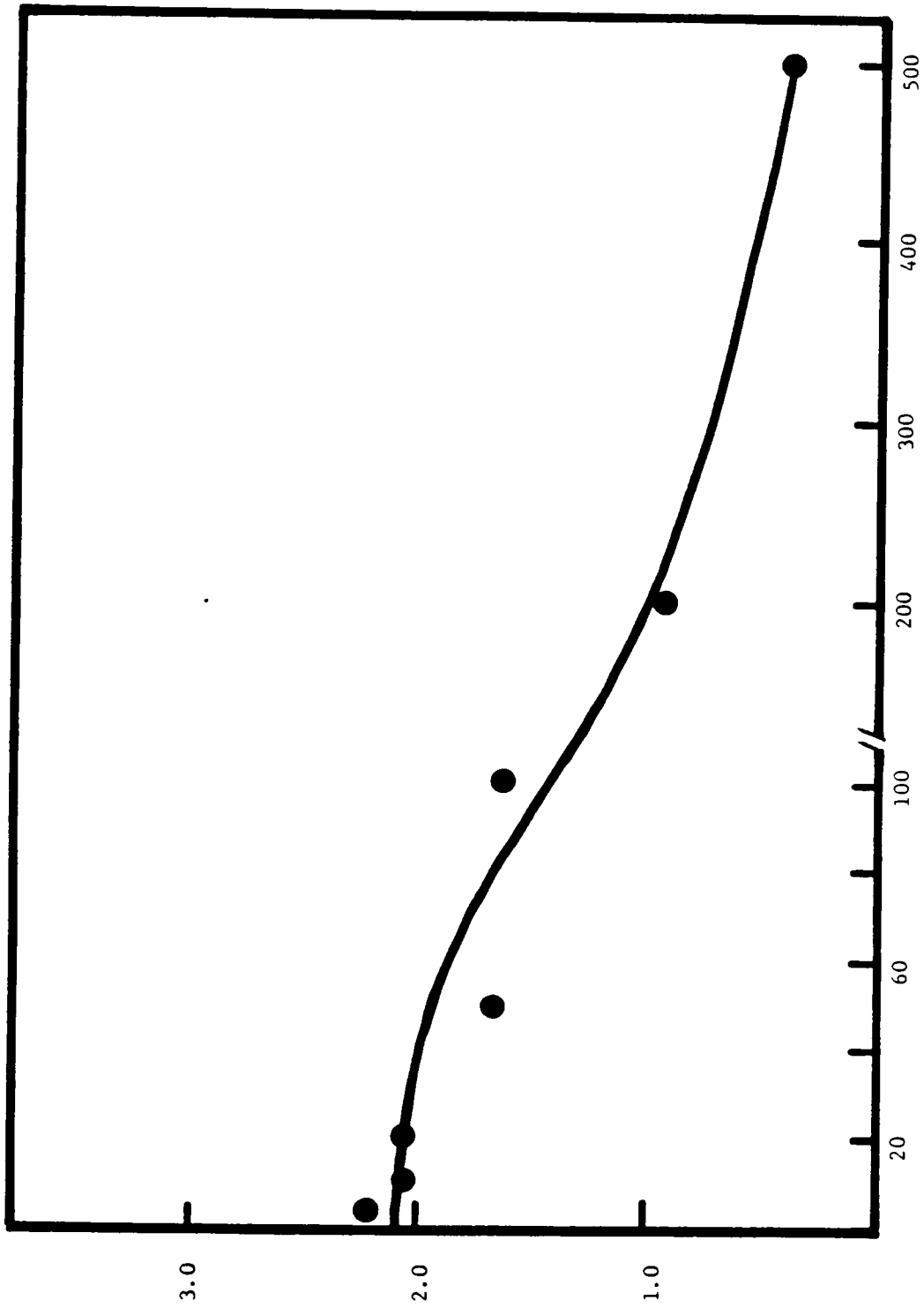

Figure 19. Fracture toughness, $K_{I,C}$, values for Udel versus strain rate.

of 0.5 or 1.0 mm/min was used. In this region the fracture toughness is somewhat independent of strain rate.

The precracks were obtained with a saw cut and then were sharpened with a razor cut. It is crucial that the precrack be very sharp and straight.

The criteria of ASTM standard E399 (114) were followed as closely as possible in obtaining the fracture toughness measurements and the important features are highlighted below:

1. Precrack fronts should not deviate more than 5% from a straight line .
2. K_{IC} values should not deviate more than 10% from the average
3. Fracture should occur in plane strain.
4. Sample should be homogeneous. However, if not homogeneous the inhomogeneity (i.e., rubber particle, void, etc.) must be small relative to a, a-w and t: a, a-w, t >>> inhomogeneity
5. The values were obtained from an average of 4-10 test specimens

3.6.2 J-Integral Analysis

For those samples which do not fail in plane strain linear elastic fracture mechanics (LEFM) is no longer applicable. Often larger sample dimensions can change the mode of failure and LEFM can be used. However, when working with limited quantities of materials, an alternative measure of fracture toughness is often used, the J-intergral analysis, according to ASTM standard E813 (117).

Three point bend test specimen with dimension of 6.4 x 12.8 x 76.2 mm were used to obtain the measurements. The precracks were introduced

with a saw and sharpened with a razor cut. The crosshead speed was 0.5 mm/min.

3.6.3 Stress-Strain Measurements-Tensile

Tensile property determinations were made using an Instron tensile tester. Dogbone samples were cut from the polymer sheet or film using a die. The samples were approximately 0.110 inches wide and 0.28 was taken as the initial length in all cases. The load cell was calibrated using a standard two kilogram weight. The sample was clamped in the pneumatic clamps and elongated at a rate of ten millimeters per minute (except where noted). Yield strength, yield strain, tensile strength, tensile strain, and modulus were calculated from the load extension plot. The results reported were an average of three to five samples.

3.6.4 Flexural Modulus

Flexural modulus was determined using a three point bend geometry. The samples measured about 52.0 x 1.7 x 13.1 mm. They were tested using a 25.4 cm span at a crosshead speed of 1.0 mm/min.

4.0 RESULTS AND DISCUSSION

4.1 Synthesis of Deuterated Polysulfones

Selectively deuterated poly(arylene ether sulfones) were prepared for deuterium NMR investigations. The availability of these model macromolecules permit structural identification of the molecular motions responsible for the low temperature relaxations which have already been observed in the dynamic mechanical spectra of these engineering polymers. Three labeled sites on the appropriate monomers, (bisphenol-A and 4,4'-dichlorodiphenylsulfone) were prepared from deuterated intermediates and characterized via chromatographic, spectroscopic and thermal analysis. These monomers were then employed, along with hydrogenous monomers to synthesize high molecular weight, selectively deuterated poly(arylene ether sulfones). These materials were characterized by FT-IR, proton NMR, intrinsic viscosities and thermal analysis. Molecular weights were controlled so that characteristic parameters (e.g. the glass temperature) were quite similar for the hydrogenous and deuterated systems.

The purity of the deuterated monomers was confirmed by comparison to commercially available hydrogenous materials using melting points and TLC. The melting points and TLC R_f values shown in Table 6 indicate the pure products that were obtained.

The structures of these partially deuterated monomers were also confirmed by proton, carbon, and deuterium NMR and FT-IR. Proton NMR spectra indicate that exchanges occur in the synthesis of the deuterated

TABLE 6

A Comparison of Melting Points and Thin Layer Chromatography for Hydrogenous and Deuterated Monomers

Monomer	Melting Point, Range °C	TLC, R_f
Bisphenol-A	156-158	0.59
D-Bis-A-I	156-158	0.57
D-Bis-A-II	155-157	0.55
4,4'-Dichlorodiphenyl Sulfone	149-151	0.72
D-DCDPS-I	149-151	0.70

Bisphenol-A monomers. These exchanges result from reaction of acetone and phenol with the hydrogen chloride catalyst. In the case of D-Bis-A-I a proton NMR singlet at 1.2 ppm is observed, which corresponds to protons on the isopropylidene moiety. Quantitative deuterium NMR results (140,141) show that the following relative levels of deuteration were obtained:

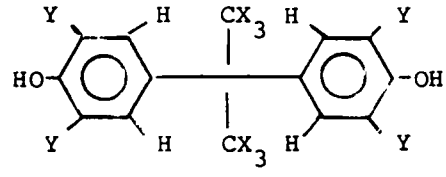

D-BIS-A-I

64% of the Deuterons in Position X
36% of the Deuterons in Position Y

However, mass spectroscopy gives more insight into the nature of the exchanges. Commercial hydrogenous Bisphenol-A monomer shows a molecular ion peak at m/e = 228. The deuterated monomer, D-Bis-A-I, exhibits a distribution of molecular ion peaks as shown in Figure 20. These data reflect the expected distribution of deuteration at the various sites. Molecules ranging from the monodeuterated (229 g/mole) to the heptadeuterated monomer (235 g/mole) are present in significant amounts. In addition, Figure 20 shows a distribution in the $M-CX_3$ peak (213-219 g/mole), again indicating a range of deuteration. The most probable loss (231-215) corresponds to a CH_2D residue.

Scrambling of the methyl deuterons most likely occurs under the acidic reaction conditions by the following mechanism:

Scheme 17

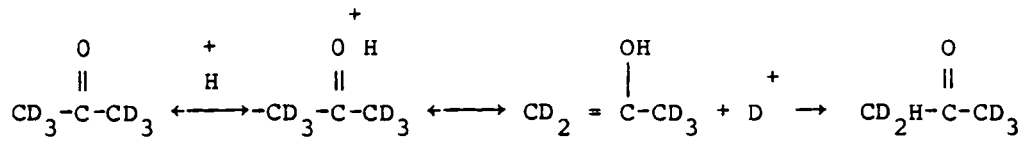

The first step involves the protonation of the ketone group and subsequent rearrangement to an enol. This structure returns to the keto form, introducing protons into the originally deuterated starting material. As this process continues more hydrogen is added to the acetone. Furthermore, the liberated D^+ can undergo exchange with the protons on the ortho and para positions of the originally unlabeled phenol.

In the case of D-Bis-A-II, for which deuterated phenol was used in the synthesis, the proton NMR spectrum has a singlet at 6.75 ppm, indicating that the phenyl rings are not completely deuterated. Figure 21 shows the proton NMR spectra of both the commercial hydrogenous Bisphenol-A and the deuterated analog, D-Bis-A-II, as well as the peak assignments. These NMR results indicate that an exchange occurs in the positions ortho to the phenol group. The liberated D^+ can exchange with the originally unlabeled acetone via the process shown in Scheme 17 to produce further deuterium scrambling. Quantitative deuterium NMR (140,141) indicates that the following pattern of deuteration was obtained:

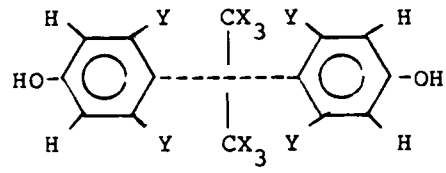

D-BIS-A-II

34% of the Deuterons in Position X
66% of the Deuterons in Position Y

The mass spectral analysis (Figure 22) of the D-Bis-A-II reveals a distribution of molecular ion peaks (232-239 g/mole), as expected.

The 4,4'-dichlorodiphenyl sulfone (D-DCDPS-I) was synthesized without exchange in deuterated form by a Friedel-Crafts acylation reaction. The structure of this monomer was confirmed by NMR, FT-IR, and mass spectroscopy. The FT-IR spectra of the commercial 4,4'-dichlorodiphenyl sulfone and the deuterated monomer are given in Figure 23. In the deuterated material the absorbances at 1547 and 1370 cm^{-1} are assigned to the aromatic carbon-deuterium stretching frequency.

The mass spectral analysis indicates that the molecular ion peaks for the deuterated monomer increased four units, as expected over the hydrogenous monomer. In addition, the isotope peaks are shown as well. The peak assignments are contained in Table 7.

The N-methyl-2-pyrrolidone potassium carbonate (NMP/K_2CO_3) synthesis technique was used to synthesize the deuterated polysulfones. Poly(arylene ether sulfones) have previously been synthesized by either potassium carbonate/dimethyl acetamide (13) or by aqueous caustic/dimethyl sulfoxide techniques (1). Although these methods are very useful, they are not entirely suitable for the synthesis of high molecular weight polymers. One of the problems associated with the later technique is the insolubility of the bisphenate intermediates. Moreover, partial hydrolysis of the activated aromatic dihalide could occur, which would create a stoichiometric imbalance and limit the molecular weight.

NMP is an aprotic dipolar solvent which effectively solvates the bisphenates that are formed. It is likely that the polymerization

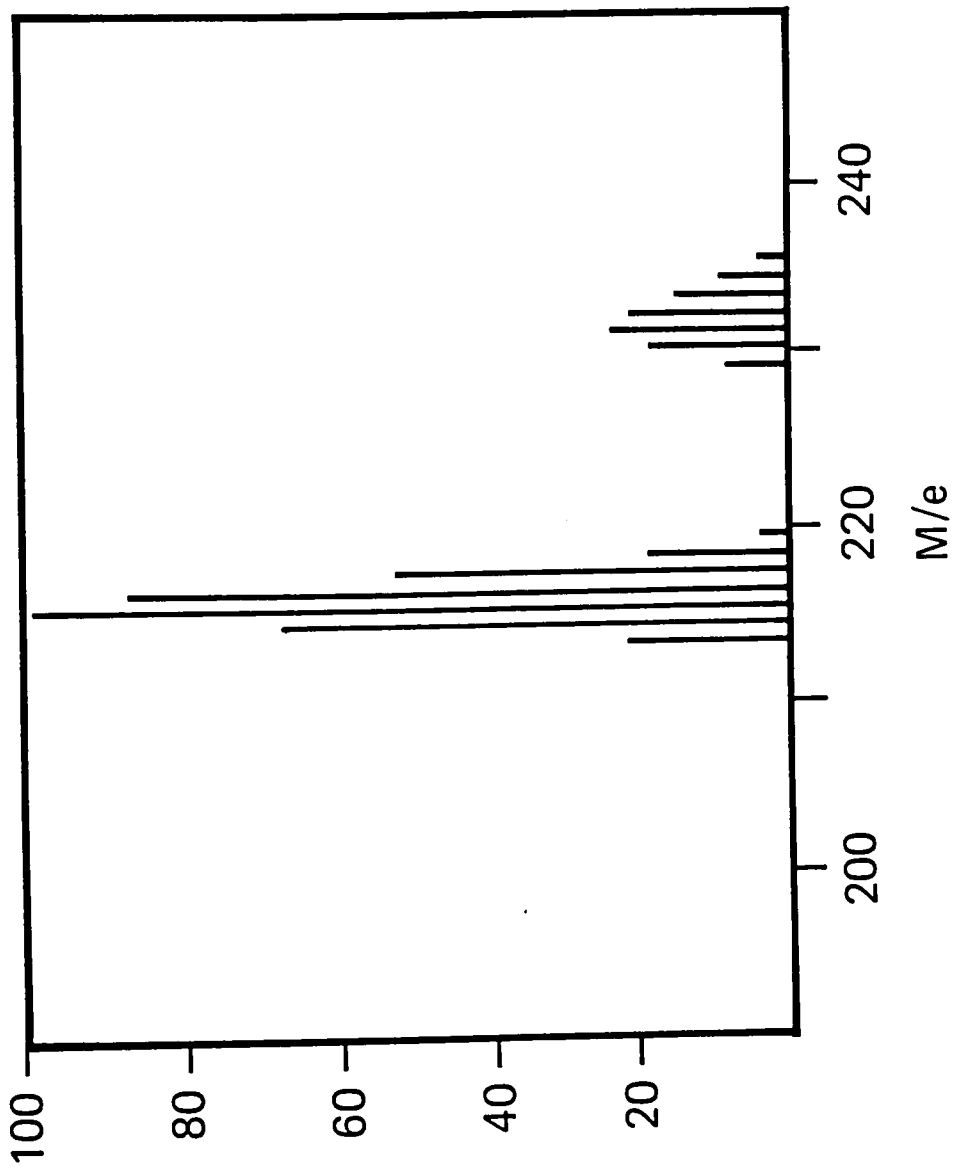

Figure 20. Mass spectrum of D-BisA-I.

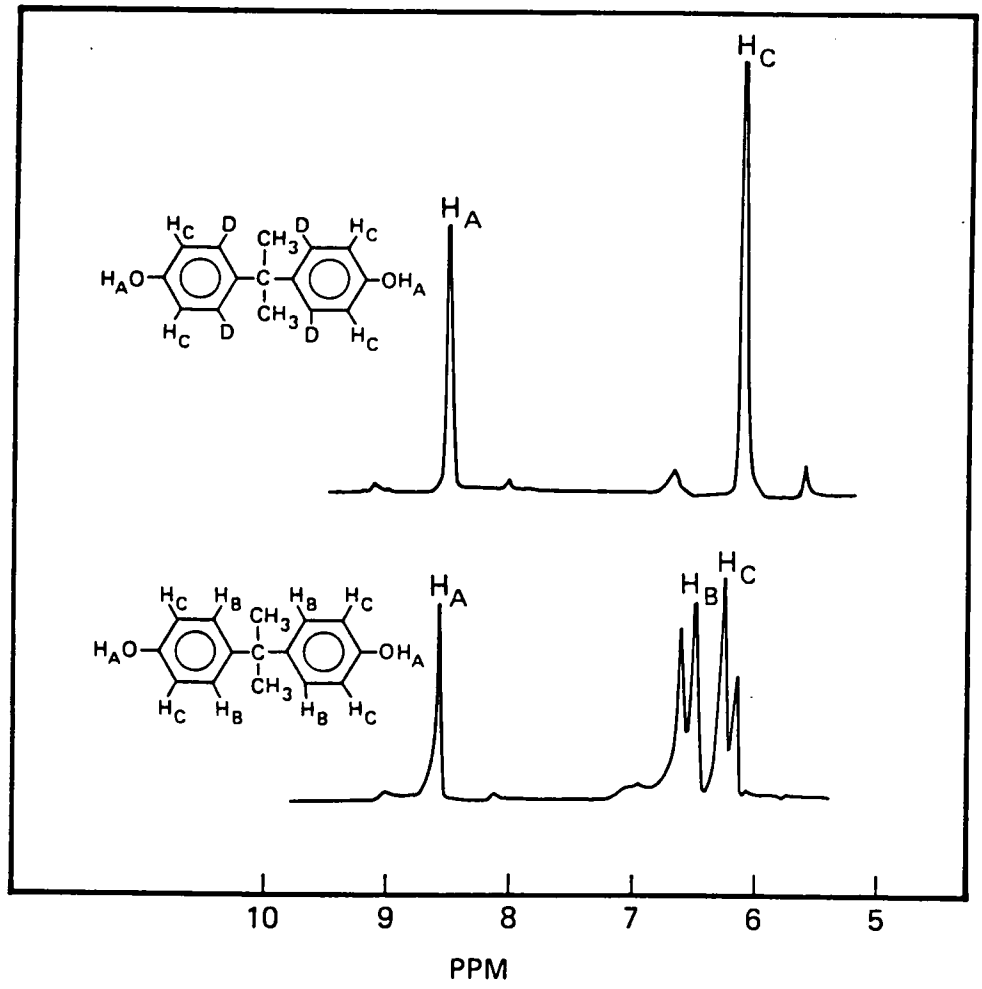

Figure 21. Proton NMR spectra of the aromatic region of (top) D-Bis-A-II and (bottom) commercial hydrogenous bisphenol-A.

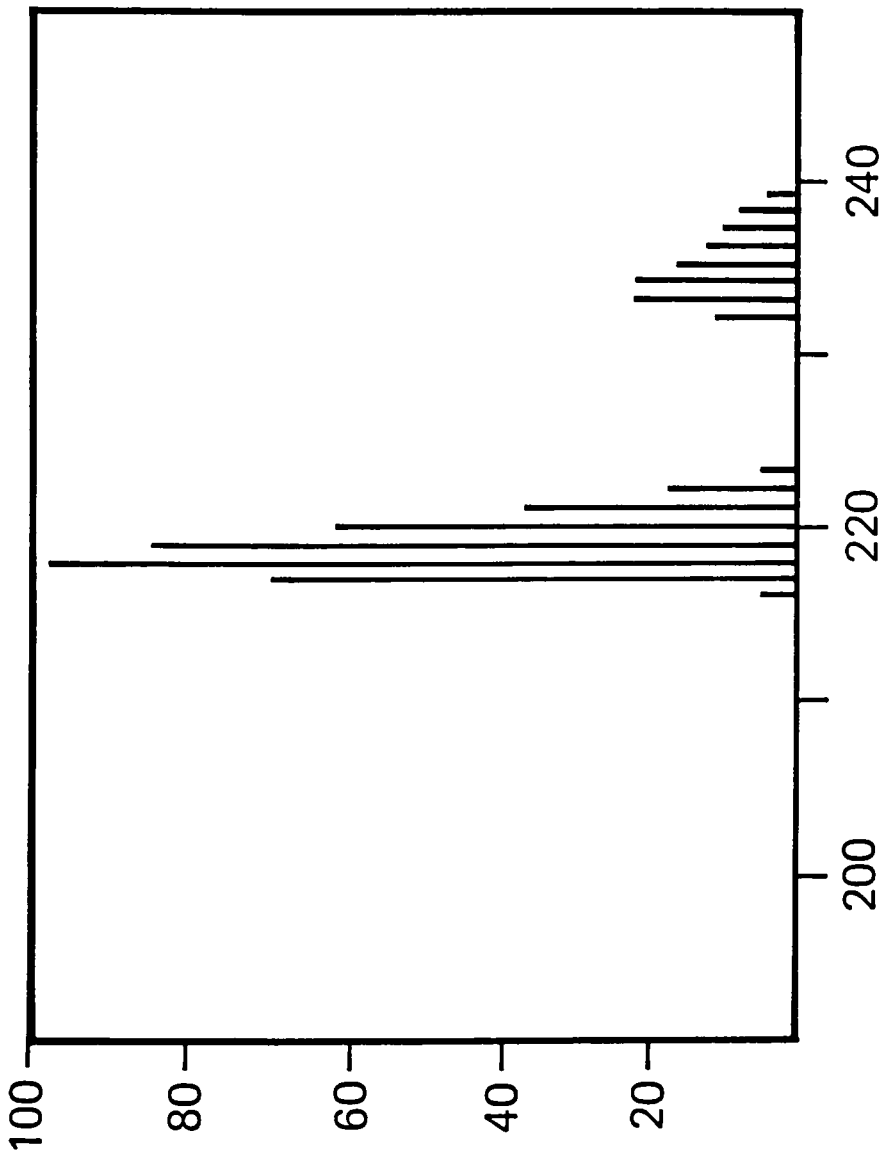

Figure 22. Mass spectrum of D-Bis-A-II.

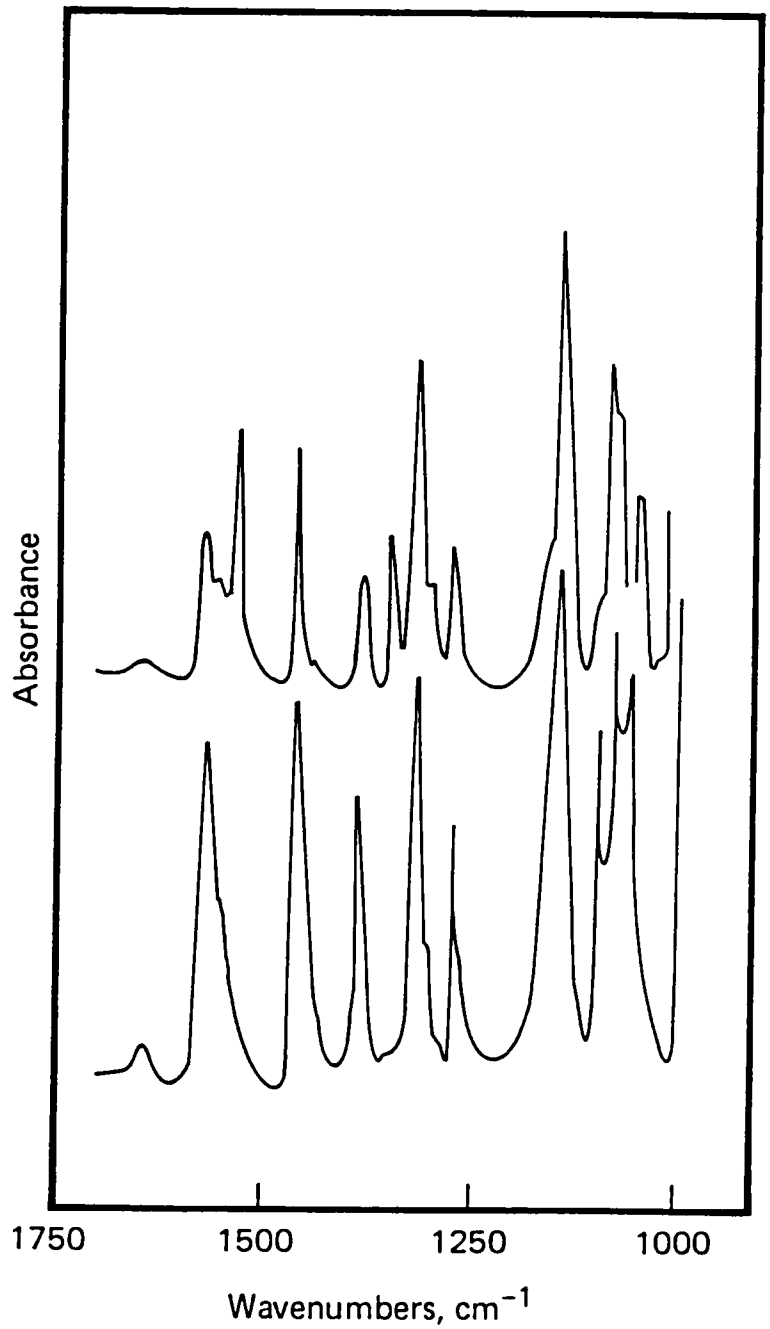

Figure 23. FT-IR spectrum of (top) D-DCDPS-I and (bottom) 4-4'-dichlorodiphenyl sulfone.

TABLE 7

Mass Spectral Data for D-DCDPS-I

m/e	% Intensity	Assignment
290	37.3	M
291	8.1	M + 1
292	26.1	M + 2
294	5.4	M + 4

proceeds first via an "uncharged" intermediate such as 4 which would be more soluble in the reaction medium than the bisphenate formed from 2.

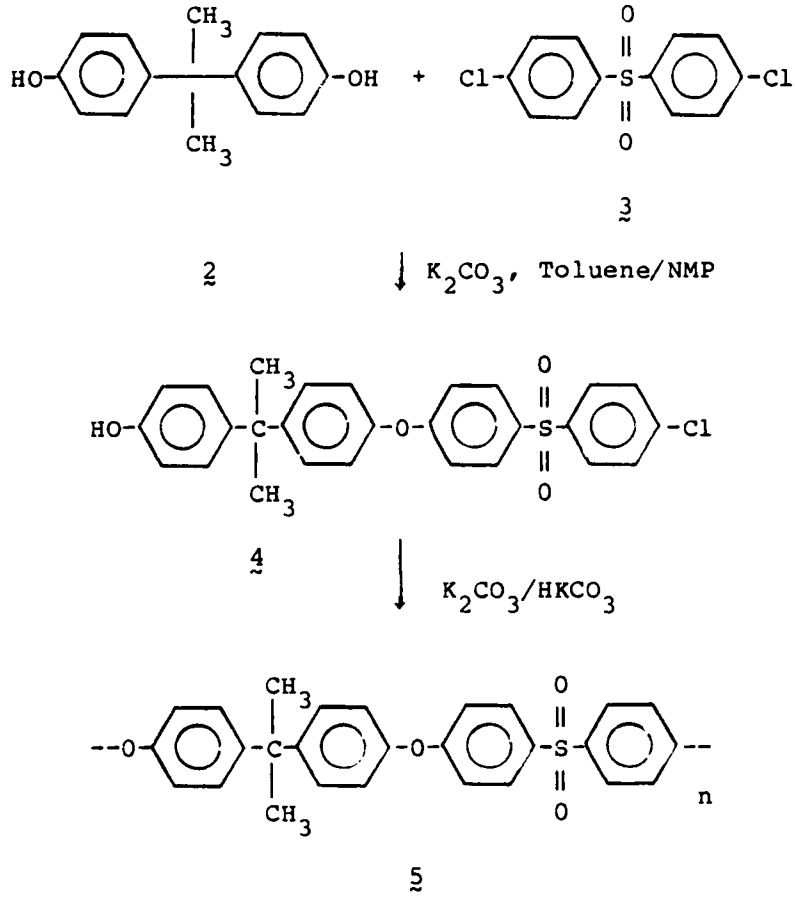

NMP solvates the starting materials, the polar intermediates, and the high molecular weight macromolecule, which is crucial in high polymer synthesis. In addition, the high temperature capabilities of NMP permit shorter reaction times over the conventional aprotic, dipolar solvents commercially used.

Furthermore, by the use of potassium carbonate in the bisphenate formation hydrolytic side reactions typical of strong bases (3,4) may be minimized, allowing the synthesis of high molecular weight macromolecules. When a strong base such as aqueous sodium hydroxide is

used to form the bisphenate, it is essential that a stoichiometric balance be maintained between the phenolic group and the base to achieve high molecular weight. An excess of the base may potentially hydrolyze the activated halide as shown below:

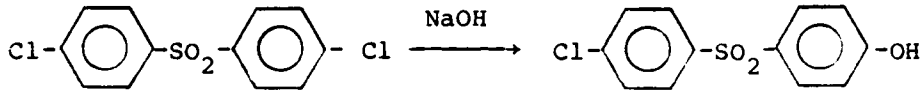

Thus, an imbalance in the stoichiometry is generated between the bisphenate and the activated halide often leading to low molecular weight. Potassium carbonate is a relatively weak base and reacts with the bisphenols only at an elevated temperature and not with the activated dihalide (13,14). So, an excess of K_2CO_3 (up to 50%) may be used without having costly hydrolytic side reactions. This is important when considering the hydroscopic nature of the K_2CO_3.

During the bisphenate formation (i.e., the reaction between the weakly acidic phenol with K_2CO_3) water and carbon dioxide are the major by-products, as shown below:

Scheme 18

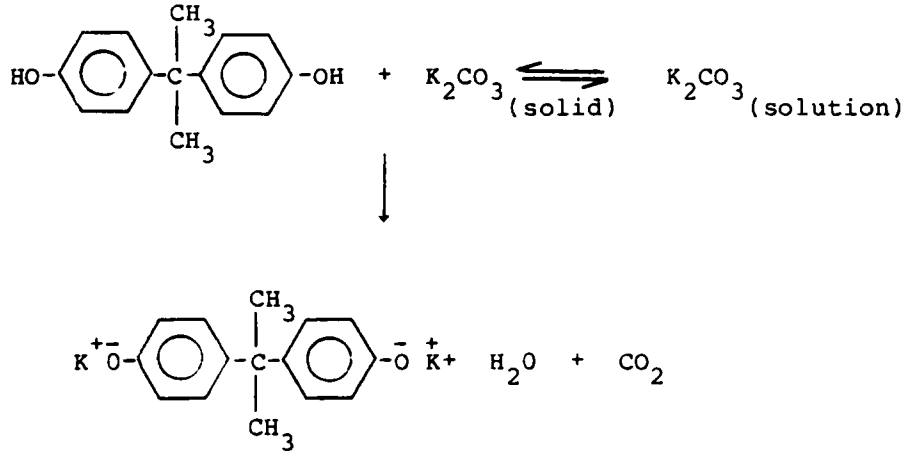

To prevent hydrolysis of the bisphenate it is crucial to remove the water as it is formed, hence shifting the acid-base equilibrium between the water and bisphenate to the right favoring high molecular weight polymer. In an effort to remove the water, toluene was used as an azeotroping agent. The reaction flask (see experimental) was equipped with a Dean Stark apparatus and condenser where the toluene was allowed to reflux. Unfortunately, toluene is relatively nonpolar, limiting the solvation of the polar species and hence serving to slow the reaction down. Furthermore, toluene is a nonsolvent for the high molecular weight polysulfone and must be removed once the bisphenate is formed and water removed. Although these polymerizations are carried out in situ in which the bisphenol, activated dihalide, K_2CO_3, toluene and NMP are charged at once, the above arguments dictate that two reaction temperatures are necessary. At first the reaction mixture is heated to 150°C, favoring the bisphenate formation with minimal polymerization, and upon removal of toluene the reaction is heated to 170-180°C to allow polymerization.

It is also believed that water can cause other side reactions. Namely, at elevated temperatures the water may hydrolyze activated halide or the water may react with the bisphenate forming potassium hydroxide which may also hydrolyze the dihalide.

In general, aromatic halides are unreactive. However, because of the electron withdrawing capabilities of the sulfone group in 4,4'-dichlorodiphenyl sulfone this monomer may react via nucleophilic displacement of the "activated" halide shown below:

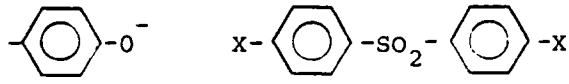

Other groups capable of activating aromatic halides include ketone and nitrile groups shown below.

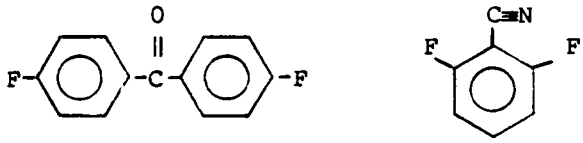

4,4'-Difluorobenzophenone 2,6-Difluorobenzonitrile

These activating groups must be ortho or para with respect to the halogen.

The rate of polymerization is controlled to some extent by the electron withdrawing abilities of the activating group (SO_2,CO,CN). The order of reactivity is $SO_2 \cong CN > CO$.

The nature of the halide is another important consideration in the polymer synthesis. The order of reactivity of the halide is F > Cl > Br. Since the fluorine atom is the smallest and most electronegative atom, it is well able to stabilize the transition state well and is actually the best leaving group.

Therefore, it is the combined effects of the electron withdrawing or activating group and of the halogen atom which determines the reactivity of the monomer. For instance, because the ketone group only weakly activates the halide, fluorine is chosen as the halide because it is a good leaving group and has less steric considerations.

Unfortunately, the fluorine containing monomers are generally more expensive.

Finally, the reaction rate of these nucleophilic aromatic substitution processes is also governed by the basicity of the bisphenate or phenate formed. That is the phenate from Bis-S is a weaker base than the phenate from tetramethyl Bisphenol-A.

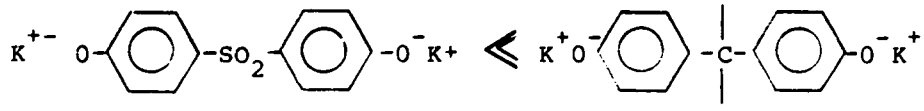

Bis S Salt TMBA Salt

However, insofar as the relative ease of phenate formation the Bis S is more reactive than TMBA.

Four Bisphenol-A polysulfone polymers were synthesized in this current series. By combining the appropriate deuterated and standard hydrogen-based monomers it was possible to prepare selectively labeled polymers. The sites and extent of deuteration and the abbreviations used for these polymers are shown in Table 8.

The intrinsic viscosities and glass transition temperatures for these polymers are given in Table 9 and confirm that a high molecular weight material was produced. The structures of each of the polymers were confirmed by proton, carbon, and deuterium NMR and FT-IR. The integration ratios of proton NMR of the synthesized polymers are in agreement with the calculated ratios based on the dilution of ordinary monomers by the deuterated monomer.

TABLE 8

The Site, Extent of Deuteration and Abbreviations for the Selectively Deuterated Polysulfones

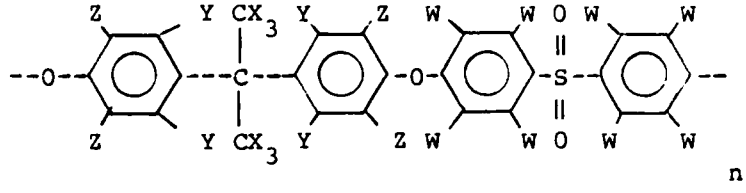

n

Abbreviation	percent of monomer units containing deuterium[a]			
	W	X	Y	Z
D-Bis-A-PSF-I	-	13	-	7
D-Bis-A-PSF-II	5	-	-	-
D-Bis-A-PSF-III	2	-	-	-
D-Bis-A-PSF-IV	-	7	13	-

[a] - indicates no measurable amount of deuterium at this site.

TABLE 9

Intrinsic Viscosity and Glass Transition Temperature Comparison for Partially Deuterated Bisphenol-A Polysulfones

Polymer	$[\eta]^{CHCl_3}$ 25°C	Tg, °C
Bis-A-PSF Hydrogenous	0.48	190
D-Bis-A-PSF-I	0.78	191
D-Bis-A-PSF-II	0.40	189
D-Bis-A-PSF-III	0.54	190
D-Bis-A-PSF-IV	0.77	190

The low temperature β relaxation which occurs at -100°C at 1 Hz has been associated with the tough, ductile mechanical properties exhibited by polysulfone and other engineering thermoplastics. At higher deformation rates the relaxation shifts to higher temperatures; it is this molecular motion which is believed to dissipate the energy associated with an impact affording a tough material.

4.2 Deuterium NMR Results

In a collaborative effort between Dr. L. W. Jelinski and coworkers (142) using solid state deuterium NMR, the molecular moieties and their relaxation times responsible for this transition have been identified. In addition, the effects of a plasticizer (water) and antiplasticizer (dichlorodiphenyl sulfone) on the β transition have been studied.

The lineshapes in deuterium NMR give detailed information concerning the amplitude and frequency of local motions. Figure 24 shows the calculated solid state deuterium NMR spectra for three models of phenyl group motion: (a) static; (b) rapid diffusion about the molecular (1,4-phenylene) axis; and (c) rapid 180° ring flips about the same molecular axis.

Figure 25 shows the deuterium NMR spectra of D-Bis-A PSF-II at various recycle times. It is important to note that the experimentally observed spectra do not correspond to either the slow or fast motion model described earlier (Figure 24). Instead, the lineshape of the experimental spectra appears to be composed of components characteristic of both the slow and fast motions. The contribution of the static components is highest at the largest recycle delay (10 sec). As the

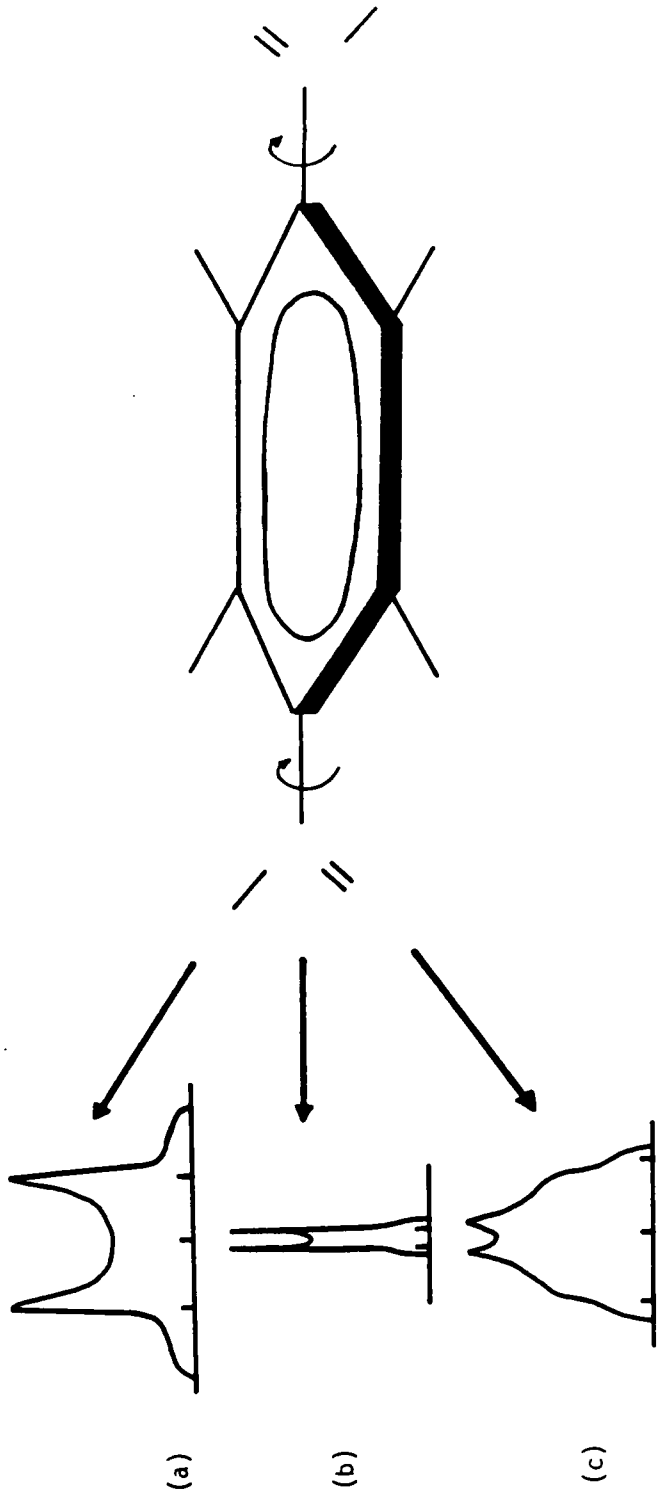

Figure24: Calculated solid state deuterium NMR spectra for three models of phenyl group motion. (a) static; (b) rapid diffusion about the 1,4-phenylene axis; (c) rapid 180° flips about the 1,4-phenylene axis. (Reference 142).

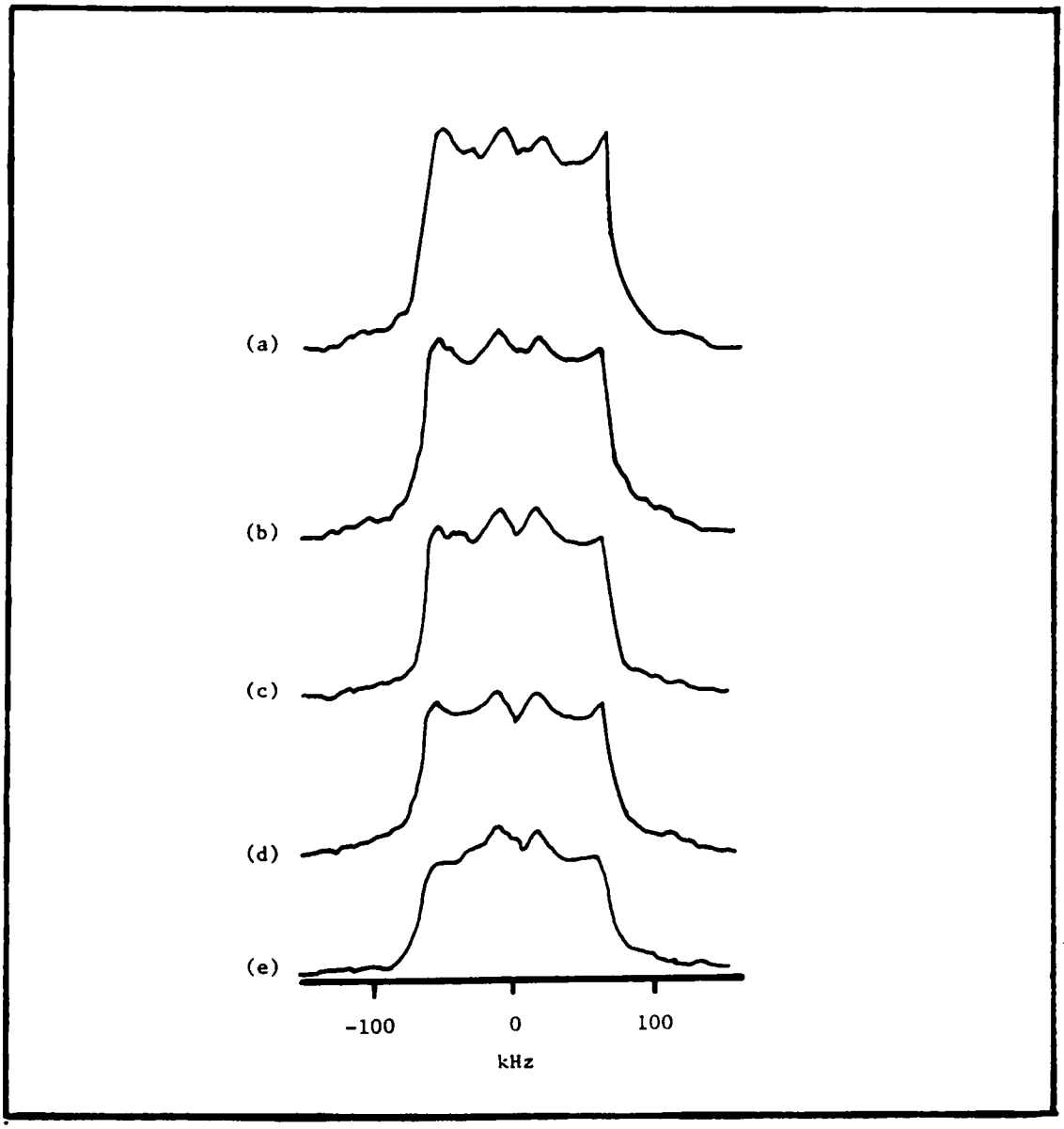

Figure 25: Solid state deuterium NMR spectra of polysulfone II obtained at 23°C and 55.26 MHz using the quadrupole echo pulse sequence. The delay between sequences, T, was set at (a) 10; (b) 5; (c) 3; (d) 2; (3) 1Δ. (Reference 142).

recycle time is lowered the contribution from this decreases, indicating only partial relaxation of the static components. This makes the mobile region (fast motion) the major contributor to the lineshape of the signal (142).

The fast motions arise partly from the ring flips of the phenylene groups. Investigations of the contribution of this to the relaxation of the mobile regions can be followed by selective excitation of the amorphous region using the amorphous quadrupole echo pulse developed by Jelinski et al. (50-52,142). From such experiments it was estimated that 45% of the phenyl rings undergo rapid 180°C flips.

Jelinski et al. found that as the temperature was increased from 23 to 46°C the constraints responsible for the inhibition of the ring flips (the static components) were relaxed as shown in Figure 26. In fact, at temperatures above 46°C only rapid 180°C ring flips were observed. The constraints inhibiting the rapid ring flips were attributed to local chain packing heterogeneities, i.e., entanglements and others.

Figure 27 contains deuterium NMR spectra of D-Bis-A PSF-II, III, and IV. Polysulfone III contains the deuterated isopropylidene linkage and clearly shows rapid rotation about the $C-CD_3$ bond. We found it interesting that each type of phenyl rings, those adjacent to the sulfone group as well as those adjacent to the isopropylidene linkage, show similar behavior.

From the above discussion it was concluded that the primary mode of motion of the aromatic rings is 180° ring flips and these motions are described by a broad distribution of frequencies.

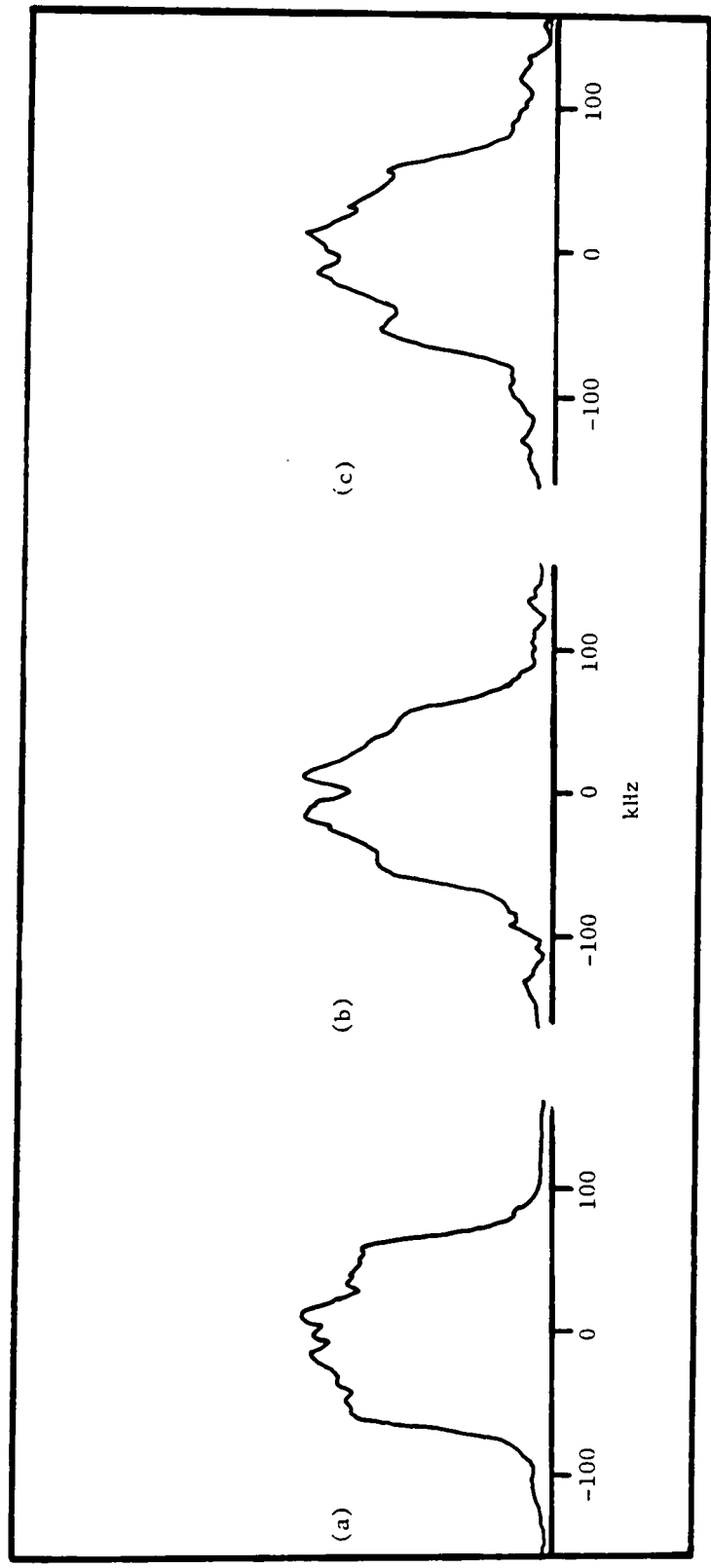

Figure 26 Solid state deuterium NMR spectra of polysulfone II obtained at 55.26 MHz using the amorphous quadrupole echo pulse sequence with a recycle delay of 2Δ. (a) 23°; (b) 46°; (c) 75°C. (Reference 142).

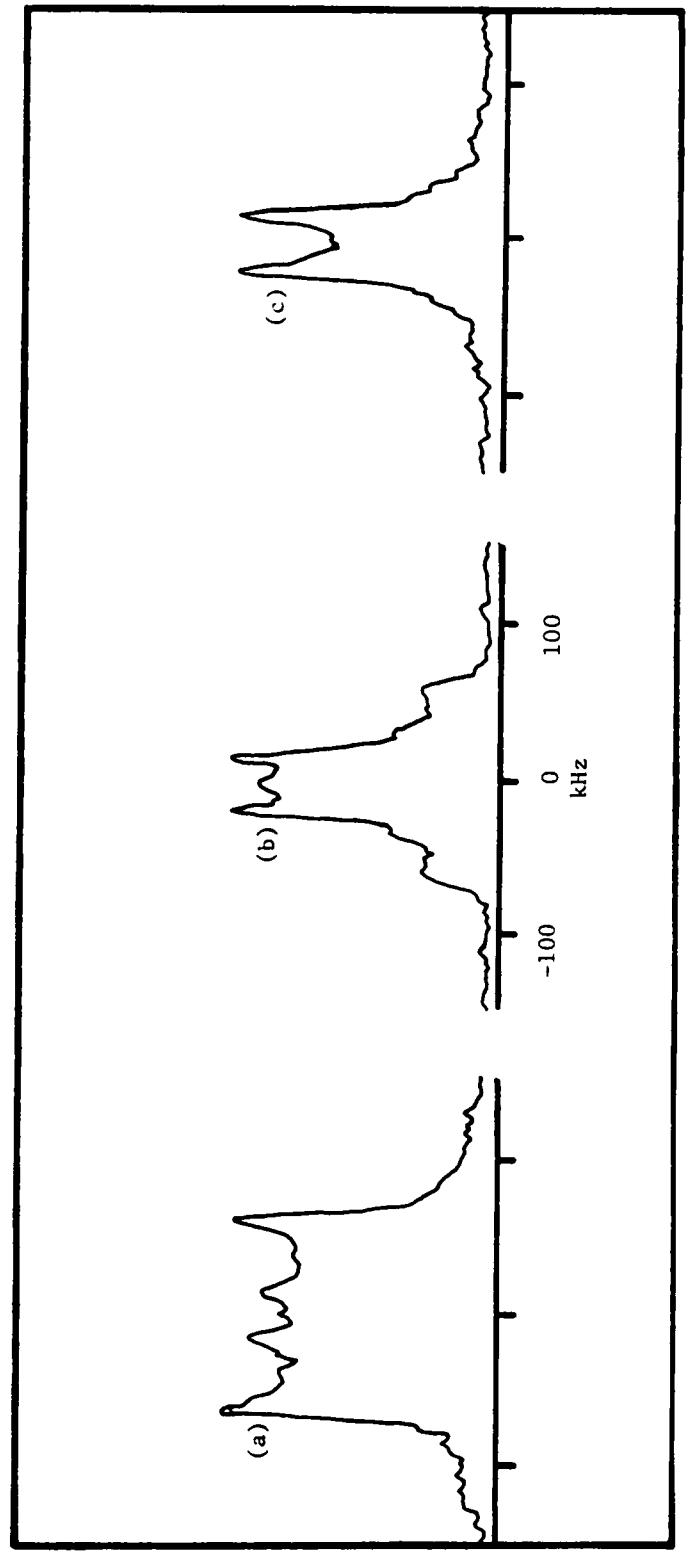

Figure 27. Comparison of the solid state deuterium NMR spectra of polysulfones II (a); III (b); and IV (c). All spectra were obtained at 23°C and 5526 MHz using the quadrupole echo pulse sequence with a recycle delay of 10 s. (Reference 142).

The next major question is how can one relate this molecular motion and hence the β relaxation to the ductile mechanical properties associated with these engineering thermoplastics. The addition of antiplasticizer to engineering thermoplastics has been shown to increase the modulus and significantly decrease the toughness. In addition, the secondary relaxations in these systems are depressed. The addition of dichlorodiphenyl sulfone (DCDPS) is known (35) to be an antiplasticizer for polysulfone. Jelinski and coworkers found that blends of DCDPS with deuterated polysulfone (20 and 40 % wt. DCDPS) change the deuterium NMR lineshapes. In these blends the static component predominated the spectra, and it is believed that free volume arguments prevent 180° ring flips.

Recently, considerable attention has been given to the semi-crystalline poly(ether ether ketone) because of its solvent resistance and good mechanical properties. However, very little has been reported on the fracture toughness, β relaxation, and molecular motions in this structure. Indeed, PEEK has a secondary relaxation (-70°C at 110 Hz) which is considerably smaller in magnitude than polysulfone. Figure 28 contains a plot of tan δ versus temperature for a quenched (amorphous) PEEK film.

Selectively deuterated PEEK was synthesized in an effort to assess molecular motions as a function of crystallinity. In addition, we plan to make fracture toughness measurements and dynamic mechanical measurements as a function of thermal history. These investigations are in progress and will be published later in the open literature.

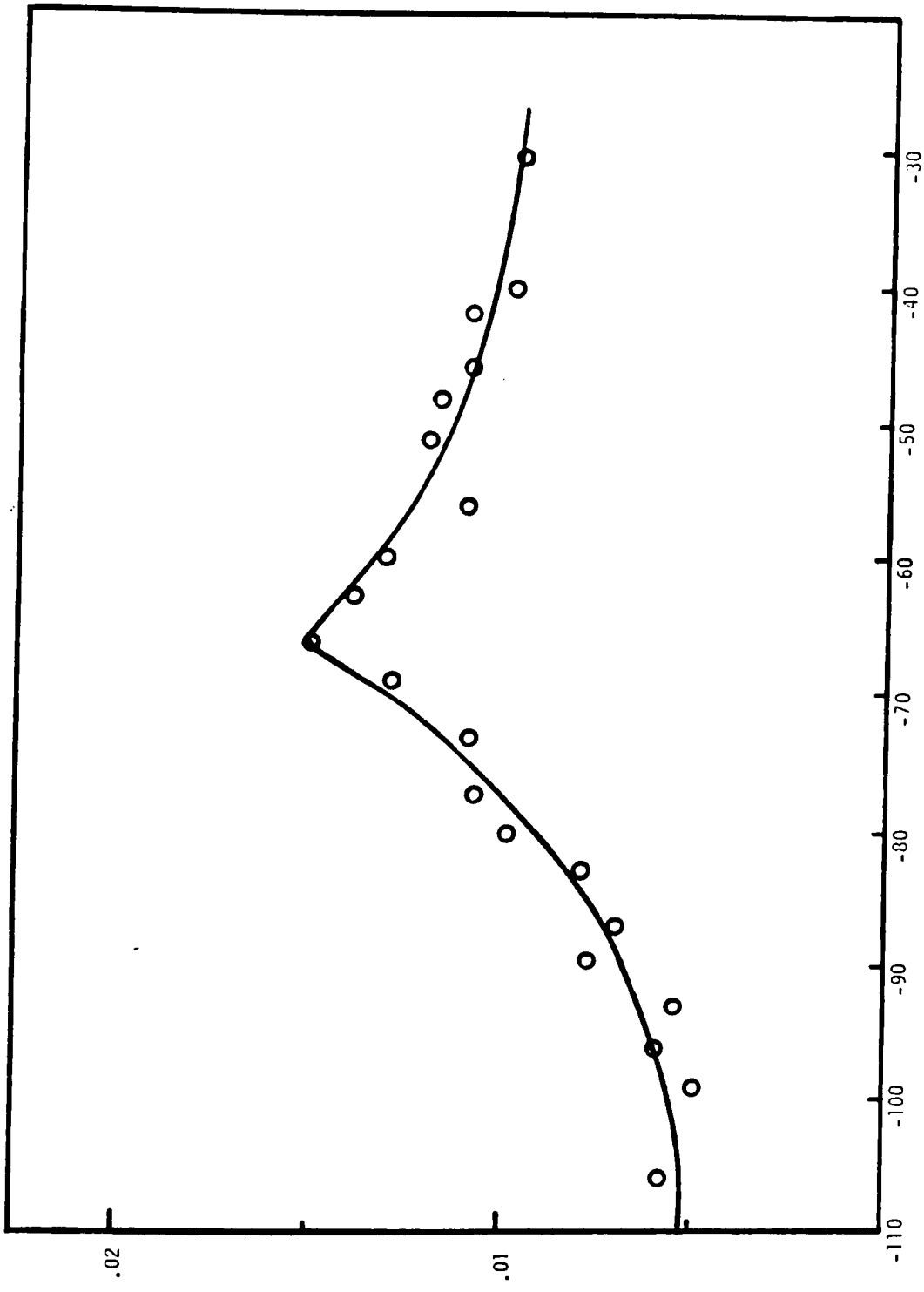

Figure 28. Tanδ versus temperature plot for quenched PEEK.

4.3 Toughening of Polymeric Materials

4.3.1 Thermoplastics

Engineering thermoplastics such as the polysulfones are a class of tough, ductile materials, and this toughness is believed to stem from localized, sub-Tg molecular motion. However, there is no doubt that the impact strength of these amorphous thermoplastics can be further increased if one initiated additional energy absorption mechanisms. Crazing and shear deformation are such energy absorption mechanisms. In recent years, the incorporation of elastomeric modifiers has served as a successful means of enhancing the fracture strength of both brittle and ductile materials. A classic example is high impact polystyrene (HIPS) in which styrene is polymerized in the presence of polybutadiene. The polybutadiene phase separates from the matrix giving rubbery particles which have good interfacial adhesion since some of the polystyrene is grafted onto the unsaturated sites promoting some miscibility. The rubbery particles, have a different (lower) modulus than the polystyrene matrix and serve as stress concentrators which can initiate energy absorbing processes such as crazing. In general, a tougher material is obtained.

Block or segmented copolymers of two dissimilar components have also been used as potential modifiers for various thermoplastics. If one segment is the same or similar to the material being modified good interfacial adhesion should result between the particles and the matrix. Polysulfone-poly(dimethylsiloxane) block copolymers blended with UDEL^{R} is such a compatible blend, in which the polysulfone in the block

copolymers is believed to provide partial miscibility, thus promoting good interfacial adhesion.

The poly(dimethylsiloxane)-polysulfone block copolymers were chosen for blending with Udel^{R} polysulfone for several reasons. One reason is the relative ease of synthesis of the perfectly alternating block copolymers, as well as the fact that well-defined copolymers result. This is important since the elucidation of structure-property relationships requires careful, well-controlled, and well-defined synthetic techniques. The synthetic route employed here, the silylamine-hydroxyl condensation, leads to the formation of perfectly alternating block copolymers where each oligomer and, hence, each block can be characterized independently before copolymerization as reported by Noshay and coworkers (143-164).

Another reason for studying this system is that many questions such as the detailed nature or cause of the improved impact resistance were left unanswered by the earlier study. The nature of the "domains" formed in these blends was only briefly addressed. Surface science instrumentation has improved drastically in the past ten years and so the possible role of the preferential segregation of the poly(dimethylsiloxane) to the surfaces of materials such as this in improving the impact resistance of these materials has not been previously considered. Thus, it is hoped that further study of these blends may lead to generalizations which can then be applied, in turn, to the modification of other polymers.

4.3.1.1 Synthesis and Properties of Block Copolymers

Polysulfone oligomers of predictable molecular weight were synthesized using the N-methyl pyrrolidone/potassium carbonate synthetic route as shown in Scheme 19. An excess of the Bisphenol-A monomer as predicted by the Carothers equation was used to obtain phenolic hydroxyl terminated oligomers of predictable molecular weights ranging from 4,000 to 15,000 Mn as determined by potentiometric titration of the weakly phenolic end groups. Table 9 contains some molecular weight characterization of these functionally terminated oligomers. For these low molecular weight oligomers a higher concentration of solids was used; upon completion the reaction mixture became fairly viscous depending on the molecular weight. In each case, the solution was dark brown indicating degradation of the solvent had indeed occurred.

The α,ω-bis(dimethylamino)-terminated poly(dimethylsiloxane) oligomer can be synthesized by a variety of methods. One convenient synthesis utilizes a base (KOH or tetramethylamonium silanolate) catalyzed equilibration of D_4 (cyclic tetramer) with a low molecular weight dimethylamino terminated poly(dimethylsiloxane) oligomer as shown in Scheme 20. The D_4 and functionally terminated oligomer were heated to 80°C prior to the addition of the catalyst. Upon addition of the catalyst the reaction mixture became extremely viscous and cloudy. However, after about six hours the viscosity decreased and the equilibration became clear. The viscosity decrease was believed to result from the incorporation of the functional end blocker and subsequent breakdown in molecular weight. Each of the oligomers were then stripped under vacuum to remove the cyclics (~10%) remaining from the

SCHEME 19

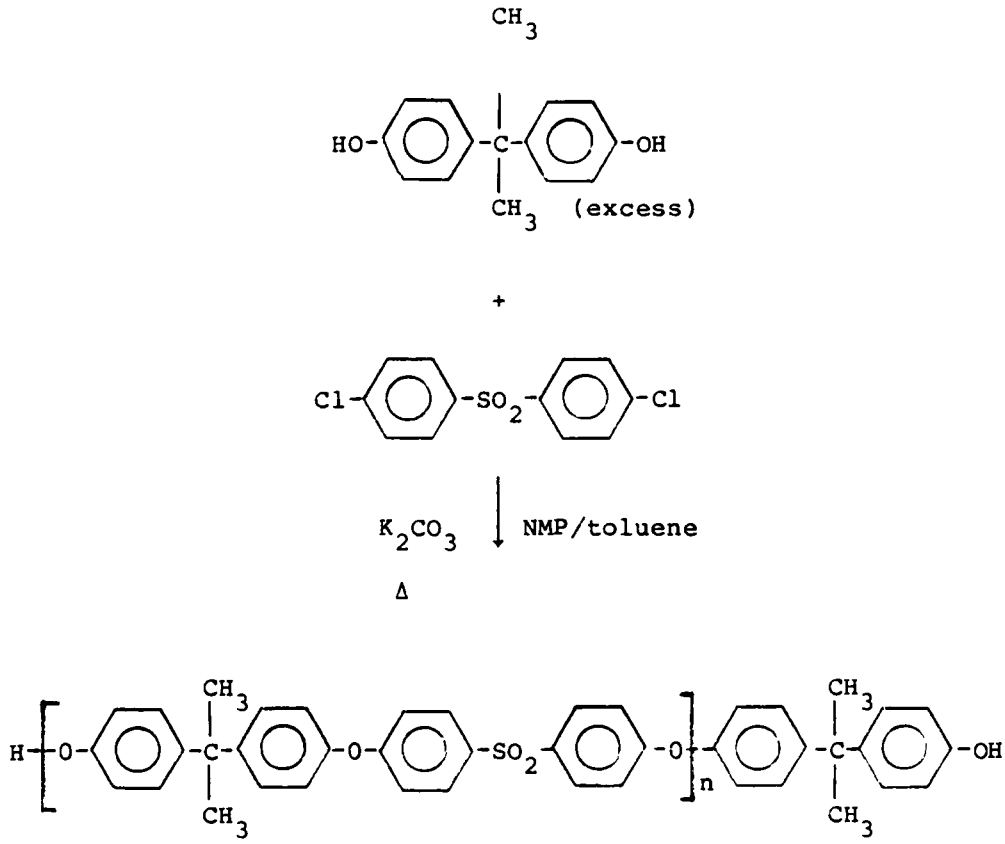
CH3
HO
C
OH
CH3
(excess)
+
Cl
SO2
Cl
K2CO3
NMP/toluene
Δ
H
O
CH3
C
CH3
O
SO2
O
n
CH3
C
CH3
OH

Table 9

Characteristics of Polysulfone Oligomer
Number Average Molecular Weight

End Group Analysis

Sample No.	Theory	Actual
1	5000	4,900
2	10,000	8,600
3	10,000	9,700
4	15,000	13,400
5	20,000	17,000

Scheme 20

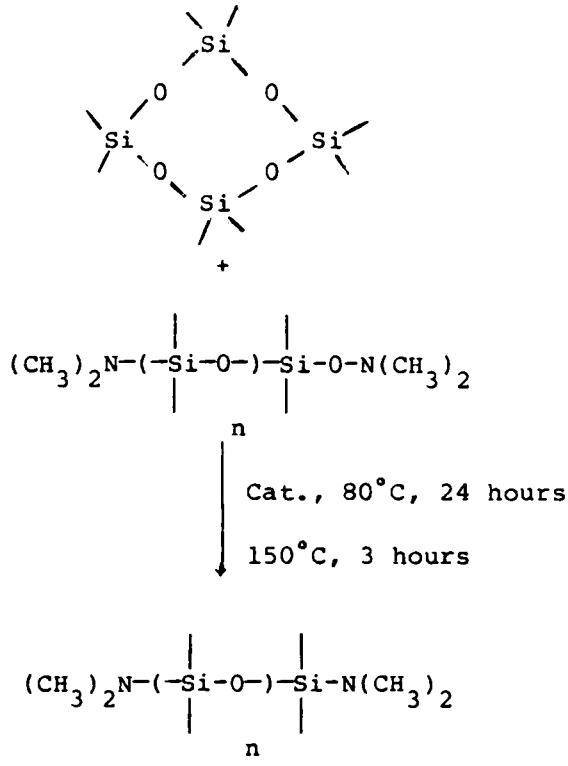
Si
O
O
Si
Si
O
O
Si
+
(CH3)2N-(-Si-O-)-Si-O-N(CH3)2
n
Cat., 80°C, 24 hours
150°C, 3 hours
(CH3)2N-(-Si-O-)-Si-N(CH3)2
n

equilibration. The siloxane block size can be controlled by the ratio of α,ω-amino-terminated siloxane oligomer to cyclic siloxane and can be measured by utilizing a potentiometric titration of the amine end groups. Table 10 contains the functionally terminated oligomers synthesized.

The poly(dimethylsiloxane)-polysulfone block or segmented copolymers were synthesized using Noshay's procedure, the silylamine-hydroxyl condensation as shown in Scheme 21 (154). This involves the interaction of preformed dihydroxyl-terminated polysulfone oligomers and bis(dimethylamine)-terminated poly(dimethylsiloxane) oligomers in chlorobenzene at reflux temperatures. The evolution of the dimethylamine by-product at these temperatures leaves an essentially pure solution of block copolymer. This is a very fast reaction due to the high reactivity of the Si-N bond of the siloxane oligomer towards the phenolic hydroxyl end groups of the polysulfone. High molecular weights are easily obtained for those preformed block lengths of moderate length (5,000 - 10,000 <Mn>).

During the polymerization of several unique phenomena were observed. Upon addition of the poly(dimethylsiloxane) to the refluxing solution of polysulfone, the developing copolymer would precipitate from solution. By dropping the temperature 10°C, the precipitated polymer would go back into solution and the mixture would once again be homogeneous. It is difficult to explain this behavior because of the complexity of the mixture. That is, both unreacted oligomers as well as copolymers may produce a rather unique blend at this point in the polymerization. One possible explanation is that the lower critical

Table 10

Characteristics of Poly(dimethylsiloxane) Oligomer Number Average Molecular Weights

End Group Analysis

Sample No.	Theory	Actual
1	5000	4,400
2	10,000	12,800
3	20,000	18,700

Scheme 21

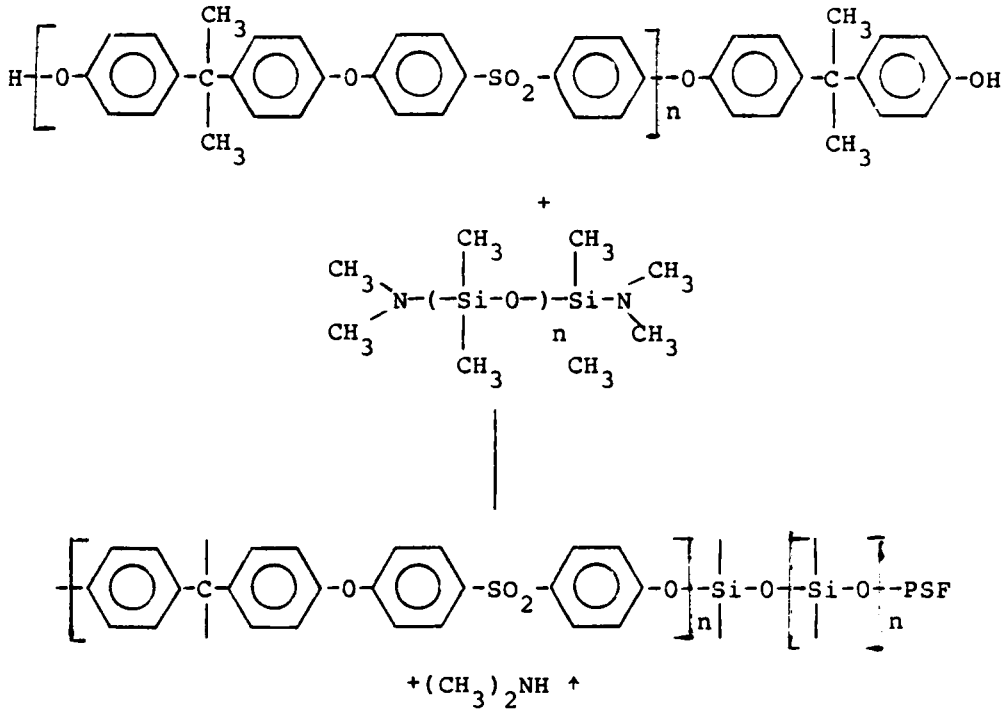

solution temperature is reached at chlorobenzene reflux temperatures. However, uneven heating effects may also cause this precipitation.

The structure of the block copolymers is very well defined and controlled because the preformed oligomers can only condense with each other and not with themselves. As a consequence, the number average segments in the block copolymer are essentially identical to those of the oligomer starting materials, although there will be a certain distribution of segments which reflects polydispersity. However, by characterizing the oligomers prior to copolymerization, the blocks in the subsequent copolymer are reasonably well characterized.

The end blocks of the block copolymers are designed to be polysulfone by controlling the final stoichiometry of the reaction. This removes the hydrolytically unstable silylamine end group. In

addition, this produces a more idealized elastomer by removing "dangling" chain end effects.

A variety of copolymers were successfully synthesized by this technique as illustrated in Table 11. The molecular weight of the oligomers ranged from 4,000-20,000 g/mol^{-1}. The copolymers utilizing the lower molecular weight oligomers were the most easily synthesized due to the abundance of reactive end groups. High molecular weights were also obtained in each of these structures as indicated by the intrinsic viscosity values, also included in Table 11. The recovered yields were all about ninety percent or higher and all of the copolymers formed clear, tough films when cast from chloroform.

An important feature involved in the synthesis of these structures is the necessity of minimizing homopolymer contamination. It is very difficult to remove any unreacted polysulfone. Furthermore, homopolymer contamination typically yields both a cloudy solution and cast film effects. The mechanical properties are no doubt altered as well. GPC was utilized to indicate the distribution of species in the copolymer. Figure 29 shows the GPC traces for several of the copolymers. It is important to note that in each case a unimodal molecular distribution is obtained.

Both the polysulfone and the poly(dimethylsiloxane) homopolymers show excellent thermal and oxidative stability. Therefore, as discussed earlier by Noshay et al. (160,164), it is not surprising that the copolymers show these properties as well. Thermogravimetric analysis measurement under nitrogen shows the onset of weight loss at 400°C as indicated in Figure 30. In addition, a "char yield", in direct

proportion to the siloxane content, is observed when samples are tested in an air atmosphere. It is believed that the poly(dimethylsiloxane) decomposes into an at least partially inorganic compound (glass) (163). This is believed to be important in flammability and for possibly other considerations.

Furthermore, these copolymers show surprisingly excellent hydrolytic stability, primarily due to the hydrophobic nature of the siloxane blocks, the two phase system and the low concentration of the water susceptible carbon-oxygen-silicon linkages (153).

The morphology of these segmented systems is fairly unique because of the contrasting properties of each of the components involved (157,163):

(A) A large difference in the glass transition temperature;
(B) A large difference in the permeability to common gases;
(C) A large difference in solubility parameters.

In addition, there is a large enough electron density contrast between the two components that SAXS and TEM analysis may be performed without further modification. This is one of the few reports in the literature in which the staining of one segment (to produce electron density contrast) was not required, and hence techniques such as SAXS and TEM could be better compared.

Robeson and coworkers (151) have extensively investigated the physical properties of these polysulfone-poly(dimethylsiloxane) copolymers as well as the morphology to some extent. However, many questions were left unanswered such as the degree of phase separation, the depression of the polysulfone Tg, and the phase separation effects on the mechanical properties. In a collaborative effort with Dr. Dinesh

TABLE 11

Characterization of PSF/PSX Block Copolymers

Sample	$\bar{M}n$ of Oligomer PSF / PSX	$[\eta]_{CHCl_3}$ 25°C	Low Temperature Transitions[a] Tg	Tc	Tm	High Temperature Transition[a] Tg
1	4,900 / 4,400	0.67	-127	-	-	147
2	4,900 / 4,400	0.60	-125	-	-	139
3	8,600 / 4,400	0.67	-128	-99	-51	189
4	4,900 / 12,800	0.55	-126	-99	(-62,-50)	120
5	9,700 / 12,800	1.27	-124	-86	-47	143
6	13,400 / 12,800	1.14	-127	-	(-62,-48)	-
7	17,000 / 4,400	1.03	-	-	-44	187
8	17,000 / 12,800	1.00	-130	-90	-43	189

[a] DSC, Perkin-Elmer-2, 10°/min.

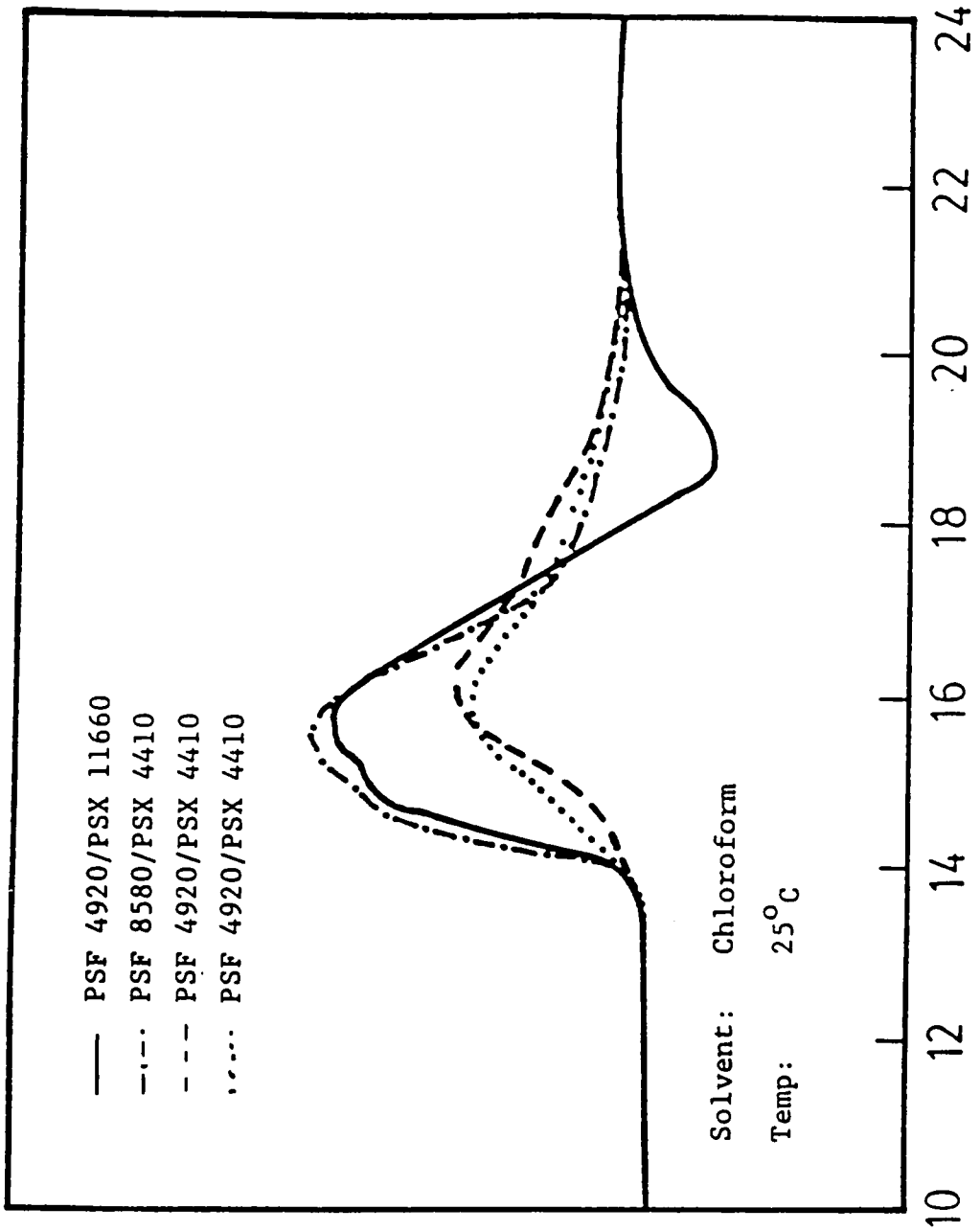

Figure 29. GPC traces for several siloxane-sulfone copolymers.

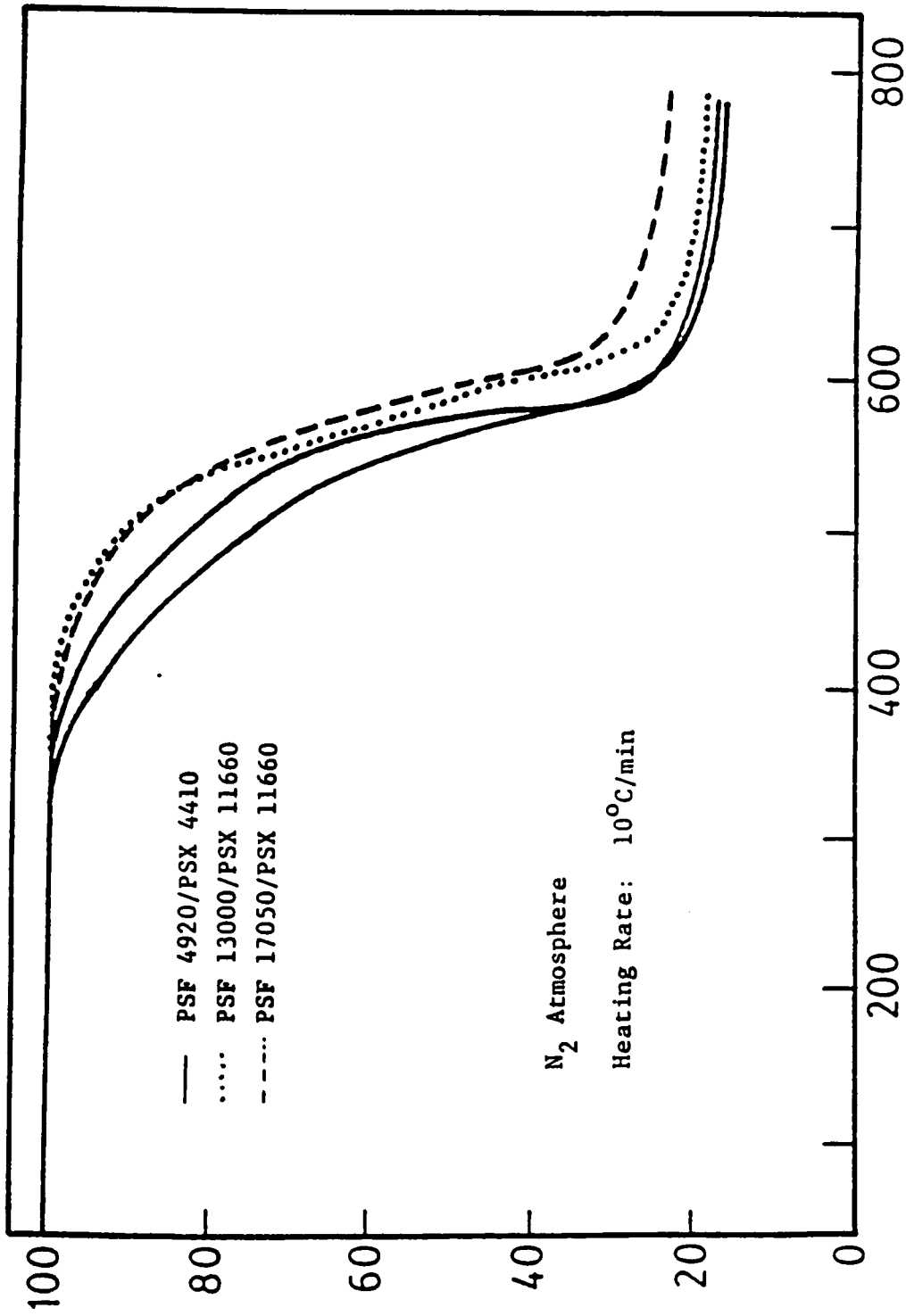

Figure 30. Thermal gravimetric analysis of several siloxane-sulfone block copolymers.

Tyagi and Professor Garth Wilkes (164) of the Chemical Engineering Department at Virginia Polytechnic Institute and State University, we have extended this early work using a wide variety of techniques, including SAXS, TEM, and thermal and mechanical analysis in an attempt to better understand how the morphology effects the properties.

It is well-known that the morphology of the copolymers can be controlled by varying the molecular weight of the oligomers (163). At lower block lengths (~2000 g/mole <Mn>) a single phase block copolymer resulted (163). However, at molecular weights above 4,000 g/mole <Mn> a two phase morphology is produced as evidenced by domain formation. The latter copolymers display two glass transition temperatures: one at -120°C due to the soft domain and another in the 160°C range due to the hard domain. Furthermore, it is interesting to note that the poly(dimethylsiloxane) blocks of higher molecular weight (>13,000 g/mole) display a low temperature melting endotherm (~-52°C). Often this is a dual melting endotherm as seen in sample 4 in Table 10. Dual melting endotherms have also been observed in PET (165) and PEEK (166). The position of the Tg for the PSX segment does not appear to be dependent on the molecular weight of either component because all of the soft segments are above their critical molecular weight. In addition, this indicates that a minimal amount of polysulfone resides within the poly(dimethylsiloxane) domains.

The dynamic mechanical storage modulus and tan δ of solution (chloroform) cast films are shown in Figure 31 for several block copolymers. The two phase morphology can clearly be seen. In each case a transition near -115°C can be observed corresponding to the glass

transition temperature of the soft segment. The melting transition of the higher molecular weight siloxane blocks can also be detected (Figures 31). Interestingly, the β transition (-100°C, 1 Hz) for the polysulfone is not observed. It is believed (35) that this transition is highly molecular weight dependent.

In each case, the storage modulus in the rubbery plateau region is proportional to the polysulfone content in the copolymer. The rubbery plateau is the highest for the copolymer in which the hard (polysulfone) segment is the greatest and can be attributed to the continuity of the polysulfone phase. In contrast, copolymer PSF 4,900/PSX 12,800 shows the largest drop in the storage modulus, suggesting that the poly(dimethylsiloxane) is the continuous phase and the polysulfone phase serves as physical junction points for the network type structure. The latter sample is referred to as a thermoplastic elastomer.

The glass transition of the polysulfone block in the copolymer shows a strong dependence on molecular weight. Both thermal analysis and dynamic mechanical analysis show that polysulfone blocks of lower molecular weight (<12,000 g/mole) experience an appreciable depression in the glass transition temperature relative to the polysulfone oligomer. This might indicate a significant amount of siloxane in the polysulfone domains or phase mixing. Furthermore, the breadth of the upper transition is extremely broad as well as being depressed. This may reflect the broad molecular weight distribution (Mw/Mn = 2) in each of the starting oligomers. The transition breadth is surprising in light of the large solubility parameter difference ($\Delta\delta \cong 3$) between the two components. Furthermore, this phase mixing (possibly with some very

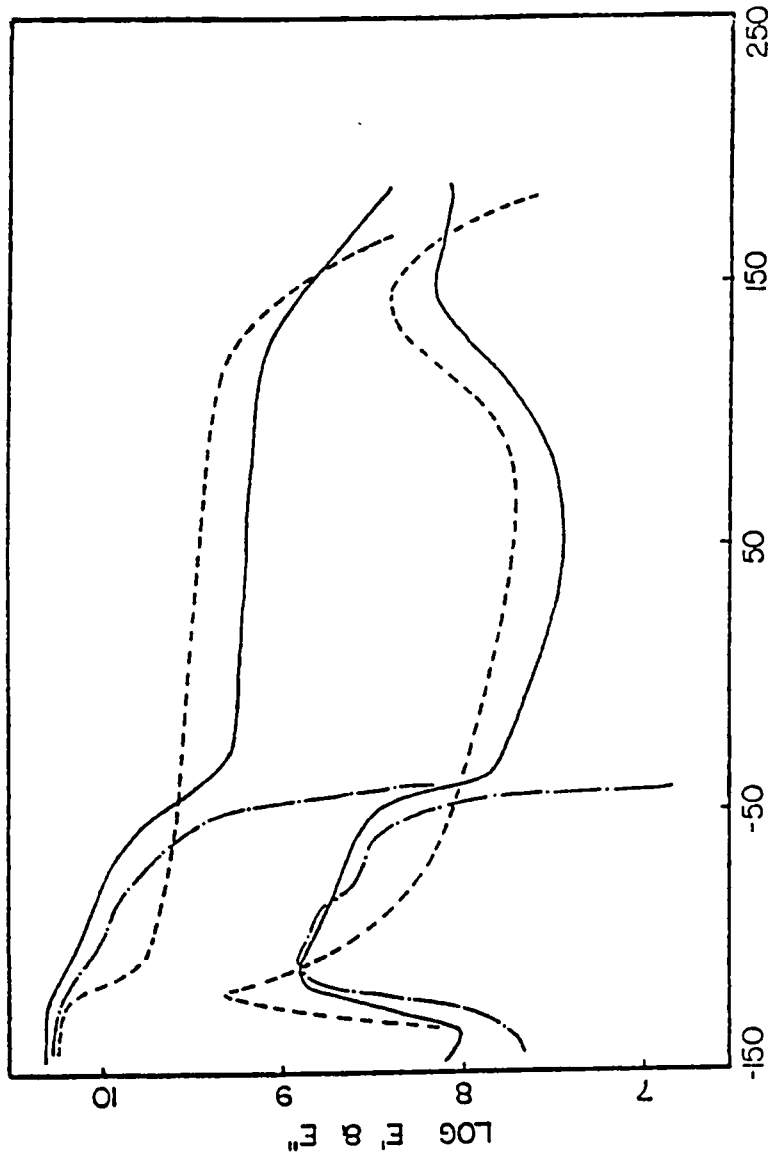

Figure 31. Dynamical Mechanical measurements for (-----) PSF-4900/PSX4400, (------) PSF9700/PSX12800 and (-----) PSF4900/PSX12800. (110 Hz). (Reference 165).

slow polysulfone blocks) will no doubt effect the mechanical properties. Robeson et al. (151) showed that a Tg of 190°C for the hard block was obtained when the polysulfone block length exceeded 12,000 <Mn>. We have found similar results by using high molecular weight polysulfone blocks. Samples 7 and 8 from Table 11 illustrate that when a 17,000 <Mn> polysulfone block is used, the Tg of the hard block approaches 190°C. This is in contrast to the low Tg's found in Samples 4 and 5 which contain 4,900 and 9,700 <Mn> polysulfone blocks.

Therefore, one must conclude that solubility parameter alone does not dictate phase separation, but block length as well as a host of other variables (i.e., thermal history, solvent, etc.) control phase separation.

Figures 32 contain TEM micrographs of copolymers 1,4,5,6 from Table 11 and provide further visual conformation of the two phase morphology. In these micrographs (50,000 magnification) the darker regions correspond to the siloxane phase while the lighter regions correspond to sulfone domains. For copolymer 1 each phase appears equally continuous. As the molecular weight of the siloxane block (copolymer 4) is increased the interdomain spacing increases and the soft segment becomes the continuous phase. As expected, as the molecular weight of both blocks is increased (copolymer 5) the interdomain spacing increases as well. The interdomain spacing measured from the micrographs is given in Table 12. Tyagi and coworkers (165) measured the interdomain spacing using SAXS, and these results are also included in Table 12. It is interesting to note the good correlation between the two techniques. There is enough electron density contrast between the two components so

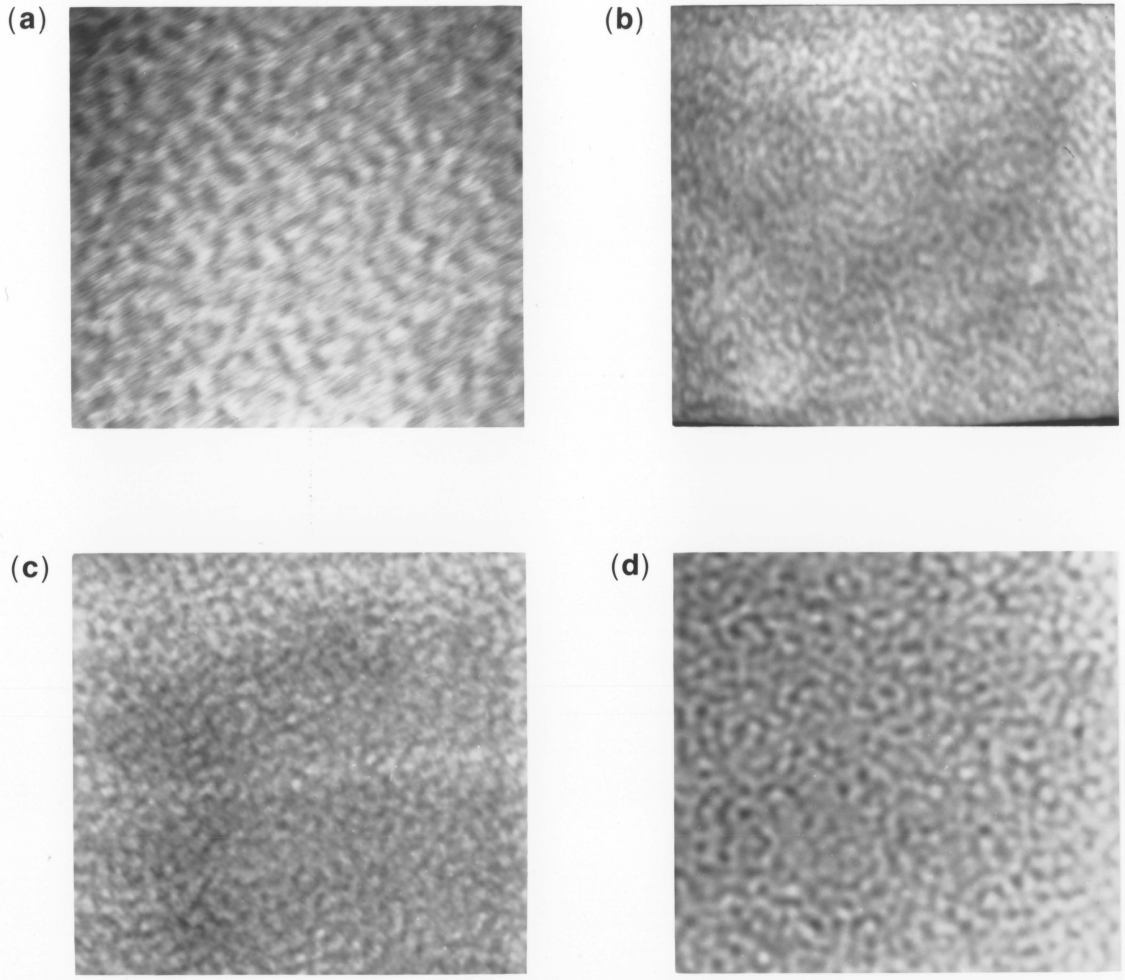

Figure 32. TEM micrographs of PSF/PSX block copolymers >(100,000×).
(A) PSF(4400)/PSX(4900), (B) PSF(4900)/PSX(12800), (C) PSF(9700)/PSX(12800) and (D) PSF(9700)/PSX(6700).

TABLE 12

Comparison Between Interdomain Spacing from SAXS and TEM

Sample	ID Spacing, nm (TEM)	ID Spacing, nm (SAXS)
PSF4900/PSX4400	16.0 ± 2.0	18.0
PSF4900/PSX12800	24.0 ± 2.0	21.0
PSF9700/PSX12800	36.0 ± 2.0	31.0
PSF9700/PSX6700	20.0 ± 2.0	24.0

that staining was not required. Thus, TEM and SAXS results could be easily compared. In addition, an extensive investigation on the morphology has been performed (164) using a variety of complementary techniques.

Another interesting feature of these segmented copolymers is the retention of their physical network structure in the melt. Matzner et al. (158) attributed this phenomenon to the large difference in solubility parameters between the two. These workers concluded that a differential solubility parameter between the two components should be preferable less than one in order to obtain good melt processability. Unfortunately, the polysulfone-poly(dimethylsiloxane) block copolymers show an extremely high melt viscosity and rheological data using a parallel plate attachment on the rheometrics instrument could not be obtained.

There are several structural modifications possible to decrease this large solubility parameter difference. For instance, tetramethyl bisphenol-A polysulfone oligomers could be used as the hard segment which has a solubility parameter of (9.4) lower than Bisphenol A polysulfone 10.2.

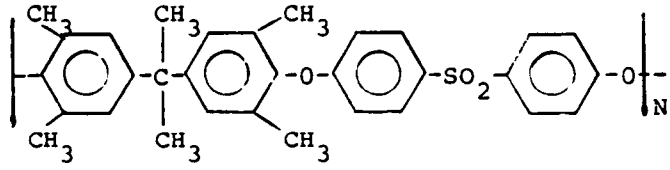

TMBA PSF $\delta = 9.4$

In addition, these segmented structures may show some interesting gas permeation characteristics.

One could also vary the soft segment structure to increase its solubility parameter. For instance, coequilibrations using the tetramer form of either diphenylsiloxane or the trimer of trifluoropropylmethylsiloxane together with dimethylsiloxane.

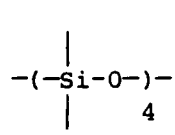

Diphenylsiloxane

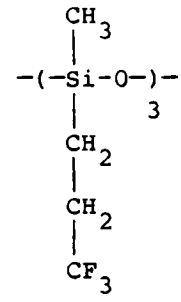

Trifluoropropylmethylsiloxane

The mechanical properties of these block copolymers are no doubt affected by the relative composition of each block in the copolymer. Figure 33 contains the engineering stress strain curve for copolymers (180) which were prepared from solution casting with chloroform. These results which are also tabulated in Table 13. These results are similar to those reported (164) earlier on the same system. The mechanical properties are affected by the amount of polysulfone contained in the system. For instance, copolymer 4, in which the polysulfone is the discrete phase, behaves as a thermoplastic elastomer (i.e., high elongations (~300%), low modulus, reversible deformations, etc.). In contrast, copolymers 1 and 5 which have a polysulfone continuous phase exhibit high modulus characteristics and undergo a yield (i.e., plastic deformation). The latter materials behave as engineering thermoplastics.

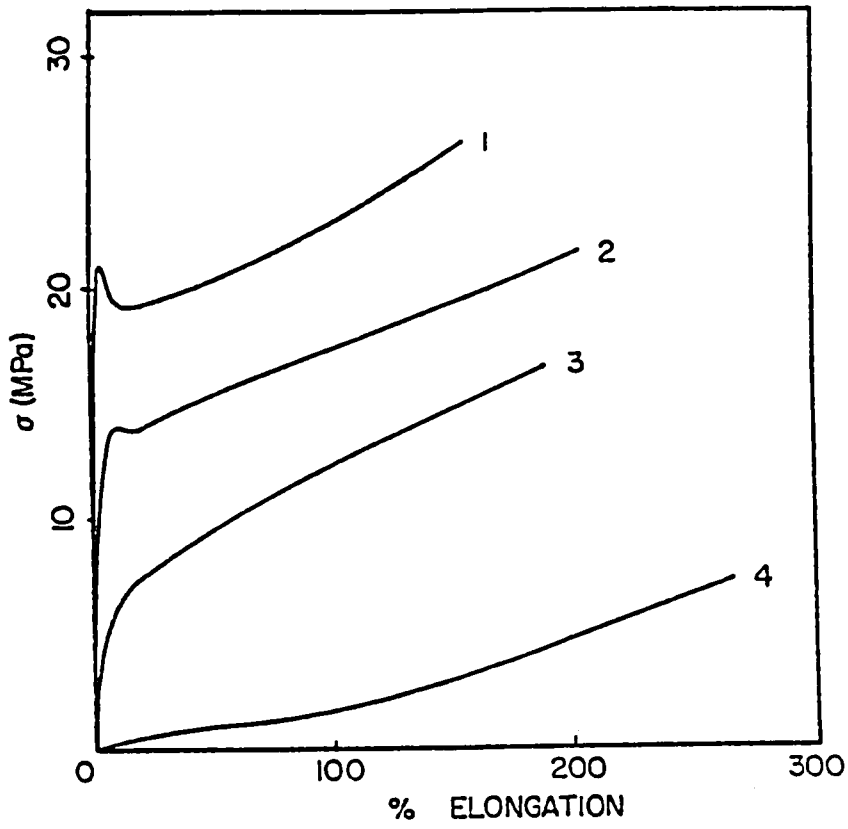

Figure 33. Stress-strain curves for (1) PSF9700/PSX6700 (2) PSF4900/PSX4400, (3) PSF9700/PSX12800 and (4) PSF4900/PSX12800. (Reference 165).

TABLE 13

Mechanical Properties of PSF/PSX Copolymers*

Sample	MW PSF/PSX	Tensile Strength (MPa)	Elong. to Break (%)	Modulus (MPa)	Yield Point
I	4900/4400	20	200	35.20	YES
II	4900/12800	6	260	0.19	NO
III	9700/12800	14	180	17.40	NO
IV	9700/6700	29	200	90.60	YES

*(Reference 165)

The above materials give rise to very well defined, perfectly alternating block copolymers. However, it is possible to synthesize random polysulfone-poly(dimethylsiloxane) block copolymers. For instance, we have synthesized phenolic hydroxyl terminated polysulfone and aminopropyl terminated poly(dimethylsiloxane) oligomers and coupled these oligomers with terephthaloyl chloride in a random fashion as shown in Scheme 22.

SCHEME 22

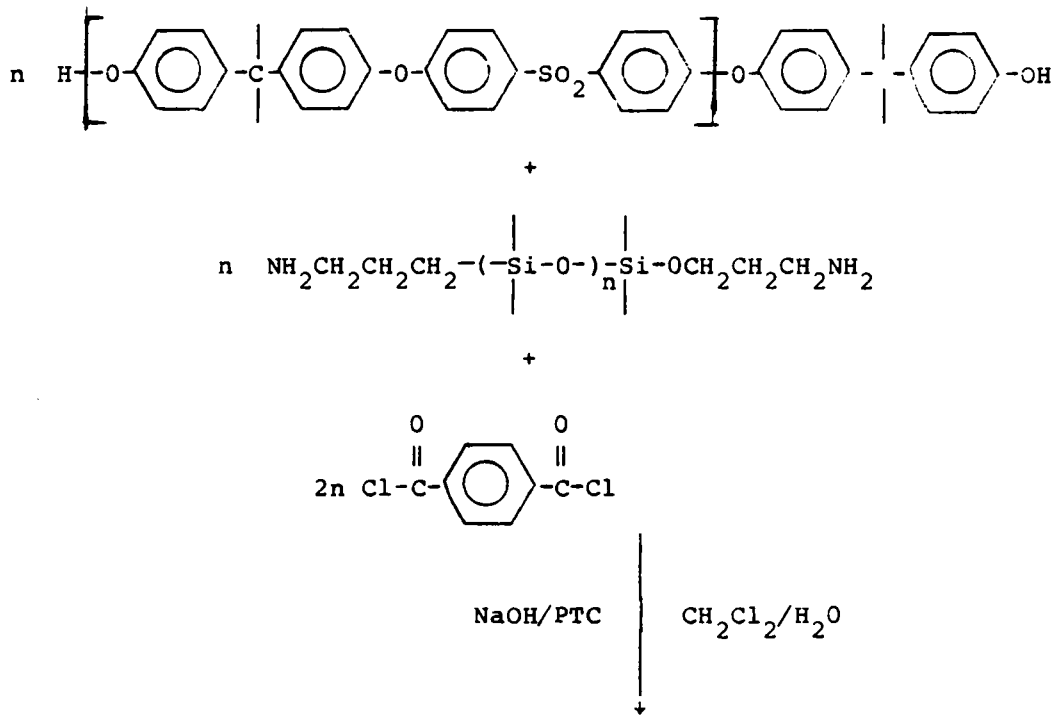

Randomly Coupled Segmented

Copolymer

The blocks in this synthesis scheme are randomly coupled by the terephthaloyl chloride, thus, giving a randomly coupled copolymer. The synthetic technique used was a modified interfacial reaction. In this

case, each of the components are soluble in the organic layer and the aqueous caustic layer was used as an acid acceptor. The phase transfer catalyst is optional. The role of the catalyst in this synthesis is still unclear.

Table 14 gives the molecular weights of the preformed oligomers and intrinsic viscosities of random copolymers. Clear, transparent films were obtained in each case, but sufficient molecular weight to obtain optimum properties was never achieved by this synthetic technique.

4.3.1.2 Homopolymer-Copolymer Blends

An interesting application for the polysulfone-poly(dimethylsiloxane) block copolymer is its use as an impact modifier additive for polysulfone homopolymer (144-147,161,163,167). Robeson and coworkers found that as little as 5-10% of block copolymer in homopolysulfone dramatically increased the impact strength. As previously discussed, we have extended their early work in an attempt to quantify the increase in fracture toughness as well as to better understand the basic energy absorption mechanisms.

We choose four copolymers to blend with the homopolysulfone, which are shown in Table 15. The blends which were made from these copolymers are listed in Table 16. The composition of the blends is listed both in terms of total siloxane content in the blend and copolymer content. As can be seen, these blends comprise four different series, each made from a different copolymer.

The blends were prepared by first solution blending, then extruding through Custom Scientific Instruments' "Maxwell" type bench-scale melt extruder, followed by compression molding of the test specimens. Due to

TABLE 14

Randomly Coupled Polysulfone-Polysiloxane
Segmented Copolymers

Sample No.	Mn of Oligomer PSF (g/mol) / PSX (g/mol)		$[\eta]_{CHCl_3}$ 25°C
1	4200	1140	0.37
2	4200	1140	0.33
3	4900	1140	0.16
4	20000*	1140	0.72

*Hq/Bp (50/50) PSF copolymer.

TABLE 15

Synthesis of Polysulfone-Poly(dimethylsiloxane) Alternating Block Copolymers (PSF-PSX)

Sample	Block (PSF)	Block (PSX)	[h]
I	4400	4900	0.67
II	12800	4900	0.55
III	12800	9700	1.27
IV	6700	9700	--

TABLE 16

Composition of Polysulfone Blends with Polysulfone-Poly(dimethylsiloxane) Block Copolymers

Series	PSX Block	PSF Block	Wt. % PSX	Wt. % Copolymer
I	4400	4900	0.5	1.0
			1.0	2.1
			2.0	4.3
			5.0	10.6
II	12800	4900	0.5	0.7
			1.0	1.4
			2.0	2.8
III	12800	9700	0.5	0.9
			1.0	1.8
			2.0	3.5
			5.0	8.8
IV	6700	9700	0.5	1.2
			1.0	2.4
			2.0	4.0
			5.0	12.2

the known extremely high melt viscosity of block copolymers of this type (158), melt extrusion was not carried out as the first step in the preparation of the blends. Solution blending in a common solvent followed by devolatilization was chosen to provide as thorough a dispersion of the copolymer in the homopolymer as possible.

Complex viscosity versus shear rate at 320°C plots are shown in Figure 34 for Blend Series III -2% PSX, IV -5% PSX and homopolysulfone. As can be seen there is essentially no difference between the blend and the polysulfone homopolymer indicating that conventional processing conditions used for polysulfone can be used for these blends. In fact, we believe that the unusual rheological behavior of the copolymer serves an important beneficial function in the blend: it discourages excessive particle breakdown during melt fabrication. The morphology block copolymer within the homopolysulfone now resembles that of styrene-diene graft systems in HIPS.

In impact modification one attempts to improve the fracture strength, preferably at a minimum sacrifice to the bulk properties (i.e., the modulus). By incorporating such small amounts of block copolymer (see Table 16), we obtained the desired impact improvement at minimal sacrifice to the bulk properties.

The tensile properties of the blends are summarized in Tables 17 and 18 yield strength, tensile strength, Young's modulus, yield strain, and ultimate strain are reported for each blend. There is a slight, but statistically significant, decrease in the yield and tensile strengths and modulus of the blends as the copolymers are added to the polysulfone. This is expected since a mechanically weaker material is

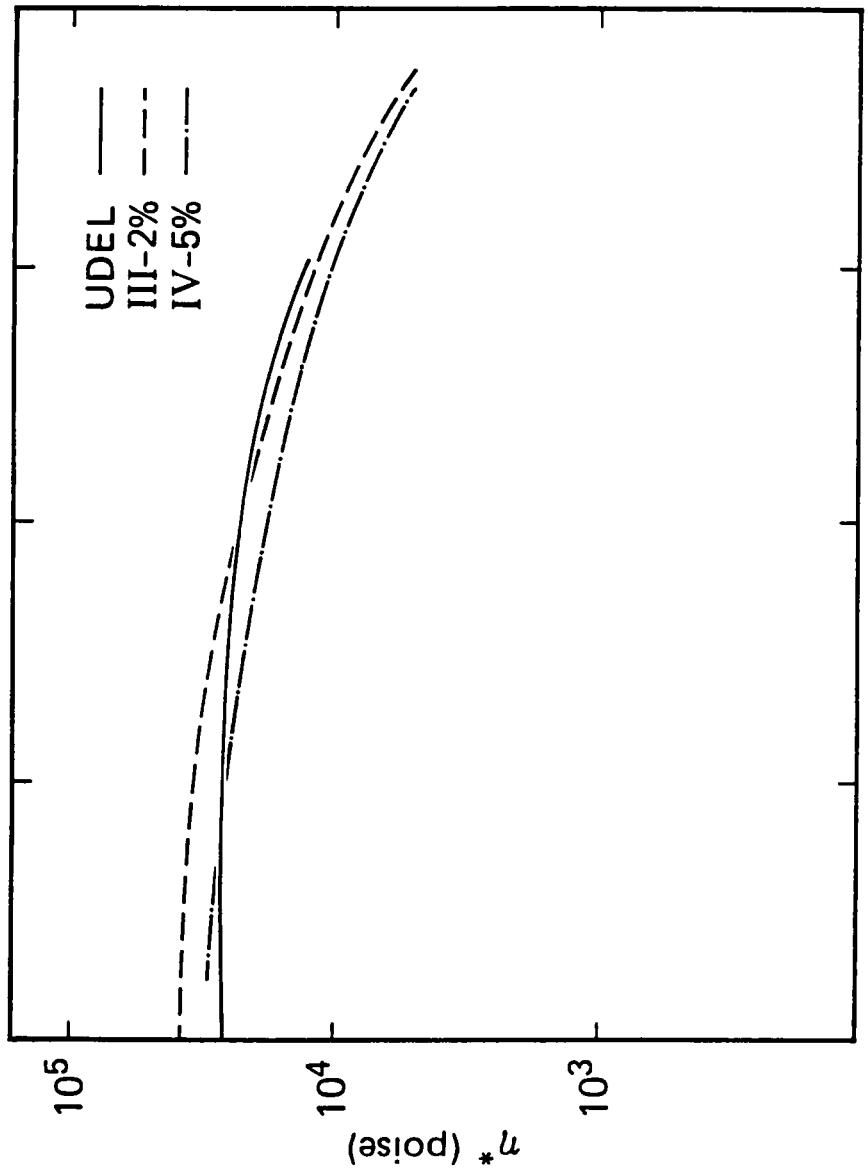

Figure 34. Complex viscosity versus shear rate at 320°C for several blends and homopolymers

TABLE 17

Tensile Properties of Polysulfone-Polysulfone/
Poly(dimethylsiloxane) Block Copolymer Blends

Sample	Yield Strength (MPa)	Tensile Strength (MPa)	Modulus (MPa)
P-1700	75.2	62.1	1180
I-0.5%	69.7	60.7	1117
1.0	63.4	57.9	1069
2.0	65.5	53.8	1103
II-0.5	71.7	63.9	1179
1.0	70.3	59.3	1152
2.0	67.6	57.2	1131
III-0.5	70.3	61.4	1166
1.0	69.7	61.4	1150
2.0	64.8	62.8	1069
5.0	56.6	56.6	1014
IV-0.5	68.3	58.6	1124
1.0	66.9	59.3	1131
2.0	62.8	53.9	1034
5.0	55.3	55.9	986

TABLE 18

Yield Strain and Tensile Strain for Poly(dimethylsiloxane)-Polysulfone Copolymer Homopolymer Blends

Sample	Yield Strain (%)	Tensile Strain (%)
Udel	8.7	110
I-0.5%*	8.1	115
I-1.0	8.3	122
I-2.0	7.9	85
II-0.5	8.2	120
II-1.0	8.4	111
II-2.0	7.6	95
III-0.5	8.9	118
III-1.0	8.2	120
III-2.0	8.2	140
III-5.0	7.8	128
IV-0.5	7.9	110
IV-1.0	8.0	120
IV-2.0	8.7	100
IV-5.0	7.6	130

*Wt. % PSX in the blend.

being added to the homopolysulfone. However, this decrease is slight since the level of additive is low.

All of the blends, as well as the polysulfone homopolymer, yielded and necked during deformation. In addition, it was observed that the blends stress-whitened extensively suggesting crazing, etc.

Previous attempts to assess the improvement in impact strength of the blends was done by an ASTM method notched Izod test. As is well known, the errors associated with this commonly used test can be extremely large. Thus, we have utilized a different technique to assess the fracture toughness in these materials.

The $K_{I,C}$ values for homopolysulfone as well as the blends are shown in Table 18. The very high toughness of the materials tended to limit the sharpness of the crack and consequently the fracture toughness may be slightly overestimated. However, the notches were consistent throughout the specimens tested and the reproducibility of the values were typically within ±10%.

The fracture toughness increases as the siloxane content in the blends is increased. In fact, for the blends containing two and five percent siloxane, the mode of fracture changed so that the plane strain criterion could not be met. This change was accompanied by the development of 45 degree shear type patterns and plastic deformation. This is indicative of a tougher material, however, with plastic deformation, LEFM no longer produces a meaningful number. Typically, if larger samples are used plane strain conditions can once again be achieved, but because of the limited sample quantities this approach was not possible. The utilization of the J_I-integral analysis is appropriate

to rank the blends with higher siloxane content. The J_I value is a measure of the energy required to initiate stable crack growth in a sample which fails in a plane stress mode. These values are also included in Table 19, and as expected, as the siloxane content increases, the $J_{I,C}$ values increase. Unfortunately, we do not have a standard or reference to compare those materials which were evaluated by the J-integral. At the sample dimensions used, neat polysulfones fails in plane strain mode and thus the J-integral could not be applied.

Since these blends do exhibit improved toughness, it was of interest to determine what morphological features give rise to these improvements in properties. To do this, the results from the mechanical property analysis and observations of the optical properties of the blends and component materials under different conditions need to be combined. In this manner, the detailed morphology can be used to substantiate and further develop the preliminary conclusions reached.

It is necessary now to consider the observations made thus far about the nature of these blends. Firstly, most of the blends are opaque. Blends of series IV are somewhat translucent, but all of the blends are turbid. Secondly, the blends undergo a great deal of stress-whitening when deformed in tension, whereas the polysulfone homopolymer does not.

It is important to consider what these observations lead to with respect to morphology. First, there has to be a dispersed phase, as expected from the turbid nature of the materials. Furthermore, microscopy indicated the block copolymers exist as particles in the polysulfone matrix which would tend to limit the size of the dispersion.

TABLE 19

Fracture Toughness of Blends

Sample	$K_{I,C}$ (Mpa $\sqrt{m}$)	$J_{I,C}$ kPa-m
UDEL	2.05	-
I - 0.5	3.5	-
- 1.0	3.3	-
- 2.0	-	3.0
- 5.0	-	-
II - 0.5	3.3	-
- 1.0	3.7	-
- 2.0	-	3.5
III - 0.5	3.6	-
- 1.0	4.0	-
- 2.0	-	4.0
- 5.0	-	5.8
IV - 0.5	3.6	-
- 1.0	3.8	-
- 2.0	-	-
- 5.0	-	7.0

The polysulfone component of these copolymer particles would provide compatibilities with the matrix. The dynamic mechanical spectrum for one of the blends is shown in Figure 35. The glass transition of the polysulfone is clearly seen at 180°C and the glass transition of the poly(dimethylsiloxane) is visible as a shoulder of the beta-relaxation of the polysulfone at -120°C. Thus, there is some evidence of phase separation in this blend as is indicated by the two distinct mechanical transitions corresponding to each component homopolymer.

To further confirm this two phase morphology SEM was conducted on liquid nitrogen fractured blend specimens. Several micrographs are shown in Figures 36. In the blend series, we observed holes which appear to have a distribution of sizes ranging from 0.15 to 5 μm.

The small holes observed in the micrographs are believed to be from the rubbery copolymer particles and the approximate size was noted to be 0.2 μm. The fact that there are no corresponding "bumps" to the corresponding holes does not lend support to the argument that these holes are a result of the soft particles in the polysulfone matrix. Recently, Kinloch (88,89) and others (81-87) have observed similar fracture topographs in acrylonitrile-butadiene rubber modified systems. It is generally thought that the rubber particle has a different coefficient of thermal expansion and upon cooling from the melt the particles are swollen within the matrix. As the crack front moves through the sample, the particle contracts to its desired size and resides in the back of the hole. This phenomenon is usually termed dilatation (88,89).

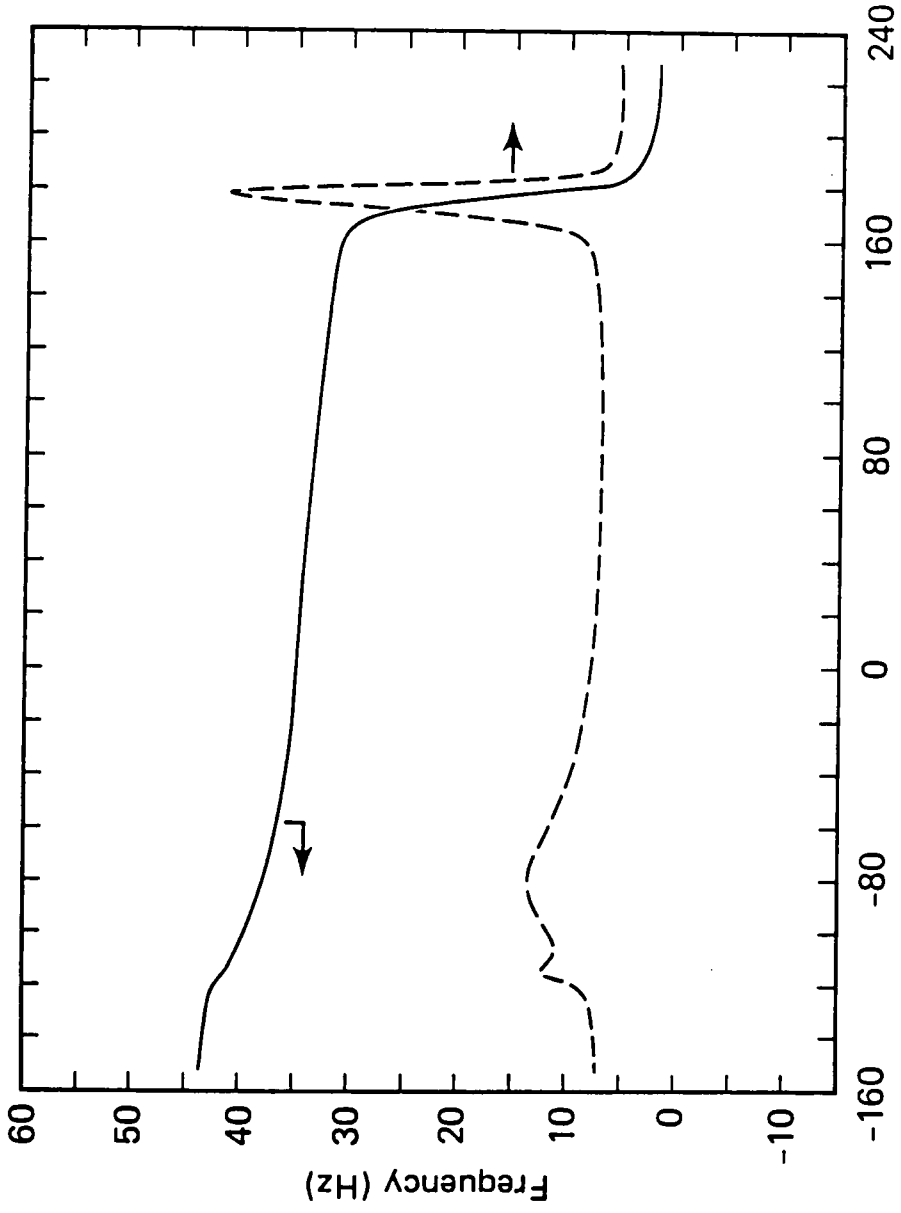

Figure 35. Dynamic mechanical analysis (DMA) (frequency versus temperature) for blend II-5%.

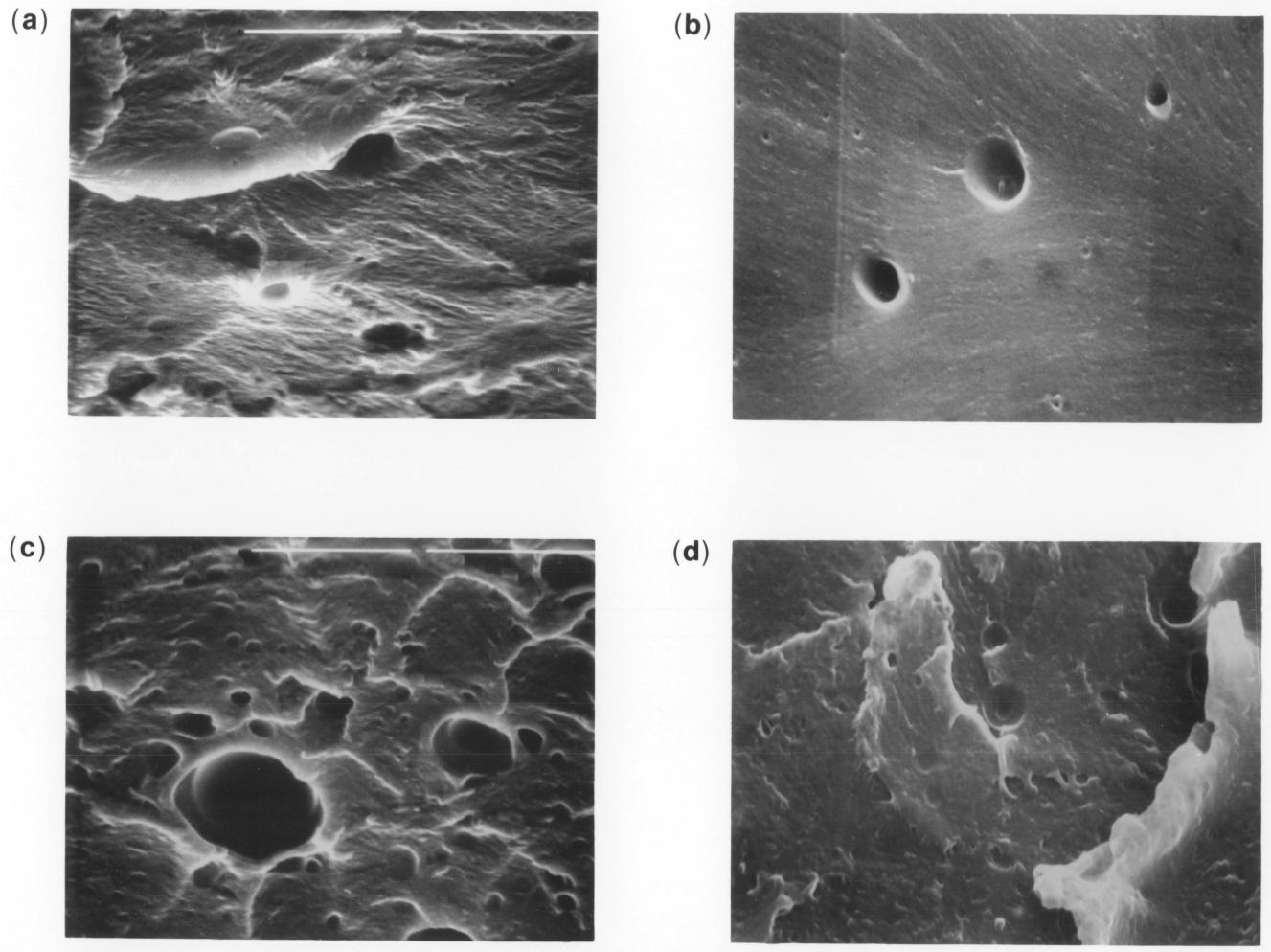

Figure 36. SEM micrographs of copolymers/homopolymer blends. (A) Series I - 1% (7000×), (B) Series I - 0.5% (7000×), (C) Series I - 2.0% (7000×) and (D) Series II - 1.0% (7000×).

To further confirm this morphology, transmission electron micrographs were obtained on thin films of a blend. A micrograph is shown in Figure 37. What is observed clearly confirms the suggested morphology for these blends. There are grey spots visible in a lighter background, but upon closer inspection, these spots are found to contain light and dark regions corresponding to the microdomains observed in the parent block copolymers. Some of the imbedded copolymer particles appear to be richer in sulfone and some richer in siloxane. (As mentioned before, the siloxane appears darker than the polysulfone in the micrographs). The average size of the particles is approximately 0.15 microns which is close to the size of the small holes which were observed in the SEM micrographs. This further indicates that the holes in the fracture surfaces resulted from the copolymer particles.

According to current understanding of toughening mechanisms in rubber modified polymers (34,67,74), the rubbery particles act to toughen the material in several different ways. One theory is that the rubber particle acts to blunt a propagating crack tip, decreasing its stress intensity and making propagation more difficult.

Another concept of toughening in plastics is that the rubber particles act as stress concentrators and initiate energy absorbing processes such as shear band formation and craze initiation. The rubbery particles are also postulated to act as craze stabilizers, and, hence, retard the breakdown of the craze fibrils (76).

In these blends, extensive stress-whitening due to crazing was observed during tensile testing. Shear band formation was also observed in the tensile testing as necking and in the fracture toughness tests as

Figure 37. TEM micrograph of PSF(4900)/PSX(4400) block copolymer blended (0.5 wt.% PSX) with homopolysulfone.

lips on the side of the test specimen. It appears also that the extent of shear band formation is greater in the blends than in the polysulfone homopolymer based on visual inspection of the fracture toughness test specimens. Thus, there appear to be two toughening mechanisms operating here in these blends: shear band formation and crazing.

We have determined that the bulk morphology of these copolymer-homopolymer blends exhibits a two-phase structure in which the copolymers exist as discrete composite particles within the matrix of the homopolysulfone. However, the surface morphology exhibits a unique characteristic, surface segregation of the block copolymers. Professor Dwight and Mr. Patel from our laboratory (168) have used XPS on series I solution cast blends to show that there is nearly a complete overlayer of siloxane on the surface at very low levels of siloxane in the bulk (1-5%) as shown in Figure 38. It is believed that the low surface energy poly(dimethylsiloxane) block tends to reside on the surface with the lowest surface energy; namely the polymer-air interface.

The ramifications of having a surface "coating" such as the siloxane are numerous. Webster, et al. (169) have shown that environmental stress cracking resistance (ESCR) is modestly improved. By changing the solubility parameter at the surface, those liquids which normally craze polysulfone do not craze the siloxane layer as effectively. ESC is believed to originate at defects in the surface and thus the presence of a rubbery layer can, in principle, relax the stress concentrating defects, thus making craze initiation more difficult.

In addition, the presence of the siloxane layer is known to improve atomic oxygen resistance (15). This is a particular problem in

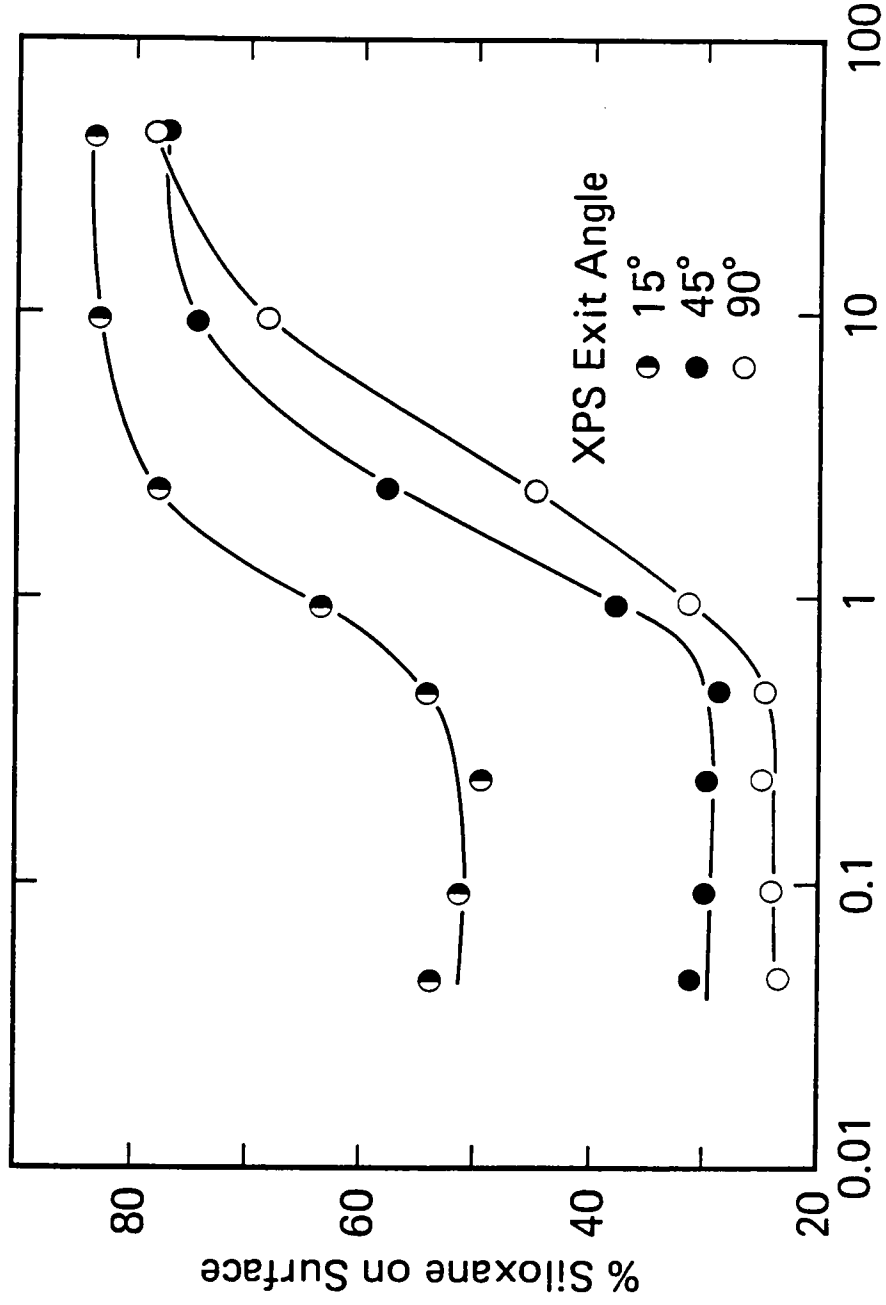

Figure 38. ESCA analysis of (5000/5000) PSF/PSX block copolymer/blend plotting percent siloxane on the surface versus percent siloxane in the bulk. (Reference 169).

aerospace applications where low earth orbits are required. The siloxane layer is believed to degrade into a protective ceramic overlayer. This may be similar to the dry etch procedures used in microlithography applications.

4.3.2 Thermosets

4.3.2.1 Introduction

In the past ten years considerable attention has been given to the impact modification of epoxy networks which will serve as matrix resins for graphite fiber composites. Kinloch et al., (88,89), Riew et al., (84) and others (85,86) have found that acrylonitrile-butadiene functionally terminated copolymers significantly improve the fracture toughness of highly crosslinked networks. The solubility parameter in these systems is designed in such a way that during the curing process the elastomeric component phase separates, giving discrete composite particles within the epoxy matrix. Although the incorporation of the elastomeric component improves the fracture toughness it is usually at the expense of the bulk properties, especially the modulus (80-89).

In an effort to obtain a better balance of properties (toughness and stiffness) functionally terminated engineering thermoplastics have been used. Specifically, poly(arylene ether sulfones) were chosen because of their tough, ductile mechanical properties, high modulus and Tg and good oxidative, thermal, and hydrolytic stability.

4.3.2.2 Synthesis and Characterization of Polysulfone Modified Epoxy Resins

Hydroxyl terminated Bisphenol-A polysulfone (Bis A PSF) oligomers were successfully synthesized by a nucleophilic aromatic substitution

reaction using the N-methyl-2-pyrrolidone (NMP) potassium carbonate route as shown in Scheme 19. Toluene was used as a dehydrating agent. The Carothers equation was used to calculate the excess of Bisphenol-A required to give the appropriate molecular weight and hydroxyl termination. Table 20 gives the oligomers synthesized as well as the intrinsic viscosities, number average molecular weight as determined by end group analysis, and glass transition temperatures.

The performed hydroxyl terminated polysulfone oligomers were reacted with a large molar excess of Epon Resin 828 in the presence of a catalytic amount of tetramethyl amonium hydroxide (TMAH). A large excess of epoxy resin was used to end cap the polysulfone oligomers giving epoxy end groups and preventing further polymerization. The reaction is illustrated in step 1 of Scheme 23. The two oligomers and catalyst are brought together in methylene chloride and stirred until homogeneous. A vacuum was applied, removing the solvent, and the mixture was heated and allowed to react for five hours at 110°C. This bulk polymerization mixture was then heated to 160°C for three hours to decompose the transient catalyst. The final step was to cure the modified resin with a stoichiometric amount of the 4,4'-diaminodiphenyl sulfone.

In the first step of the reaction the incorporation of the polysulfone oligomer into the epoxy resin is considered to be crucial otherwise a blend would result. The chemistry of the phenoxide-epoxy reaction is fairly well established because the commercially available polyhydroxy ethers are made using this technique. Several techniques were used to characterize and monitor this reaction.

TABLE 20

Characteristics of Hydroxyl Terminated Polysulfone Oligomers

NO.	Mn g/mole Theory	Via End Group Analysis	Tg,**°C
1	3,000	3100	-
2	5,000	5300	180
3	7,000	6200	180
4	10,000	8200	183
5	15,000	14600	189

*Potentiometric titration

**DSC, heating rate 10°C/min.

Scheme 23

step 1

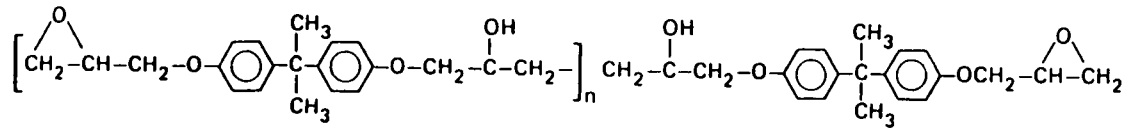

EPON Resin 828 (excess)

+

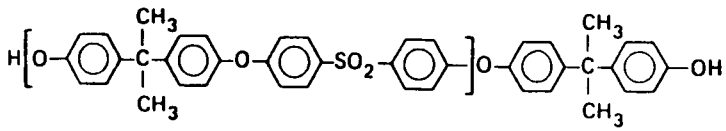

Polysulfone

110°C, 4-1/2 hrs.

TMAH

Epoxy capped polysulfone and
Epoxy resin

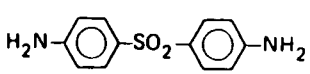

step 2 Diamino diphenyl sulfone (DDS)

Crosslinked Network

Therefore, in an attempt to assess more accurately the first stage of the reaction between polysulfone and epoxy oligomers, reverse phase HPLC was used. Four samples were prepared for this investigation: the EPON resin 828, the polysulfone oligomers, blends of the epoxy, and polysulfone oligomers and the reaction between the polysulfone and epoxy oligomers. The retention times for these samples depend on their interaction with the column. Figure 39 provides the HPLC chromatograms for each of the samples. The EPON resin 828 (a) shows two peaks indicating n can be 1 or 2 in 1 below.

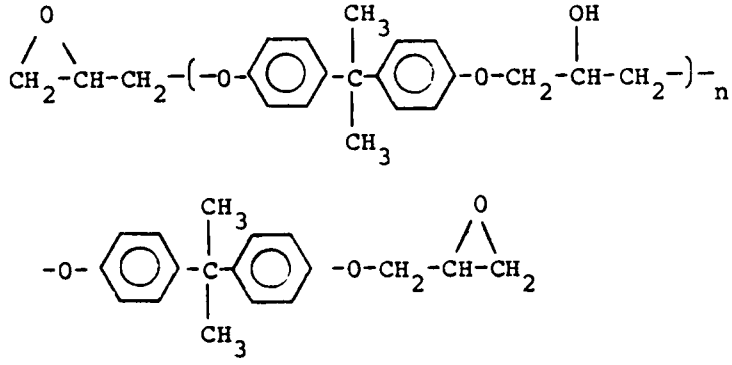

Blends of the polysulfone and epoxy oligomers gave identical retention times as those of the starting oligomers (a,b). However, in the final case of the polysulfone modified epoxy resin a new peak developed, indicating a reaction had indeed occurred. Furthermore, the peak corresponding to the polysulfone oligomer was no longer present, leading us to believe the "capping" reaction was both successful and quantitative.

In an attempt to better understand the chemistry of these systems, high molecular weight polysulfone-epoxy or poly(hydroxy ether) polymers were synthesized according to Scheme 2 below.

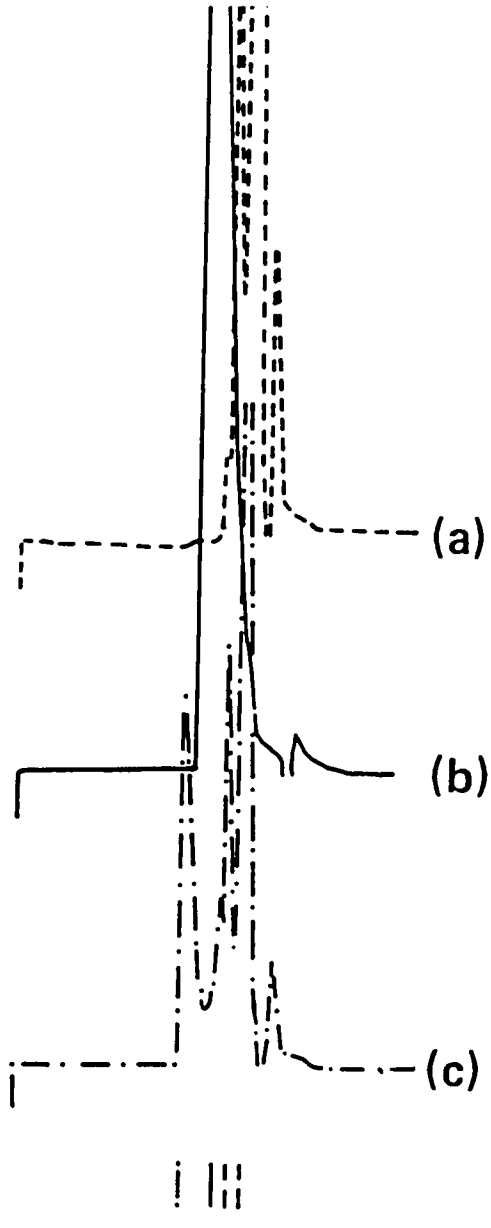

Figure 39. HPLC chromatograms for (a) Epon Resin 828, (b) polysulfone oligomer (5300 gmol Mn) and (c) Epon Resin 828 chemically modified with 15 wt.% polysuflone oligomer (5300 gmol Mn).

Scheme 24

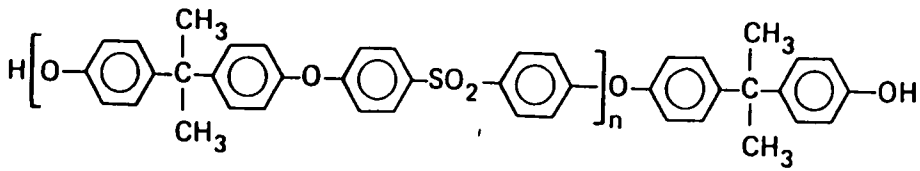

Bis A PSF

+

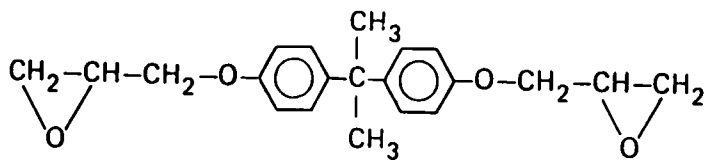

DGEBA

TMAH | DMSO/Toluene (dehydrating agent)

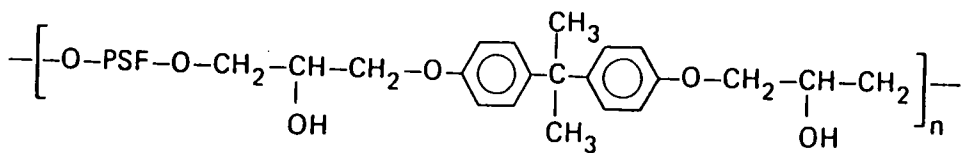

(and Branched Products)

In this synthesis, dimethylsulfoxide (DMSO) was chosen as the solvent with toluene as a dehydrating agent. As before TMAH was used in a catalytic amount. Table 21 contains the polymers synthesized along with their glass transition temperatures and intrinsic viscosities. High molecular weight was obtained as determined by the intrinsic viscosity measurements shown in Table 21.

GPC chromatograms of the starting oligomers (Table 20) and high molecular weight epoxy-polysulfone copolymers (Table 21) are shown in Figures 40 and 41. In each case the copolymers were shifted to lower elution volumes indicating higher molecular weight. In addition, copolymer 2 (Table 21) showed a bimodal molecular weight distribution which suggests branching.

Unfortunately, it is very difficult to make any substantial correlations between the latter solution reaction and the former bulk polymerization.

4.3.2.3 Synthesis and Characterization of Phenolic Hydroxyl Terminated Polysulfone Modified Epoxy Networks

The polysulfone modified epoxy resins were cured with a stoichiometric amount of 4,4'-diaminodiphenylsulfone (DDS) as illustrated in Step 2 of Scheme 23. The networks synthesized as well as the composition and block type of polysulfone are given in Table 22. In each case either ten or fifteen percent by weight of polysulfone oligomer or polymer was reacted or blended into the epoxy network. The molecular weight and weight percent polysulfone added determined the curing procedure. As described in the experimental section a second post-cure was required for the higher molecular weight oligomers

TABLE 21

Synthesis of High Molecular Weight
Polysulfone-Poly(Hydroxy Ether) Copolymers

Sample	Mn, Polysulfone Oligomer	$[\eta]_{25^\circ C}^{CHCl_3}$	Tg*°C
(1)	5300	0.6	189
(2)	9700	0.9	189

*DSC 10°/min. heating rate

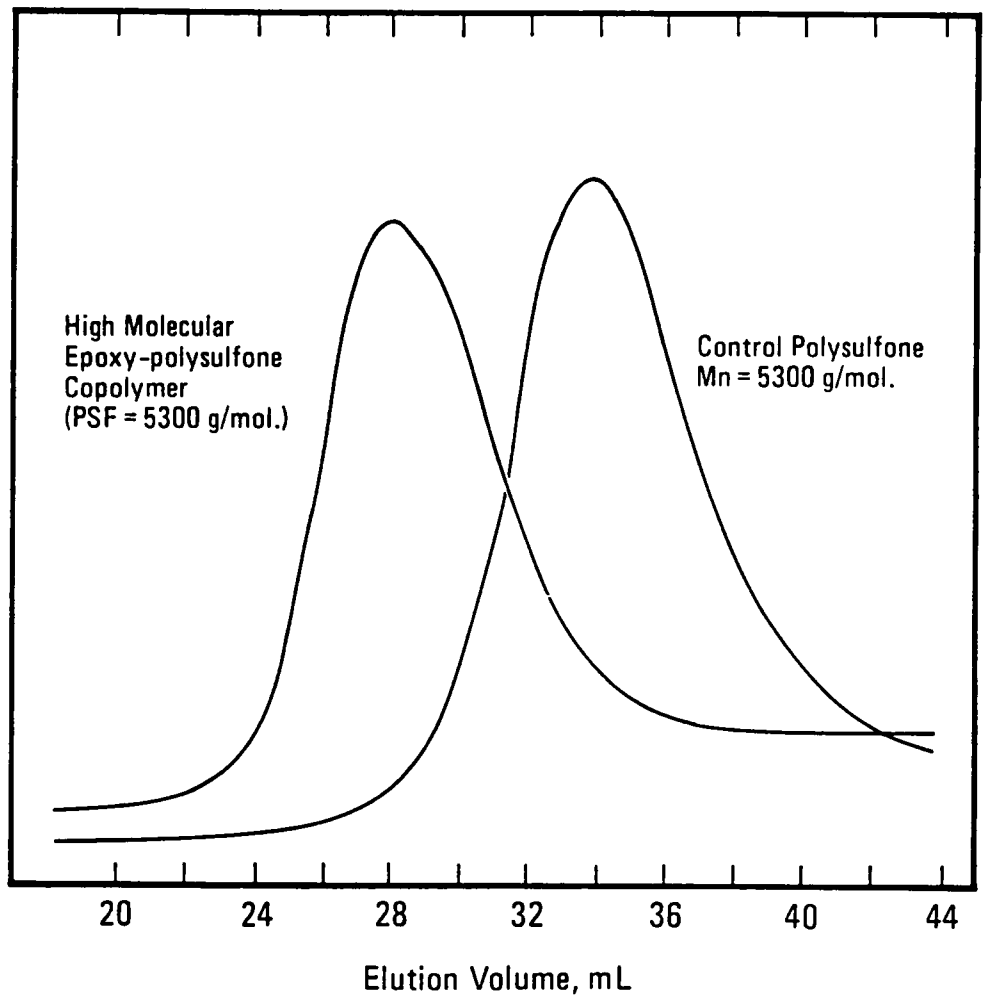

Figure 40. GPC chromatograms of 5300 Mn polysulfone oligomer and high molecular weight epoxy-sulfone copolymer.

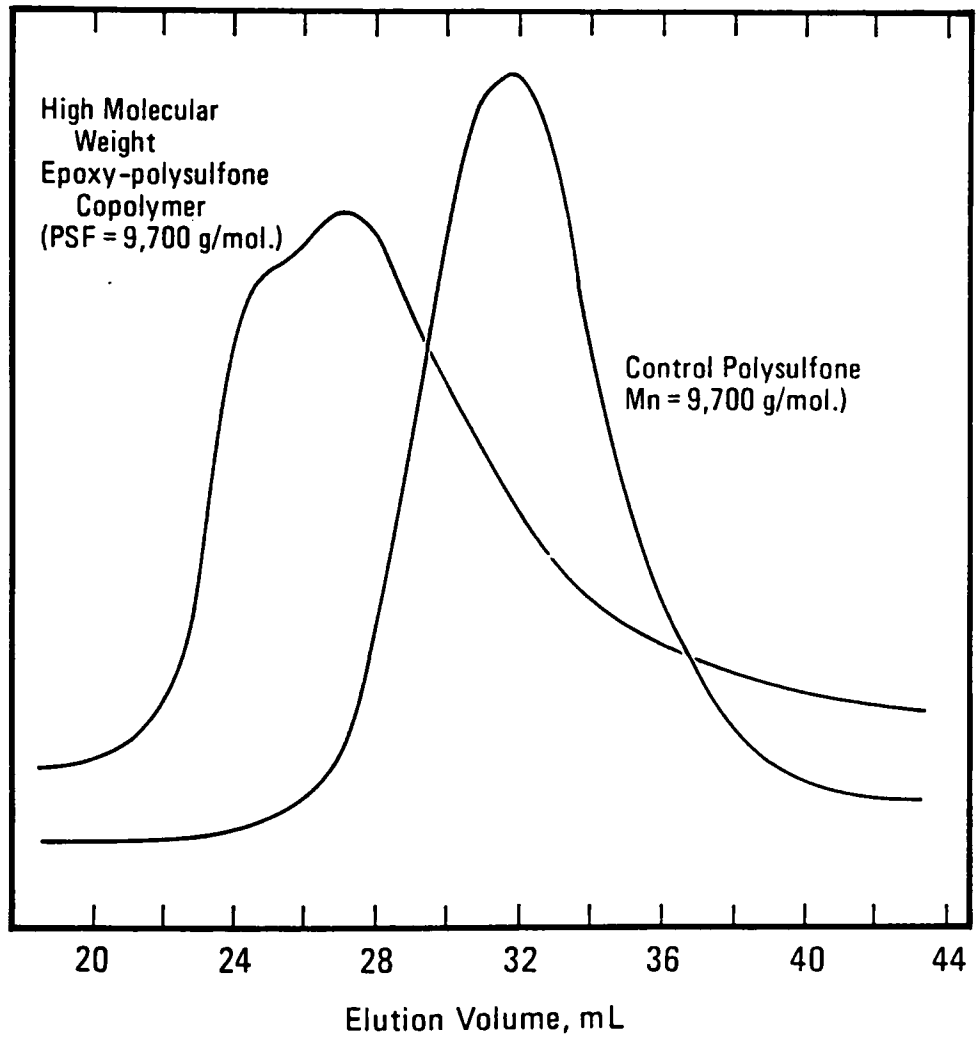

Figure 41. GPC chromatograms of 9700 Mn polysulfone oligomer and high molecular weight epoxy-sulfone copolymer.

TABLE 22

Characteristics of Bis-A Polysulfone Modified Epoxy Networks

	Bis-A Polysulfone			Network
No.	Mn g/mol	Tg(°C)	(wt.%)	Tg(°C)
1	3100	---	15	187
2	5300	180	10	
3	5300	180	10	
4	6200	180	10	187
5	6200	180	15	192
6	8200	183	10	198
7	8200	183	15	200
8	14600	189	10	196
9	14600	189	15	198

(numbers 6-9 on Table 22). Extremely high melt viscosities were associated with these modified epoxy resins. In fact, those resins which contained higher molecular weight polysulfone oligomers were solid at room temperature and did not show tack unless heated (40°C (104°F)). This loss in room temperature tack may complicate composite fabrication. Table 22 also contains the glass transition temperatures of these networks. DSC scans do not show any further exotherms which indicate that these systems are fully cured. Our synthetic approach to modifying the epoxy resins with polysulfone oligomers is similar to the chemistry involved in the ATBN, CTBN, and siloxane rubber modifiers. In these systems the solubility parameter is controlled in such a way that these oligomers are miscible with the epoxy resin in the initial stages of the cure but will phase separate during the later stages. In our system, the solubility parameters are such that the polysulfone is miscible with the epoxy resin in the first stage of the reaction giving a clear homogeneous solution. This promotes good mixing and a chemical reaction. During the curing process, the thermoplastic component separates within the reacting medium to form a second dispersed phase. The solubility parameter of the epoxy resin has been estimated to be 9.4 which is lower than that of the bisphenol A based polysulfone, 10.2. No doubt this difference promotes the phase separation of the components, as observed in SEM studies which we will discuss later in the text.

4.3.2.4 Synthesis and Characterization of Amine Terminated Polysulfone Oligomers and Amine Terminated Polysulfone Modified Epoxy Networks

The amino terminated polysulfone oligomers may be used together with the curing agent, diaminodiphenyl sulfone, in a one step modification process. The phenolic hydroxyl terminated polysulfones had to be reacted with the epoxy resin using tetramethyl amonium hydroxide as a catalyst, and upon completion of the reaction the catalyst had to be decomposed. Thus, by using an amine terminated polysulfone these steps may be avoided.

Amine terminated bisphenol-A based polysulfone (Bis-A PSF) oligomers of predictable molecular weight were successfully synthesized (170) via nucleophilic aromatic substitution (Scheme 25) using a modified Carothers Equation. Due to the strong activating ability of the amine group in p-aminophenol, a strong base was required to form the metal phenate. Hence the DMSO/aqueous sodium hydroxide route was necessary. Table 23 contains the molecular weight and glass transition temperatures of the various amine terminated polysulfones synthesized.

The amine terminated polysulfones were used together with diaminodiphenyl sulfone to cure Epon Resin 828 as shown in Scheme 26. Table 24 contains the thermal properties of the modified resins and, for comparative purposes, a control (Epon Resin 828 cured with DDS). In both the control and the modified networks we got high Tg's which are in the 190-200°C range. The DSC scans show no exotherms after the Tg which clearly indicates quantitative reactions.

Scheme 25

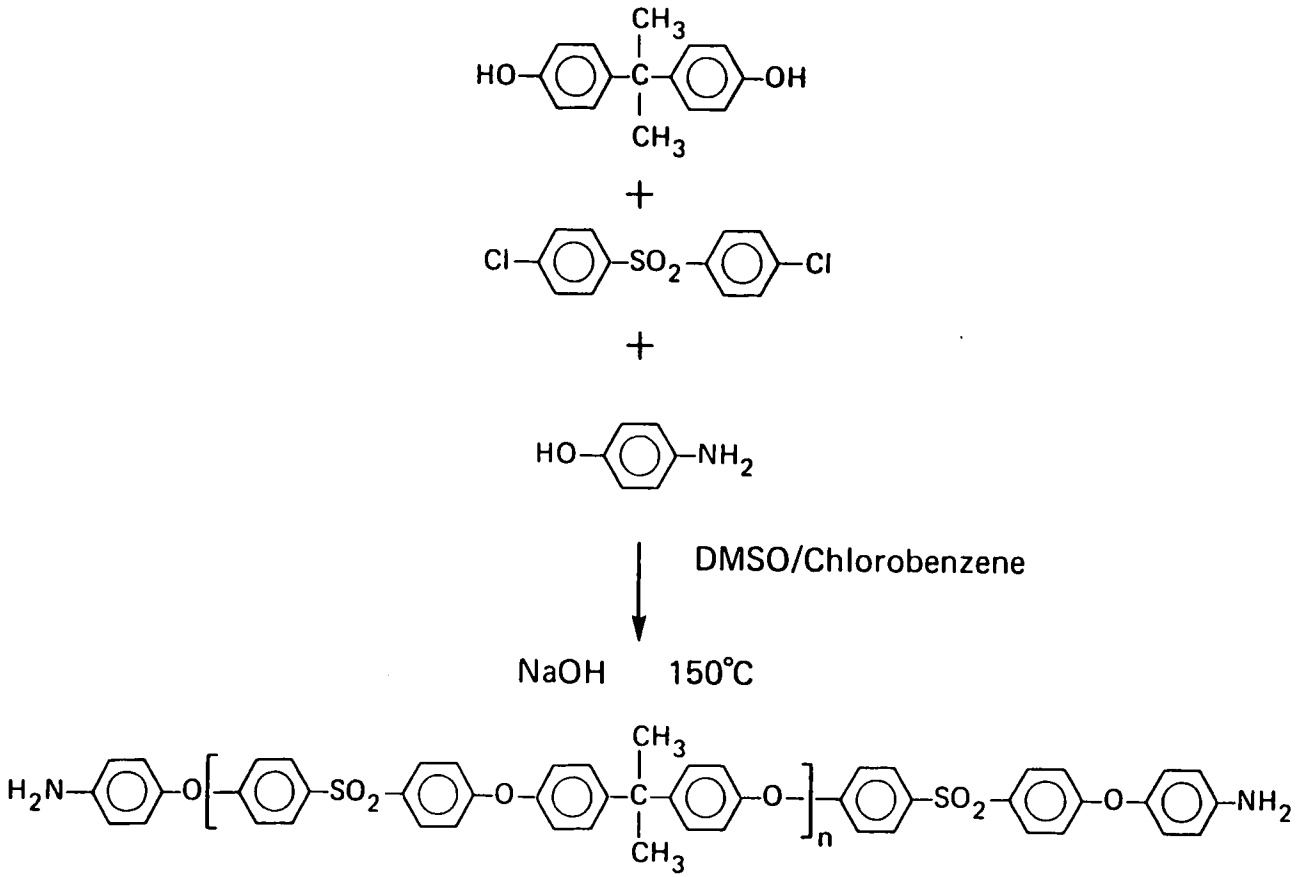
HO
CH3
C
CH3
OH
+
Cl
SO2
Cl
+
HO
NH2
DMSO/Chlorobenzene
NaOH
150°C
H2N
O
SO2
O
C
CH3
CH3
O
n
SO2
O
NH2

TABLE 23

Characteristics of Amine Terminated Polysulfone Oligomers

No.	Mn g/mole	$[n]^{25°C}_{CHCl_3}$	Tg(°C)
1	4100	0.16	148
2	7100	0.18	167
3	13100	0.22	178

Scheme 26

Synthesis of Polysulfone Modified Epoxy Networks

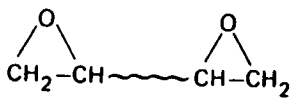

Epon Resin

+

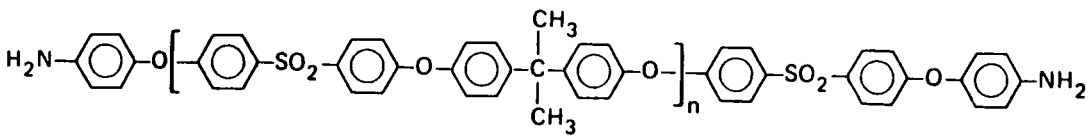

Bis-A Polysulfone

+

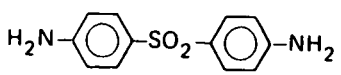

DDS

↓

MODIFIED
CROSSLINKED
EPOXY NETWORK

4.3.2.5 Mechanical Properties of Modified Epoxy Networks

The main objective of this investigation is to improve the toughness of the epoxy networks by the addition of the ductile polysulfone at a minimum sacrifice to the bulk properties. Rubber modifiers typically show improved fracture properties, at the expense of the bulk properties, especially the modulus.

The $K_{I,C}$ values for the phenolic hydroxyl terminated polysulfone modified epoxy networks are given in Table 25. There are several important observations to be made here, first as the amount of polysulfone is increased in the matrix (from ten to fifteen percent) the fracture toughness increases as well. In addition, as the block length of the polysulfone oligomer increases the fracture toughness also increases and then levels off.

Unlike the rubber modifiers, polysulfone is a ductile engineering thermoplastic with a high modulus. Therefore it is not surprising that the bulk properties in these modified networks are retained. Table 25 also contains the flexural modulus of the control and the modified networks. In each case, the modulus of the polysulfone modified networks decrease about 10-15 percent, which is considerably better than the rubber modifiers.

In a similar fashion the amine terminated polysulfone modified network also showed an improvement in fracture toughness. Table 16 gives the $K_{I,C}$ values for the neat and the modified networks synthesized by the one-step process. The polysulfone content was held constant at fifteen weight percent in each case. The fracture toughness appears to be sensitive to the molecular weight of the oligomer and increases with

TABLE 24

Thermal Properties of Modified Networks

No.	PSF Mn g/mole	PSF (wt.%)	Network Tg(°C)
1	Epon resin 828/ DDS control	0	195
2	4100	15	193
3	7100	15	187
4	13100	15	190

TABLE 25

Mechanical Properties of Bis-A Polysulfone Modified Epoxy Resins

No.	PSF Mn	PSF (wt.%)	Flex. Mod. (N/M^2)	Fract. Tough., $K_{I,C}$ ($N/M^{3/2}$)
1	Control		2.5×10^9	0.6×10^6
2	3100	15	2.1×10^9	0.6×10^6
3	5300	10	2.0×10^9	0.9×10^6
4	5300	15	2.0×10^9	0.9×10^6
5	6200	10	1.9×10^9	0.9×10^6
6	6200	15	2.3×10^9	1.1×10^6
7	8200	10	---	1.0×10^6
8	8200	15	2.2×10^9	1.3×10^6
9	14600	10	2.2×10^9	1.0×10^6
10	14600	15	2.3×10^9	1.2×10^6
11	polysulfone control			2.4×10^6

increasing molecular weight. This is consistent with our previous results on the phenolic hydroxyl terminated polysulfones.

In addition, only a minimum sacrifice in flexural modulus was observed for each of these modified networks as shown in Table 26.

To further illustrate this point, Figure 42-44 contain dynamic mechanical spectra of a 8200 g/mol phenolic hydroxyl terminated polysulfone modified network, a 13,300 g/mol amino terminated polysulfone oligomer and a control (Epon 828 cured with DDS). In each case a high modulus may be observed up to the Tg of the epoxy network. In other words, these materials exhibit dimensional stability over a wide temperature range. This is typical of the elastomer modified systems. Each of these materials show a large tan δ damping transition at 190-195°C which corresponds to the Tg of the epoxy network. The glass transition temperature of the polysulfone is in this same temperature range and generally cannot be detected. However, the Tg's of polysulfone oligomers are molecular weight dependent, and this temperature dependence usually levels off at <Mn>'s of 12,000-14,000 g/mol. As expected, tan δ of the 8200 g/mol polysulfone modified network (Figure 42) shows a small shoulder on the range damping peak of the epoxy network Tg. If this is the glass transition temperature of polysulfone this suggest a two phase morphology. The next section will discuss the morphology in more detail.

4.3.2.6 Morphology

In a close examination of the fracture surfaces with scanning electron microscopy (SEM) the two phase morphology alluded to be the dynamic mechanical results is confirmed. Figure 45 contains SEM

TABLE 26

Mechanical Properties of Modified Epoxy Networks

No.	PSF Mn g/mole	Modulus (N/M^2)	Fract. Tough., $K_{I,C}$ (N/M^{372})
1	Epon Resin 828/ DDS Control	2.5×10^9	0.6×10^6
2	4100	1.8×10^9	0.6×10^6
3	7100	-----	0.8×10^6
4	13100	1.9×10^9	1.0×10^6

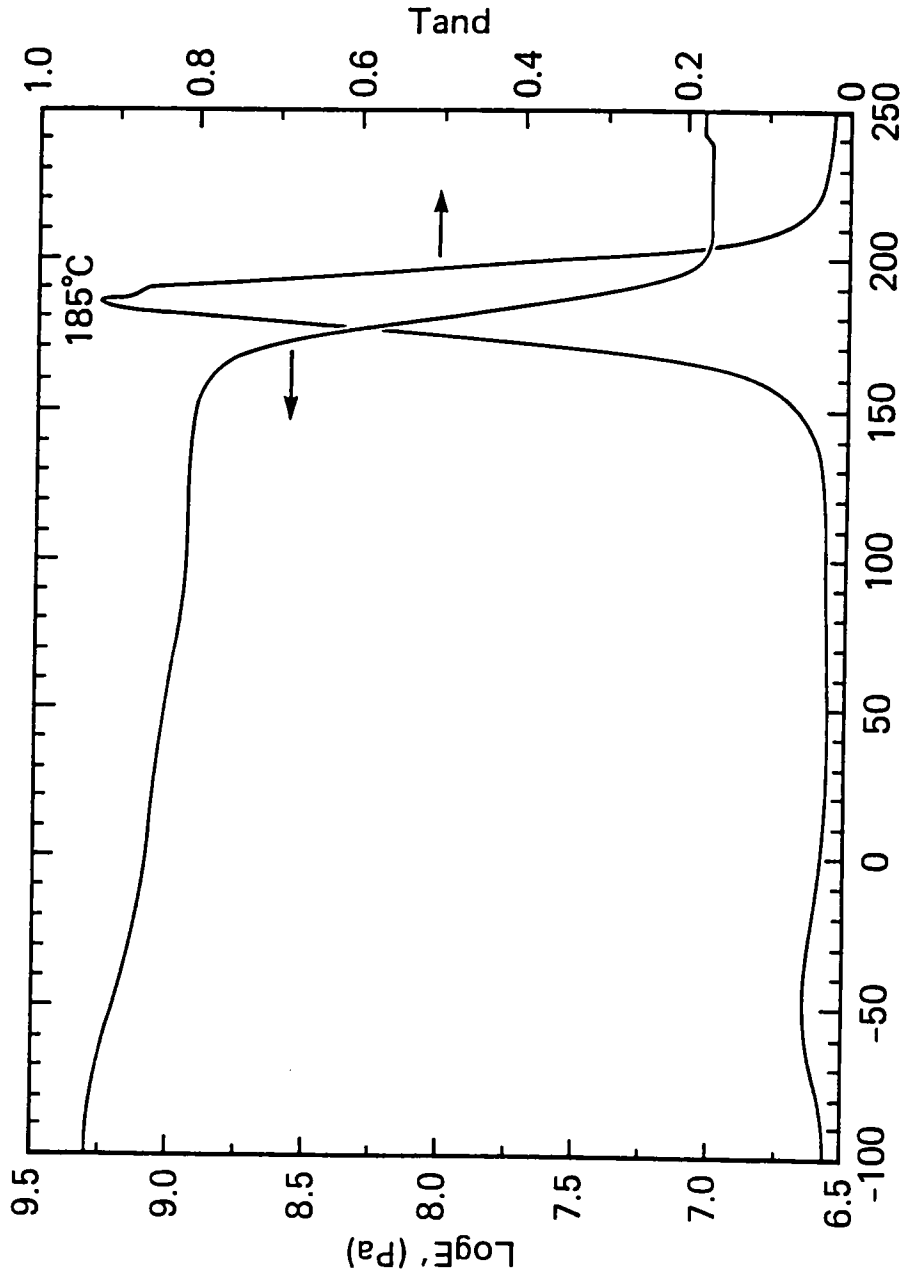

Figure 42. Dynamic mechanical thermal analysis of control (Epon Resin 828 with DDS), measured at 1 Hz.

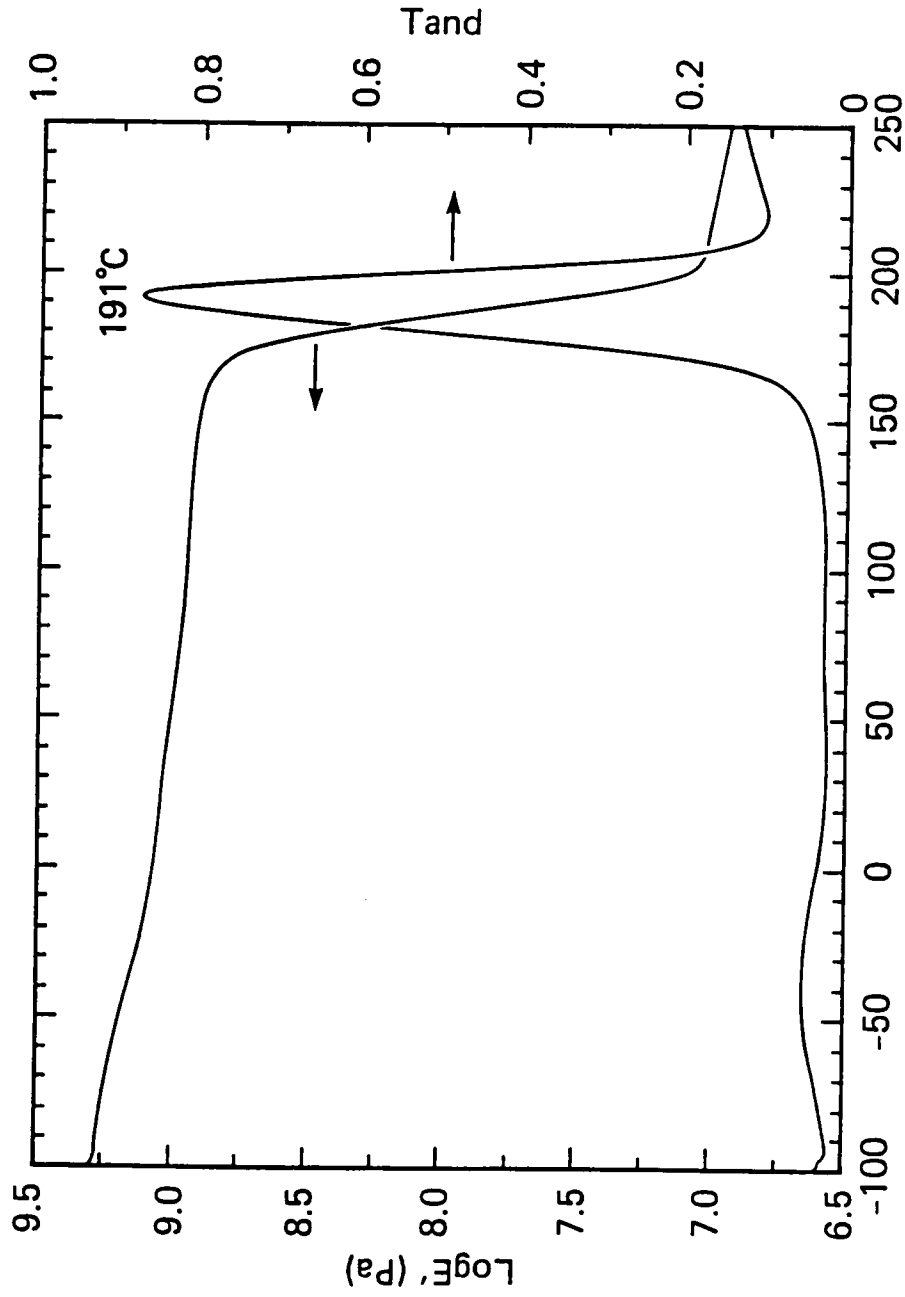

Figure 43. Dynamic mechanical thermal analysis of 13,100 g/mol amine terminated polysulfone modified epoxy network (15 wt.% PSF) measured at 1 Hz.

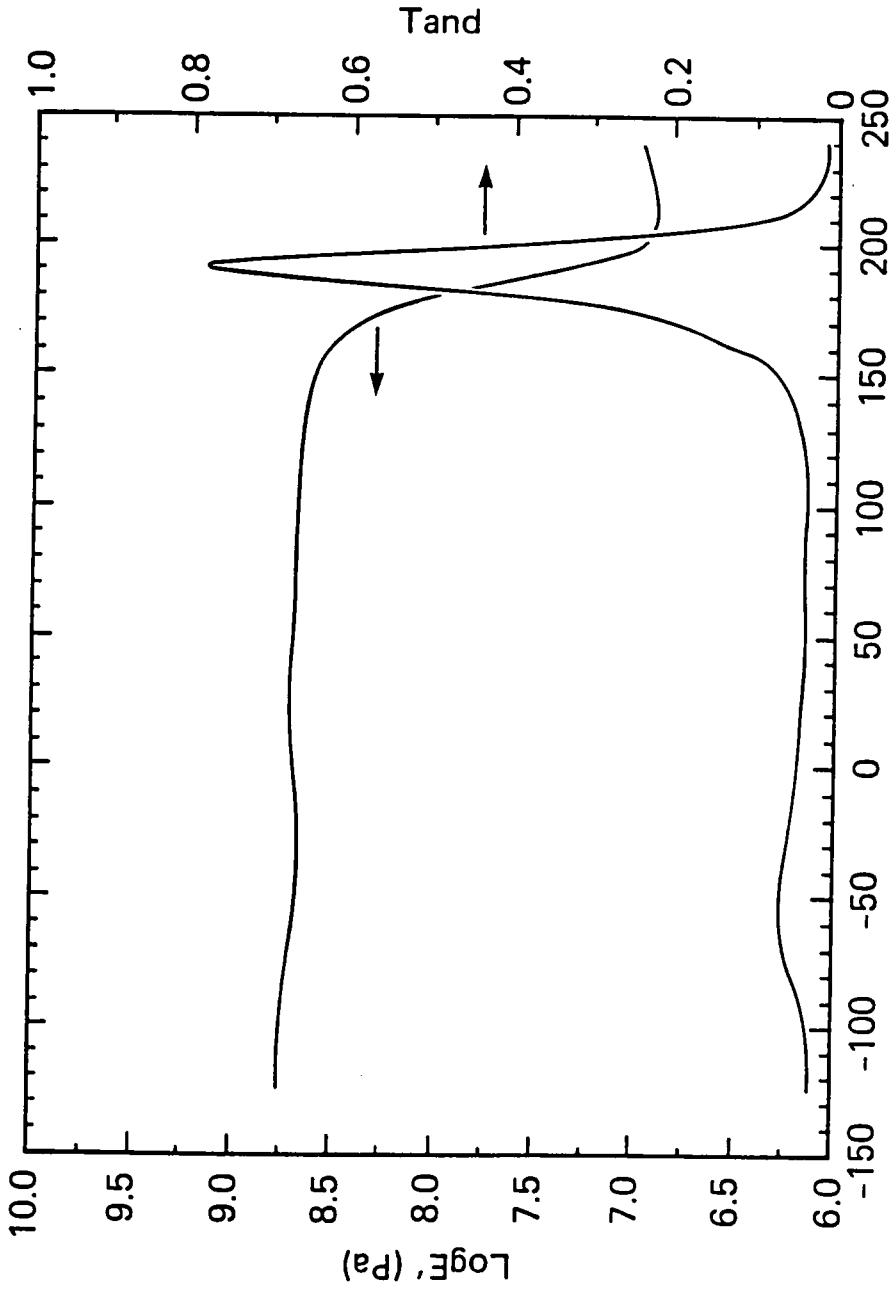

Figure 44. Dynamic mechanical thermal analysis of 8200 g/mol phenolic hydroxyl terminated polysulfone modified epoxy network (15 wt.% PSF), measured at 1 Hz.

micrographs of the phenolic hydroxyl terminated polysulfone modified networks containing fifteen percent by weight polysulfone. In the case using the 3100 g/mol polysulfone oligomer a single phase morphology was observed. However, in the 5300 g/mol polysulfone oligomer a two phase morphology develops, and this two phase morphology becomes more pronounced and defined with increasing polysulfone molecular weight. In addition, as the molecular weight of the functional modifier increased the average particle size increased from 0.3 to 0.8 μm for the 5300 to the 14,600 g/mol modified networks. As the amount of polysulfone incorporated into the network increased from ten to fifteen percent by weight, the frequency of particles increased but the size remained the same.

In each case their exist both an even distribution and size of composite particles within the matrix. Figure 46 contains low magnification SEM micrographs of several low modified networks clearly illustrate this point. In addition, these micrographs show river patterns and a rough surface which is generated with increasing thermoplastic molecular weight and content.

Finally, in those samples containing higher molecular weight modifiers, small rings around each particle were observed.

Figure 47 contains the SEM micrographs of the amine terminated polysulfone modified networks. This one step modification process produces a two phase morphology as well for polysulfone oligomers of sufficient molecular weight. As expected, the 4100 g/mol modifier produced a single phase morphology. The higher molecular weight modifiers produced a two phase morphology consisting of polysulfone

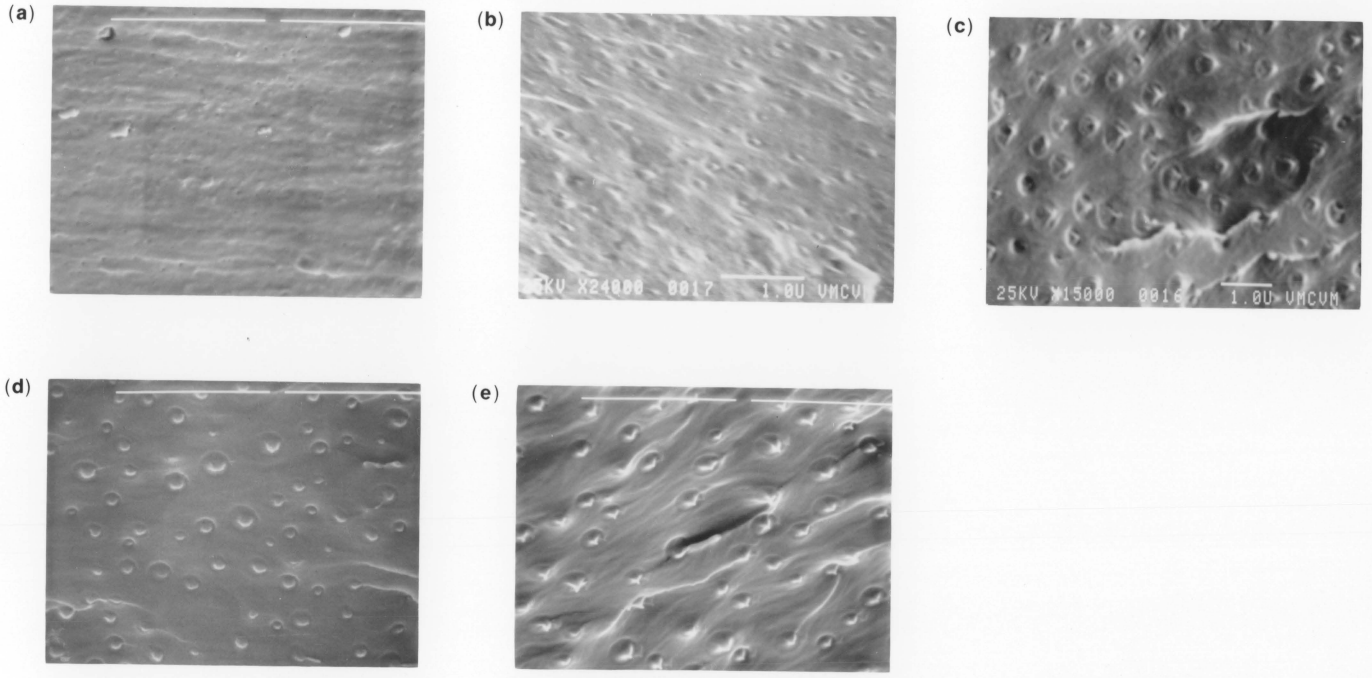

Figure 45. SEM micrographs of phenolic hydroxyl terminated polysulfone (15 wt.%) modified epoxy networks. Molecular weight of oligomers. (A) 3100 g/mol (10,000×), (B) 5300 g/mol (24,000×), (C) 6200 g/mol (15,000×), (D) 8200 g/mol (10,000×) and (E) 14,600 g/mol (10,000×).

(a)

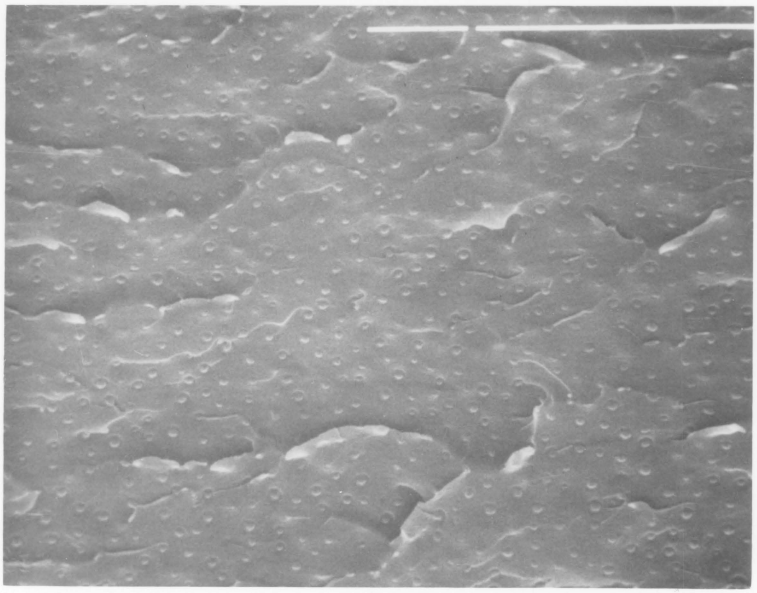

(b)

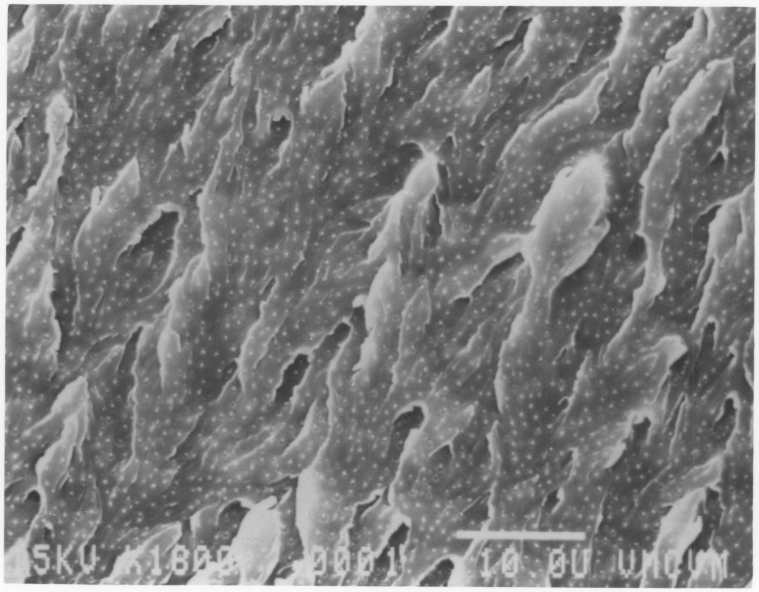

Figure 46. (A) Phenolic hydroxyl terminated polysulfone (8200 g/mol) modified network (15 wt.% PSF) (2000×). (B) Amine terminated polysulfone (13,100 g/mol) modified network (15 wt.% PSF) (1600×).

(a)

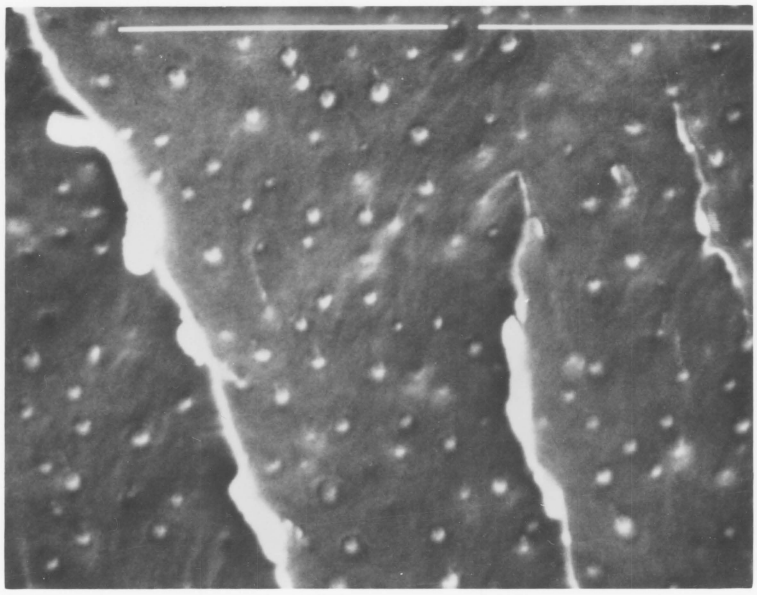

(b)

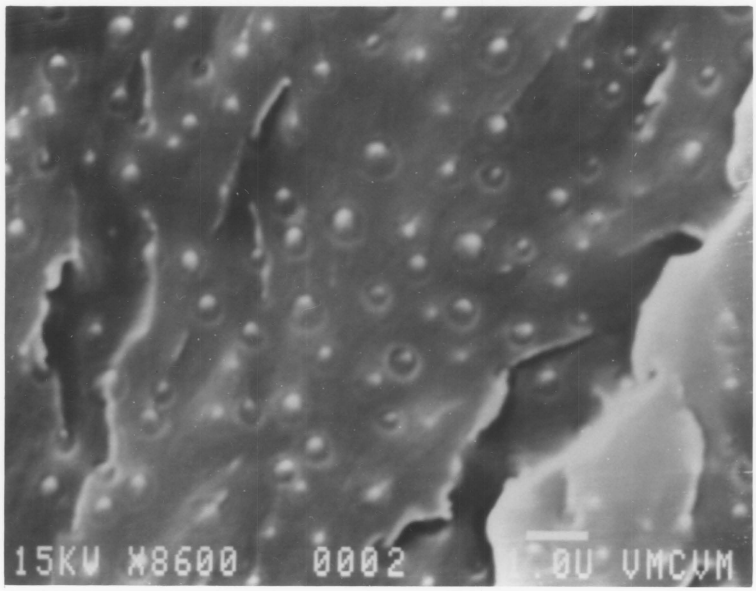

Figure 47. SEM micrographs of (A) 7100 g/mol amine terminated sulfone modified network (10,000×) and (B) 13,100 g/mol amine terminated sulfone modified network (8600×).

composite particle embedded within the epoxy matrix. In a similar fashion to the previous case, the particles were of even distribution and size and showed the small rings around the particles. However, this dispersed phase is somewhat smaller than that generated for two step modification process. It is conceivable that in the two step process chain extension may occur.

4.3.2.7 Toughening Mechanisms

The fracture surface of a typical rubber epoxy network generally consists of holes in which the rubber is believed to reside within. The toughening of these materials may result from a cavitation/dilatation mechanism recently discussed by Kinloch (88,89). The SEM micrographs of the polysulfone modified networks reveal particles on each side of the fracture surface with no corresponding holes. The thermal coefficients of expansion are very similar for each of the two components, hence dilitation of the particle was not observed. We believe that the mechanisms for toughening of these systems are different from those for the rubber modified systems. The first observation is that as the molecular weight of the polysulfone oligomer increases the size of the particle increases. In addition, the fracture toughness also increases and levels off as the molecular weight of the polysulfone increase.

Furthermore, when these modified networks are viewed at an angle, the composite particles appear to be plastically deformed and even drawn. This effect is particularly pronounced when the highest molecular weight polysulfone oligomer was used, 14,600 g/mol. Figure 48 contains a high magnification SEM micrograph of this sample. This polysulfone oligomer was of sufficient molecular weight to give a glass

transition temperature similar to the commercially available, high molecular weight polysulfone, Udel^{R}. This oligomer gave good films with tough, ductile mechanical properties. To confirm this observation, the samples were heated above the Tg of the polysulfone, 197°C, for twenty minutes. If the polysulfone had indeed plastically deformed, it would relax with this treatment. Figure 49 contains a SEM micrograph at 60°C of the 14,600 Mn polysulfone modified network after heating. As expected, the polysulfone composite particles relaxed and even flowed with the heat treatment. Moreover the average particle size increased from about 0.8 to 1.2 μm.

We believe that the toughening of these network structures upon the addition of the polysulfone results, in part, from the ductile nature of the polysulfone composite particles. It follows that as the molecular weight of the polysulfone increases and approaches the critical molecular weight for ductile properties, the fracture toughness of the modified networks increases as well.

Furthermore, a closer examination of the SEM micrographs of those networks modified with the higher molecular weight polysulfone oligomers have small rings around each of the particles. It has been noted by several authors (94) that these particles, having a different modulus than the matrix, serve as stress concentrators. Theories such as the cavitation/dilatation reviewed by Kinloch propose that this stress concentration may plastically deform the local area surrounding the particle. Thus, this local plastic deformation of the epoxy matrix may explain the rings around the composite particles. However, Kramer and coworkers (66) found that the size of the discrete phase influences the

(a)

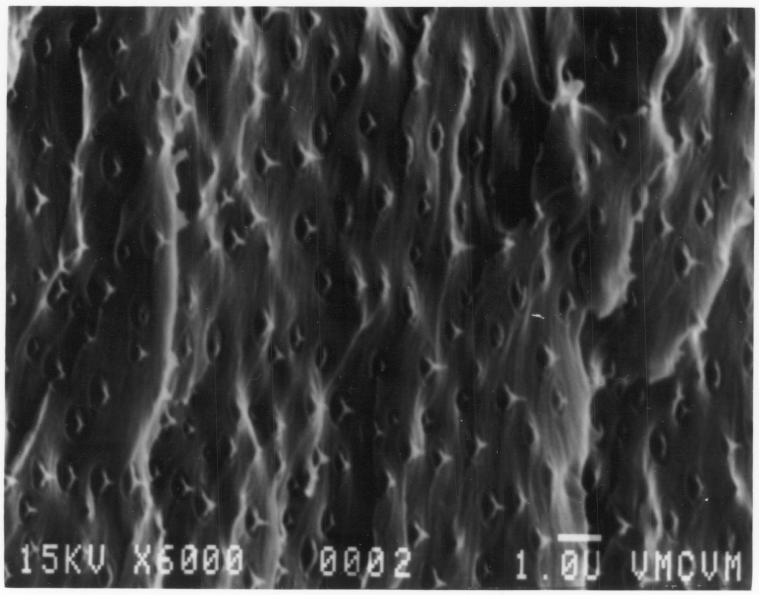

(b)

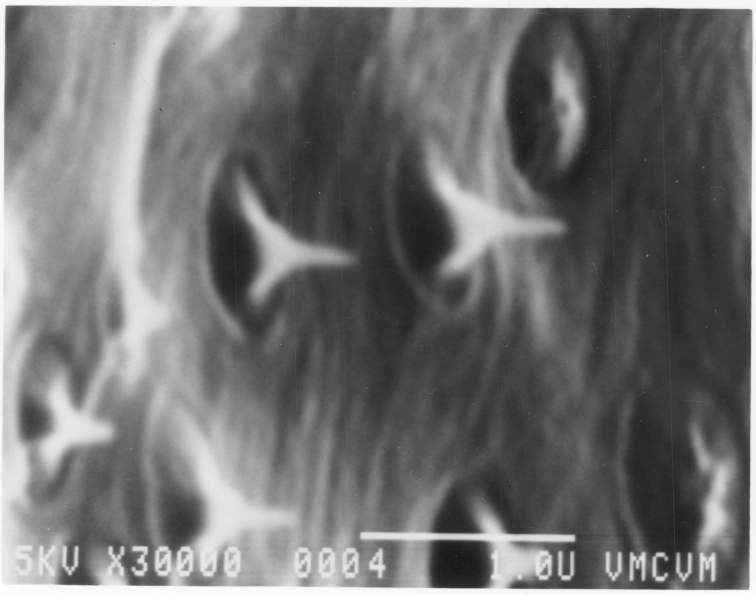

Figure 48. SEM micrograph of phenolic hydroxyl terminated polysulfone modified network (A) 6000× and (B) 30,000×.

(a)

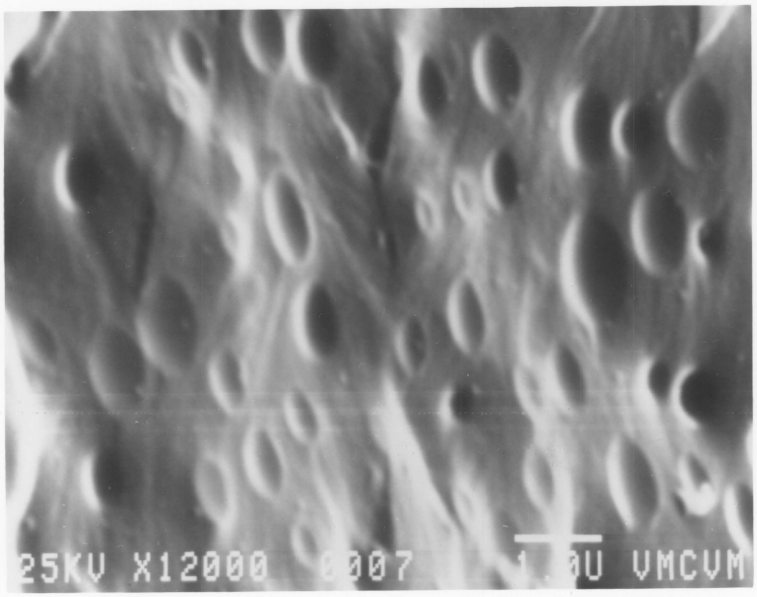

(b)

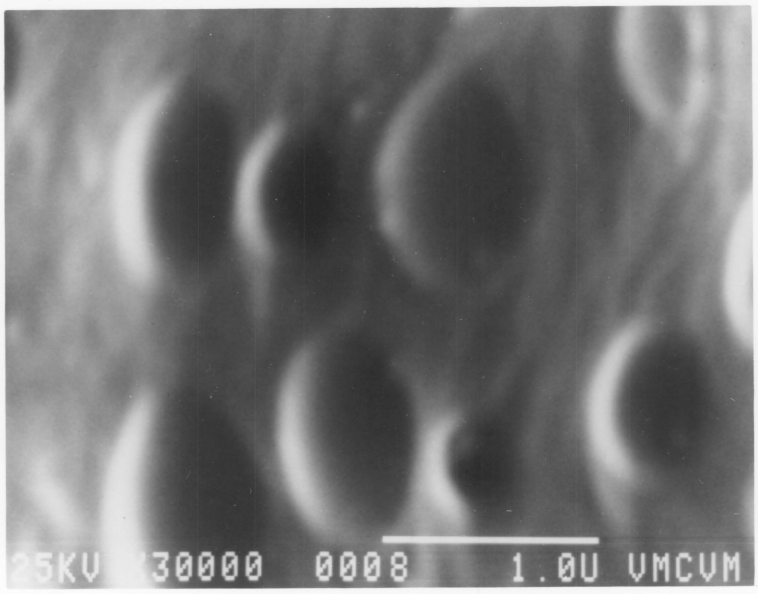

Figure 49. SEM micrographs of 14,600 polysulfone modified network after heat treatment (A) 12,000× and (B) 30,000×.

efficiency of the initiation of the energy absorption mechanism available to highly crosslinked epoxy networks is local plastic deformation, and small particles are more efficient at initiating these mechanisms. The optimum particle size found for these networks is in the 1.0-1.5 μm range (66). We believe that the thermoplastic composite particles triggers off the local plastic deformation in the matrix. However, the mechanism may be somewhat more complicated. Polysulfone modifiers of low molecular weight are miscible with the epoxy network. We believe that the relatively broad molecular weight distribution (Mw/Mn = 2) associated with the polysulfone allows a considerable amount of the modifier to be miscible with the matrix which may influence the toughening mechanisms.

Not only does the molecular weight of the oligomers used play a significant role in determining the fracture properties, but as one may expect, the amount of these modifiers in the matrix also improves the fracture properties. This increase is only noticed for those samples with higher molecular weight block. In addition, it has been reported (71) that as the frequency of the particles increases, the stress fields created by the particle interact, resulting in improved fracture toughness.

Another important factor believed to be responsible for the improved impact strength is the good interfacial adhesion between the particle and the matrix due to chemical linkage. Previous attempts to modify brittle materials with hard particles such as glass may have failed because of poor interfacial adhesion (79).

4.3.2.8 Optical Properties of the Modified Networks

In general, materials which contain a discrete phase that is larger than ~0.1 micron are opaque. This is the case for many of the rubber modified epoxy networks such as the acrylonitrile-butadiene, siloxane, and acrylate elastomers.

The polysulfone modified epoxy networks remain transparent upon curing despite their two phase morphology. We believe that the refractive index values for the polysulfone and the epoxy network are similar.

4.3.2.9 Preparation of Non-Functional Polysulfone Modified Epoxy Networks

One of the major issues involved in impact modification is the nature of the interface between the particle and the matrix. In the previous examples interfacial adhesion was forced because of the chemical linkage and partial miscibility between the two components. If a blend of the commercial Udel^{R} gives similar properties it would be most advantageous in terms of both economics and time.

Udel^{R} is methoxy or chloride end capped, thus precluding any reaction with the epoxy resin. Buchnall (101) modified epoxy networks with polyether sulfone (Victrex) but found little to no improvement in fracture properties. Polyether sulfone has a higher solubility parameter (11.2) than Bis-A PSF (10.2) which may prevent good interfacial adhesion and/or controlled particle size.

Blends of Udel^{R} and Epon Resin 828 were prepared as described in the experimental section. The modified resin was then cured with a stoichiometric amount of diaminodiphenyl sulfone into a highly

crosslinked network. An additional post-cure (see experimental) was required because of the high viscosity associated with the modified resin. In each case, 10 and 15 percent by weight polysulfone was added. The thermal properties of the blends are shown in Table 27. In each case high glass transition temperatures were obtained which are comparable to the control also shown in the table.

Table 28 gives the flexural modulus and fracture toughness values for the modified resins. Unexpectedly, the fracture toughness increased with the modifier in a similar fashion to the chemically reacted systems. However, one might anticipate that the values would be quite dependent on mixing conditions.

The addition of the modifier only caused a minimal sacrifice in the flexural modulus as illustrated in Table 28. This is further illustrated in dynamic mechanical spectra (Figure 50). The Tg of the sulfone is in the same region as the epoxy network transition.

4.3.2.10 Morphology and Toughening Mechanisms

Figure 51 contains an SEM micrograph of a $K_{I,C}$ fracture surface of an Udel^{R} modified network. Discrete composite particles ranging from 0.8-1.0 μm in size. However, good interfacial adhesion was not observed in this case and holes were even present. This was confusing in light of the improvement in fracture toughness. A closer examination of the fracture topography revealed large "globular" regions. Figure 52 contains such a region. These regions were easily removed upon treatment with chloroform leading us to believe they were unmixed polysulfone. Figure 53 contains a treated fracture surface and only holes exist. It is interesting that these samples become opaque upon

treatment with solvent, but the chemically reacted materials do not.

The toughening in these systems is not believed to result from the composite particles. We did not observe regions of plastic deformation of the matrix in the vicinity of the particle nor was the adhesion sufficient to ductilly tear the polysulfone. The regions of unmixed polysulfone are believed to contribute to the improvement in fracture toughness. Figure 54 contains a SEM micrograph of a $K_{I,C}$ fracture surface at a low magnification. The topography of the surface is considerably rougher than the chemically modified system, and the unmixed polysulfone is probably responsible.

Table 27

Thermal Properties of Udel® Modified Networks

No.	Udel® wt.%	Udel® Tg, °C	Network Tg, °C
1	Epon Resin 828/DDS (control)		195
2	10	190	197
3	15	190	195

Table 28

Mechanical Properties of Udel^{R} Modified Epoxy Networks

No.	wt.% Udel^{R}	Flex. Mod. (N/M^2)	Fract. Tough. $K_{I,C}$ ($NM^{3/2}$)
1	Epon Resin/DDS (control)	2.5×10^9	0.6×10^6
2	10	2.1×10^9	0.8×10^6
3	15	1.9×10^9	1.1×10^6

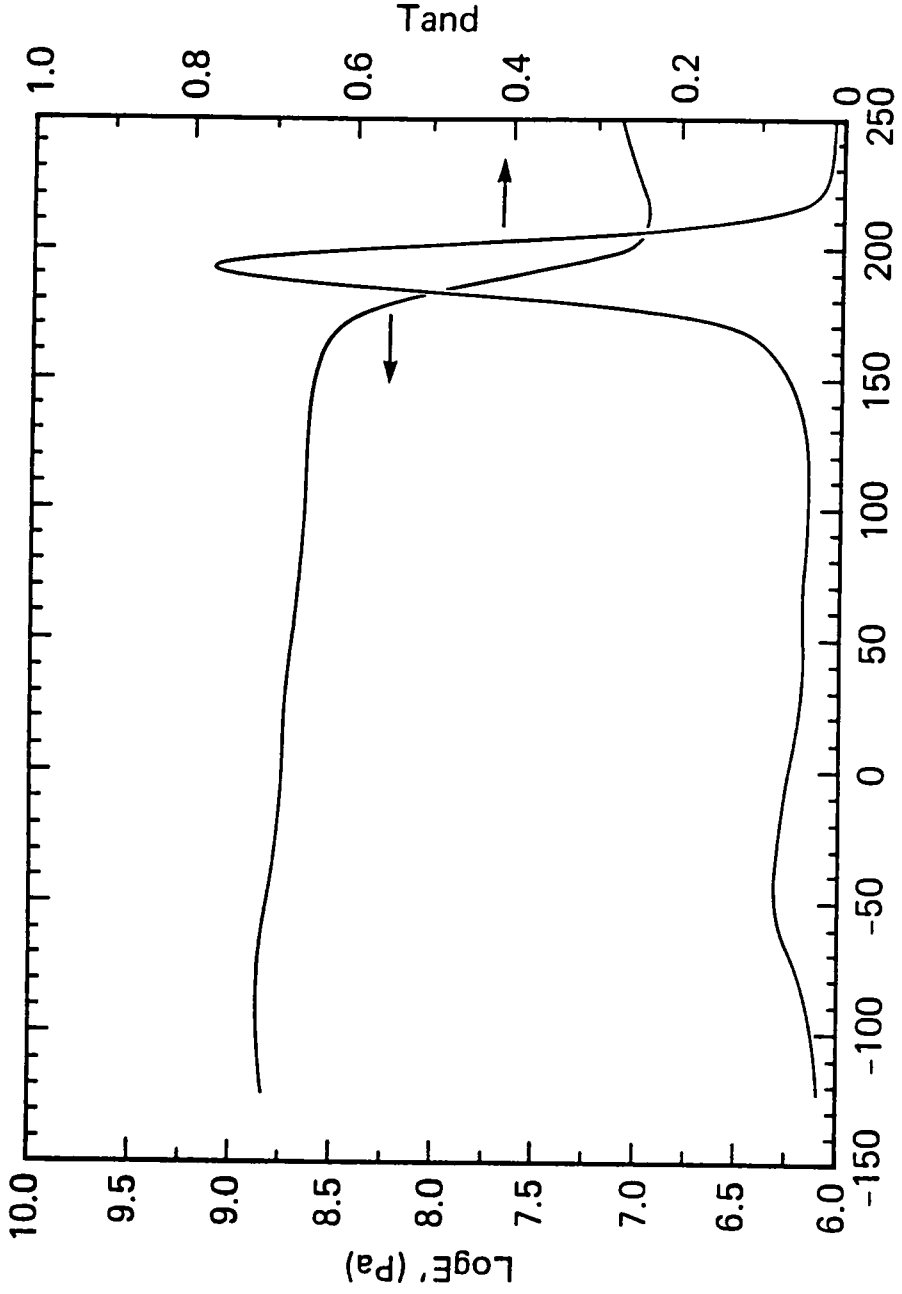

Figure 50. Dynamic mechanical thermal analysis of Udel modified (15 wt.%) epoxy network, measured at 1 Hz.

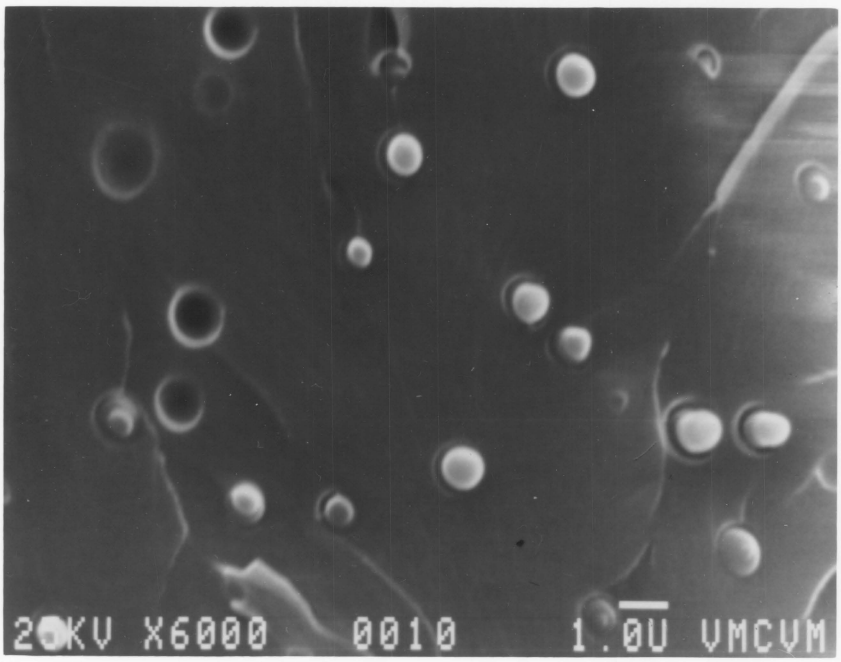

Figure 51. SEM micrograph of a $K_{I,C}$ fracture surface of a Udel (15 wt.%) modified network (6000×).

(a)

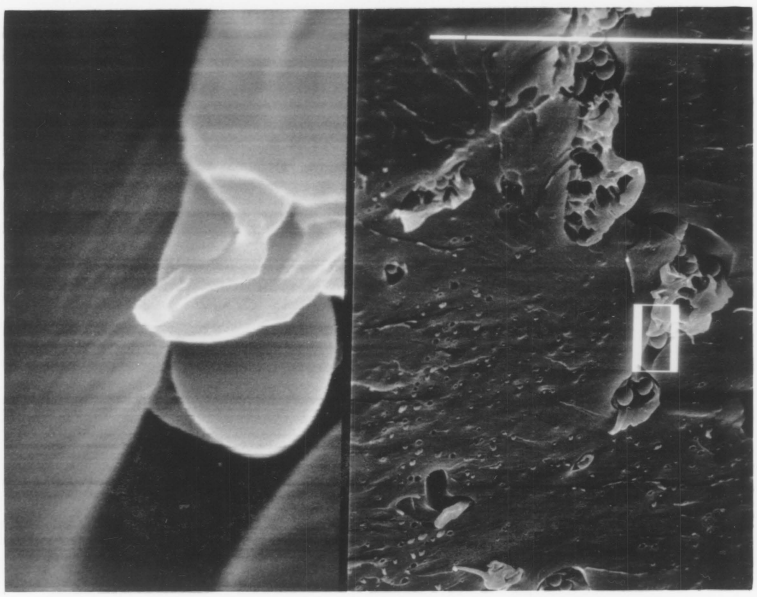

(b)

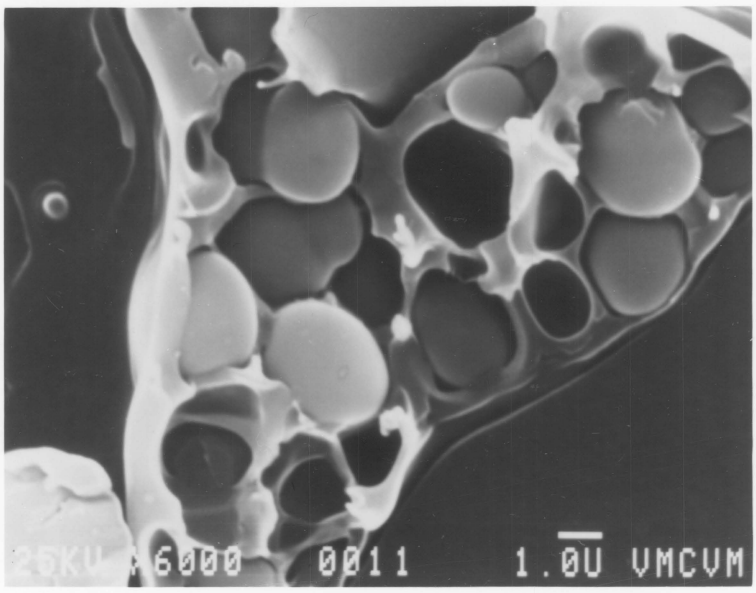

Figure 52. SEM micrograph of a Udel (15 wt.%) modified network. (A) 1000× on left and 10,000× on right and (B) 6000×.

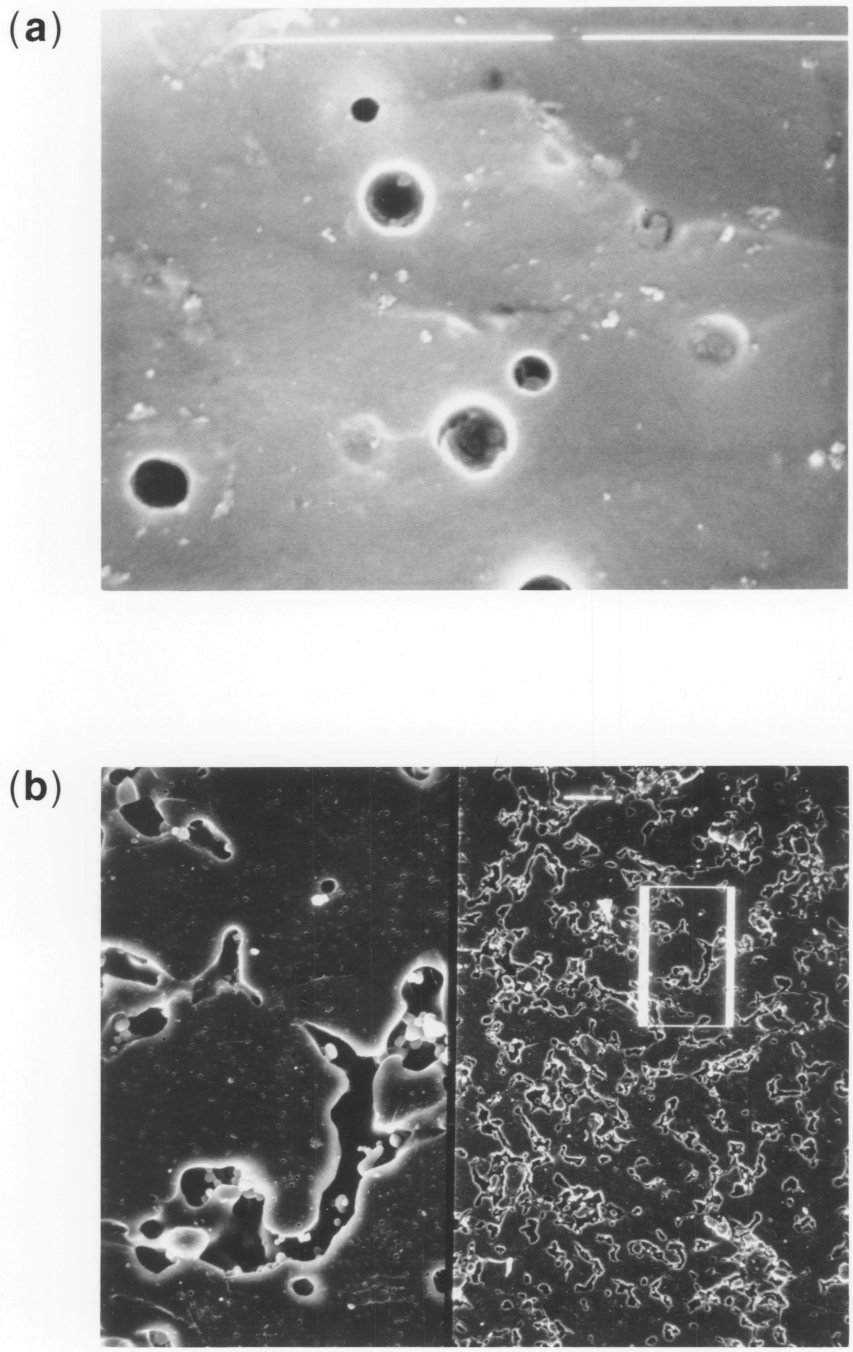

Figure 53. SEM micrograph of Udel modified network after chloroform rinse (A) 10,000× and (B) 100× on left and 500× on right.

(a)

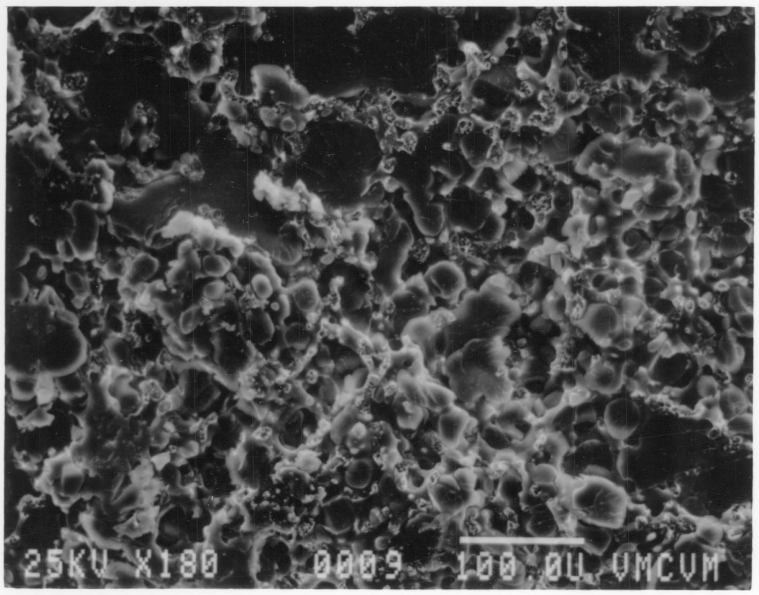

(b)

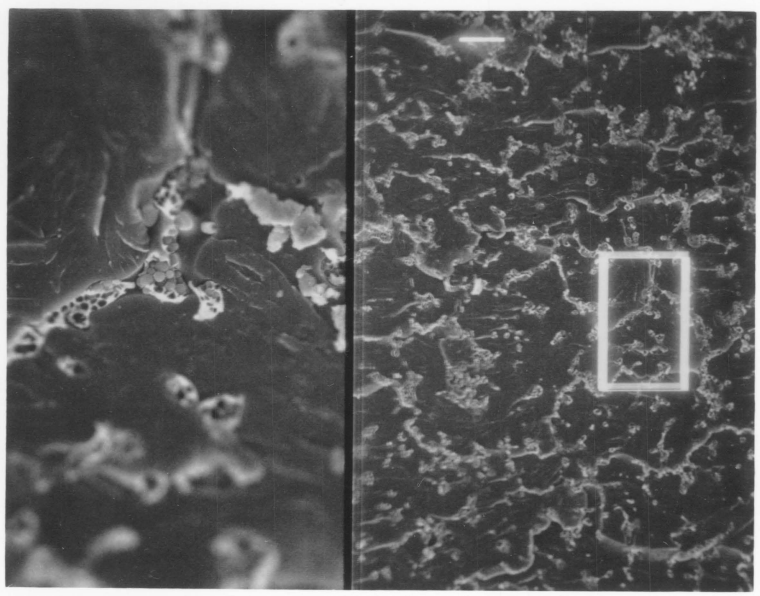

Figure 54. Fracture topography of a Udel modified network. (A) 100× and (B) 100X on left and 500× on right.

5.0. CONCLUSIONS

This thesis discussed both the synthesis and properties of Poly(arylene ether sulfones) and related structures. The tough, ductile mechanical properties which has been associated with the major secondary relaxation in the dynamic mechanical spectra were examined together with the deformation mechanisms (crazing and plastic deformation) available to these structures. In addition, these engineering polymers were used as modifiers for highly crosslinked epoxy networks to provide toughness while maintaining the modulus.

Several selectively deuterated poly(arylene ether sulfones) were synthesized for deuterium NMR investigations in a collaborative effort with Dr. L. W. Jelinski. Deuterium NMR provided highly specific information about molecular motion which complemented the molecular motion obtained using dynamic mechanical analysis.

Polysulfones have the ability to craze and deform in a plastic or ductile fashion. The initiation of these energy absorption mechanisms leads to a material of sufficiently improved strength. Perfectly alternating block copolymers of polysulfone with poly(dimethylsiloxane) were synthesized and blended with polysulfone homopolymer. The block copolymer was shown by SEM, TEM and DMA to exist as discrete composite particles within the homopolymer matrix and served as a stress concentrator capable of initiating either craze formation or decavitation. The toughness was evaluated by both $K_{I,C}$ and $J_{I,C}$ measurements.

Phenolic hydroxyl terminated polysulfone oligomers of various molecular weights were synthesized and used to chemically modify epoxy

resins. The polysulfone phase separated into discrete composite particles within the matrix of the epoxy network. These particles were able to initiate a localized plastic deformation within the epoxy matrix as well as plastically deform themselves. The incorporation of the ductile engineering thermoplastic to the brittle epoxy network uniquely provided toughness at a minimal sacrifice to the modulus.

6.0 REFERENCES

1. R. N. Johnson, A. G. Farnham, R. A. Clendinning W. F. Hale and C. N. Merrian, J. Polym. Sci. [A-1] 5, 2375 (1967).

2. W. A. Hale, A. G. Farnham, R. N. Johnson and R. A. Clendining, J. Polym. Sci.: Part A-1, 5, 2399 (1967).

3. R. N. Johnson and A. G. Farnham, J Poly. Sci.: Part A-1, 5, 2415 (1967).

4. R. N. Johnson, Encyclopedia of Polymer Science and Technology, 11, p. 447 (1969).

5. H. A .Vogel, J. Polym. Sci. [A-1] 8, 2035 (1970).

6. T. E. Atwood et al., Polymer, 18, 359 (1977).

7. T. E. Atwood et al., Polymer, 18, 365 (1977).

8. T. E. Atwood et al., Polymer, 18, 391 (1977).

9. T. E. Atwood et al, Polymer, 18, 369 (1977).

10. J. F. Bunnett and R. F. Zahler, Chem. Rev., 49, 273 (1951).

11. S. R. Schulze and A. L. Baron, Adv. Chem. Series, 91, 589 (1969).

12. J. B. Rose, Polymer, 15, 456 (1974).

13. R. Viswanathan, Ph.D. Thesis, Virginia Polytechnic Institute and State University, Blacksburg, Virginia, June, 1981; R. Viswanathan, B. C. Johnson, T. C. Ward and J. E. McGrath, NASA Langley Final Report, Research Grant NSG 1599, May 1981; R. Viswanathan, B. C. Johnson and J. E. McGrath, Polymer (London), (25)12, 1827 (1984).

14. D. K. Mohanty, Ph.D Thesis, Virginia Polytechnic Institute and State University, June 1983.

15. B. C. Johnson, Ph.D Thesis, Virginia Polytechnic Institute and State University, June 1984.

16. H. R. Kircheldorf and G. Bier, J. Polym. Sci. Polym. Chem.Ed., 21, 2283 (1983).

17. H. R. Kircheldorf and G. Bier, Polymer (London), 25, 1151 (1984).

18. D. Wu, Ph.D. Thesis, Virginia Polytechnic Institute and State University, June, 1987.

19. H. A. Vogel, Brit. Pat, 1060546 (1963).

20. S. M. Cohen and R. H. Young, J. Polym. Sci. [A-1], 4, 722 (1966).

21. M. E. A. Cadby et al., Polymer, 6, 589 (1965).

22. W. H. Bonner, U. S. Patent 3065205 (to DuPont) (1962).

23. I. Goodman, J. E. McIntyre and W. Russel, British Patent 917227 (1964).

24. Y. Iwakure, K. Uno and T. Takigchi, J. Polym Sci., [A-1] 6, 3345 (1968).

25. B. M. Marks, U. S. Patent 3442857 (1969).

26. K. J. Dahl, British Patent 1387303 (1975).

27. J. B. Rose, British Patent 4398020 (1983).

28. H.M. Colguhoun, Polymer Preprints, 25, 17 (1984).

29. D. Wu, et al., Polymer Preprints, 26(2), 277-280 (1985).

30. J. R. Fried and H. Kalkanogm, J. Polym. Sci.; Poly. Lett. Ed., 20, 381 (1982).

31. J. Heiboer, Br. Polym. J., 1, 3 (1969).

32. L. L. E. Struik, "Physical Aging in Amorphous Polymers and Other Materials", Elsevier, Amsterdam 1978.

33. S. E. B. Petrie, J. Macromol. Sci. - Phys., B12(2), 225 (1976).

34. A. J. Kinloch and R. J. Young, "Fracture Behavior of Polymers", App. Sci. Pub., London (1983).

35. L. M. Robeson, A. G. Farnham, and J. E. McGrath, "Molecular Basis of Transitions and Relaxations", D. J.Meir, Ed., Gordon and Brench, N.Y. (1978).

36. M. Baccaredda, E. Butta, V. Frasini, and S. dePetris, J. Polym. Sci. Polym. Phys. Ed., 5, 1296 91967).

37. J. E. Kurz, J. C. Woodbrey, and M. Ontu, J. Polym. Sci. Polym. Phys. Ed., 8, 1169 (1970).

38. T. Suzuki, K. Adachi, and T. Kotaka, Polym. J., 13, 385 (1981).

39. G. Allen, J. McAinsh, and G. M. Jetts, Polymer, 18, 85 (1971).

40. C. I. Chung and J. A. Sauer, J. Polym. Sci. Polym. Phys. Ed., 9, 1097 (1971).

41. L. M. Robeson, A. G. Farnham, and J. E. McGrath, Polym. Prepr. Am. Chem. Soc. Div. Polym. Chem., 16(1), 476 (1975).

42. L. M. Robeson, A. G. Farnham, and J. E. McGrath, Appl. Polym. Symp., 26, 373 (1975).

43. J. Schaefer, E. O. Stejskal, and R. Buchdal, Macromolecules, 10, 384 (1977).

44. T. R. Steger, J. Schaefer, E. O. Stejskal, and R. A. McKay, Macromolecules, 13, 1127 (1980).

45. J. Schaefer, E. O. Stejskal, T. R. Steger, M. D. Sefcik, and R. A. McKay, Macromolecfules, 13, 1121 (1980).

46. J. Schaefer, M. D. Sefcik, E. O. Stejskal, R. A. McKay, W. T. Tixon, and R. E. Cais, Macromolecules, 17, 1107 (1984).

47. P. T. Inglefield, A. A. Jones, R. P. Lubianez, and J. F. O'Gara, Macromolecules, 14, 288 (1981).

48. N. G. Boyle, V. J. McBrierty, and A. Eisenberg, Macromolecules, 16, 80 (1983).

49. A. N. Garroway, W. M. Ritchey, and W. B. Moniz, Macromolecules, 15, 1051 (1982).

50. L. W. Jelinski, J. J. Dumais, and A. K. Engel, Macromolecules, 16, 403 (1983).

51. L. W. Jelinski, J. J. Dumais, P. I. Watnick, A. K. Engel, and M. D. Sefcik, Macromoelcules, 16, 409 (1983).

52. L. W. Jelinski, Macromoelcules, 14, 1341 (1981).

53. M. D. Sefcik, J. Schaefer, E. O. Stejskal, and R. A. McKay, Macromolecules, 13, 1132 (1980).

54. H. W. Spiess, J. Molecular Struc., 111, 119 (1983).

55. L. W. Jelinski, J. J. Dumais and A. L. Cholli, Polym. Prepr. Am. Chem. Soc. Div. Polym. Chem., 25(1), 348 (1984).

56. D. A. Torchia and A. Szabo, J. Magn. Res., 44, 107 (1982).

57. H. W. Spiess, J. Phys. Chem., 72, 6755 (1980).

58. H. W. Spiess and H. Sillesen, J. Magn. Res., 42, 381 (1981).

59. J. G. Powles and J. H. Strange, Proc. Phys. Soc., 82, 6 (1983).

60. L. W. Jelinski, et al., Macromolecules, 16, 1019 (1983).

61. S. G. Turley and H. Keskkula, Polymer, 21, 466 (1980).

62. H. Keskkula, S.G. Turley, and R. F. Boyer, J. Appl. Polym. Sci., 15, 351 (1971).

63. E. R. Wagner and L. M. Robeson, Rubb. Chem. Tech., 43, 1129 (1970).

64. E. Sacher, Polymer, 21, 1234 (1980).

65. J. G. Williams and K. Nikpur, Plast. Rubb.: Mater Appl., 3, 163 (1978).

66. A. M. Donald and E. J. Kramer, J. Mat Sci., 17, 1765 (1982).

67. C. K. Riew, E. H. Rowe and A. R. Siebert, in "Toughness and Brittleness of Plastics" edited by D. Deanin and A. M. Crugnola, ACS Adv. in Chem. Ser. 154 (ACS, 1976) p. 326.

68. E. H. Merz, G. C. Clauer and M. Baer, J. Polym. Sci., 22, 325(1956).

69. S. Strella and S. Newman, J. Appl. Polym. Sci., 9, 2297 (1965).

70. P. W. R. Kung-Dougless et al., J. Mat Sci., 15, 1109 (1980).

71. J. N. Goodier, Trans. Am. Soc. Mech. Eng., 55, 39 (1933).

72. J. D. Moore, Polymer, 12, 478 (1971).

73. C. B. Bucknall, "Toughened Plastics", Applied Science Publishers Ltd., London (1977).

74. C. B. Bucknall, Adv. Polym. Sci., 27, 121 (1978).

75. R. N.Howard and C. B. Bucknall, Pure and Appl. Chem., 46, 227 (1976).

76. R. P. Kambour and D. R. Russell, Polymer, 12, 237 (1971).

77. C. B. Bucknall, D. Clagton and W. E. Keast, J. Mat. Sci., 10, 253 (1970).

78. R. P. Kambour, Macromol. Rev., 7, 1 (1973).

79. A. M. Donald and E. J. Kramer, J. Mat. Sci., 17, 2351 (1982).

80. W. G. Potter, "Epoxide Resins"; Springer-Verlag: New York, 1970.

81. C. A. May, G. Y. Tanaka, Eds.,"Epoxy Resin Chemistry and Technology," Marcel Dekker: New York, 1973.

82. "Epoxy Resin Chemistry"; R. S. Bauer, Ed.; Advances in Chemistry No. 114; American Chemical Society: Washington, D.C., 1979.

83. H. Lee and K. Neville, Handbook of Epoxy Resins, McGraw Hill, N.Y., 1967.

84. C. K. Riew and J. K. Gillham, "Rubber-Modified Thermoset Resins", Advances in Chemistry Series No. 208 (1984).

85. R. S. Bauer, Ed., "Epoxy Resin Chemistry II" ACS Symposium Series No. 221, (1984).

86. "Jeffamine Polyoxypropyleneamines", Technical Brochure, Jefferson Chem. Co., Inc., (1978).

87. J. R. Buner, J. L. Rushford, W. S. Rose, D. L. Hunston and C. K. Riew, J. Adhesion, 13, (1982).

88. A. J. Kinloch, S. J. Shaw, D. A. Tod and D. L. Hunston, Polymer, 24, 1341 (1983).

89. A. J. Kinloch, S. J. Shaw and D. L. Hunston, Polymer, 24, 1355 (1983).

90. R. C. Laible and F. J. McGarry, Polym. Plast. Technol. Eng., 27 (1976).

91. C. Bucknall and T. Yoshii, British Polym. J., 10, 53 (1978).

92. A. C. Meeks, Polymer, 15, 675 (1974).

93. E. J. Kramer, J. Mat. Sci., 14, 1381 (1978).

94. J. A. Schmitt and H. Keskkula, J. Appl. Polymer Sci., 3, 132 (1960).

95. C. B. Bucknall and R. R. Smith, Polymer, 6, 437 (1965).

96. S. K. Bhattacharya, Polym. Comp., 9, 2297 (1965).

97. F. F. Lange, and K. C. Radfor, J. Mat. Sci., 6, 1197 (1971).

98. F. F. Lange, Phil Mag., 22, 983 (1970).

99. F. Ramsteiner, Polymer, 20, 839 (1979).

100. S. Sahu and L. J. Broutman, Polym. Eng. Sci., 12, 2511 (1977).

101. L. Nicholais and L. Nicodemo, Polym. Eng. Sci., 13, 469(1973).

102. J. Leidner and R. T. Woodhams, J. Appl. Polym. Sci., 18, 1639 (1974).

103. F. F. Lange, Phil. Mag., 22, 983 (1970).

104. C. B. Bucknall and I. K. Patridge, Polymer, 24, 639 (1983).

105. A. R. Wedgewood and J. C. Seferis, Polymer, 22, 966 (1981).

106. J. Diamant and R. J. Moulton, 29th Natl. Sampe, Symp., Vol. 29, 422 (1984).

107. A. A. Griffith, Phil. Trans. Royal Soc., 221A, 163 (1920).

108. A. A. Griffith, Proc. 1st International Congress on App. Mechanics, Delft, 55 (1924).

109. E. Inglis, Trans., Institute of Naval Architects, London, 219.

110. G. R. Irwin, First Symp. on Naval Structural Mechanics, (1958).

111. G. R. Irwin and J. A. Kies, Welding J. Research Supplement, 31, 95 (1952).

112. E. Orowan, proc. 1950 Conference at M.I.T., John Wiley, NY, 139 (1952).

113. J. P. Hickerson, Elements of Experimental Fracture Mechanics, Sandia Laboratories for the U.S. Atomic Energy Commission, 1974.

114. ASTM Standard E399.

115. F. J. Loss, Naval Research Lab. Report, (1976).

116. R. Y. Ting, J. Mat. Sci., 16, 3059 (1981).

117. ASTM Standard E813.

118. J. R. Rice, J. Appl. Mech., 35, 379 (1968).

119. P. C. Paris et al., "Elastic Plastic Fracture", ASTM STP 668, J. D Landes et al., Eds., American Soc. Testing and Materials, 5-36 (1979).

120. M. K. v. Chan and J. G. Williams, Int. J. Fracture, Martinus Nijhoff Pub., Netherlannds (1783).

121. D. S. Dugdale, J. Mech. and Phys. of Solids, 8, 100 (1960).

122. P. J. Hine, D. A. Duckett and I. M. Ward, Polymer, 22, 1745 (1981).

123. D. S. Matsumoto and M. T. Takemori, Polym. Comm., 24, 44 (1983).

124. R. A. W. Fraser and I. M. Ward, Polymer, 19, 220 (1978).

125. G. L. Pitman and I. M. Ward, Polymer, 20, 895 (1979).

126. M. Parvin and J. G. Williams, J. Mat. Sci., 10, 1883 (1975).

127. A. M. Donald and E. J. Kramer, J. Mat. Sci., 16, 2977 (1981).

128. W. Doll, L. Konczol and M. G. Schinker, Polymer, 24, 1213 (1983).

129. P. Prentice, Polymer, 24, 344 (1983).

130. R. Schirrer, M. C. Konczol and W. Doll, Coll. Polym. Sci., 259, 812 (1981).

131. G. W. Weidmann and W. Doll, "Deformation, Yield and Fracture of Polymers", Plastics and Rubber Institute, 224 (1982).

132. Elio Passaglia, Polymer, 23, 754 (1982).

133. H. R. Brown and I. M. Ward, Polymer, 14, 464 (1973).

134. W. Doll, U. Seidelmann and L. Konczol, J. Mat. Sci., 15, 2389 (1980).

135. A. M. Donald and E. J. Kramer, J. Mat. Sci., 17, 1871 (1982).

136. E. J. Kramer, J. Mat. Sci., 14, 1381 (1978).

137. C. S. Henkee and E. J. Kramer, J. Polym. Sci. Poly. Phys. Ed., 22, 721 (1984).

138. A. M. Donald and E. J. Kramer, J. Polym. Sci. Polym. Phys. Ed., 20, 899 (1982).

139. E. J. Kramer, "Crazing in Polymers" Advances in Polym. Sci., 52/53, H. H. Kausch, Eds., Springer-Verlag, N.Y., 1983).

140. J. L. Hedrick, R. A. Patsiga and J. E. McGrath, Polymer Preprints, 24, 88(1984).

141. J. L. Hedrick et al., J. Polym. Sci.: Polym. Chem. Ed., accepted (1986).

142. L. W. Jelinski et al., Macromolecules, 19, 1884 (1986).

143. A. Noshay, M. Matzner, and C. N. Merriam, German Offen. 1,913,749 (Union Carbide Corp.) (1969); C. A. 71, 125475f(1969).

144. A. Noshay, M. Matzner, B. P. Barth and R. K. Walton, German Offen. 1,913907 (Union Carbide Corp.) (1969); c. A. 72, 44528u(1970).

145. A. Noshay, M. Matzner, and C. N. Merriam, German Offen. 1,913,908 (Union Carbide Corp.) (1969); C. A. 72, 22289q (1970).

146. A. B. Noshay, M. E. Matzner, B. P. Barth and R. K. Walton, German Offen. 1,927,787 (Union Carbide Corp.) (1970); C. A. 72, 79930w (1970).

147. A. Noshay, M. Matzner, B. P. Barth and R. K. Walton, U.S. Patent 3,536,657 (Union Carbide Corp.) (1970).

148. A. Noshay, M. Matzner and C. N. Merriam, U.S. Patent 3,539,656 (Union Carbide Corp.) (1970).

149. A. Noshay, M. Matzner and C. N. Merriam, U.S. Patent 3,539,657 (Union Carbide Cor.) (1970).

150. A. Noshay, M. Matzner, and C. N. Merriam, Polym. Prepr., Am. Chem. Soc., Div. Polym. Chem. 12(1), 247(1971).

151. A. Noshay, M. Matzner and C. N. Merriam, J. Polym. Sci., Part A-19(11), 3147 (1971); C. A. 76, 100111z (1972).

152. A. Noshay, M. Matzner and C. N. Merriam, in "Macromolecular Syntheses." Wiley, New York (in press).

153. A. Noshay and M. Matzner, M., Angew. Makromol. Chem. 37, 215(1974).

154. A. Noshay, M. Matzner and T. C. Williams, Ind. Eng. Chem., Prod. Res. Deve. 12(4), 268(1973); C.A. 80, 109042t(1974).

155. A. Noshay, M. Matzner, B. P. Barth and R. K. Walton, Am. Chem. Soc. Div. Org. Coat. Plast. Chem., Pap 34(2), 217(1974); also see Adv. Chem. Ser. (in press).

156. L. M. Robeson, A. Noshay, M. Matzner and C. N. Merriam, Angew. Makrromol. Chem. 29/30, 47(1973); C. A. 79, 19957v(1973).

157. M. Matzner, A. Noshay and J. E. McGrath, Polym. Prepr., Am. Chem. Soc. Div. Polym. Chem. 14(1), 68(1973); Trans. Soc. Rheol., 21/22, 109 (1977).

158. M. Matzner, A. Noshay, L. M. Robeson, C. N. Merriam, R. Barclay, Jr., and J. E. McGrath, Appl. Polym. Symp. 22, 143(1973); C.A. 80, 71813e(1974).

159. M. Matzner, A. Noshay, D. L. Schober, and J. E. McGrath, Ind. Chim. Belge 38, 1104(1973).

160. N. W. Johnston and B. L. Joesten, J. Fire Flammability 3, 274(1972); C.A. 78, 30693f(1973).

161. French Patent 2,050,554 (Union Carbide Corp.) (1971); C.A. 76, 114135x(1972).

162. J. D. Strachman and T. C. Williams, German Offen. 1,913751 (Union Carbide Corp.) (1969); C.A. 72, 22292k (1970).

163. A. Noshay and J. E. McGrath, "Block Copolymers Overview and Critical Survey", Academic Press, New YHork, p. 403 (1977).

164. G. L. Wilkes, et al., Polymer (London), accepted (1987).

165. D. J. Blundell and B. N. Osborn, Polym., 24, 953(1983).

166. P. J. Holdworth and A. Turner-Jones, Polym., 12, 704(1982).

167. D. C. Webster, J. L. Hedrick and J. E. McGrath, Proc. from SAMPE, Reno, NV (1984).

168. N. Patel, M.S. thesis, VPI & SU, 1986.

169. D. C. Webster, Ph.D. Thesis, Virginia Polytechnic Institute and State Uiversity (1984).

170. M. J. Jurek and J. E. McGrath, Polymer Preprints, 26(2), 283 (1985), M. J. Jurek, Ph.D. Thesis, VPI & SU, 1987.

The vita has been removed from the scanned document